

ACKNOWLEDGEMENT

Firstly, I would like to express my sincere gratitude to my advisors Assoc. Prof. Dr. Hakan YALÇINER and Assist. Prof. Dr. Ayşe P. BALKIS for the continuous support of my Ph.D. study and related research, for their patience, motivation, and immense knowledge. Their guidance helped me in all the time of research and writing of this thesis. I could not have imagined having a better advisors and mentor for my Ph.D. study.

Besides my advisors, I would like to thank the rest of my thesis committee: Prof. Dr. Tahir ÇELİK, Prof. Dr. Khaled MARAR, Prof. Dr. Özgür EREN, Assoc. Prof. Dr. Ertuğ AYDIN, Assist. Prof. Dr. Atila KUMBASAROĞLU and Assist. Prof. Dr. Salaheddin SABRI, for their insightful comments and encouragement, but also for the hard questions, which incanted me to widen my research from various perspectives.

My sincere thanks also goes to Assist. Prof. Dr. Atila KUMBASAROĞLU, Ahmet İ. TURAN, and Alper ÇELİK, who provided me an opportunity to join their team as an intern, and who gave access to the laboratory and research facilities. Without they precious support it would not be possible to conduct this research.

Last but not the least, I would like to thank my family: my parents and to my brothers and sister for supporting me spiritually throughout writing this thesis and my life in general.

ABSTRACT

An experimental study was performed to investigate the effects of polypropylene fibers on uncorroded and corroded reinforced concrete beams. Three different volume fractions of polypropylene fibers having 0, 0.5, and 1.5%, were tested at four corrosion levels of 0% and approximately 5, 7, and 9%. A full scale of an accelerated corrosion pool was used for the accelerated corrosion process. Reinforced concrete beams were used for an under monotonic bending test. The contribution of the actual corrosion levels of transverse and longitudinal reinforcement bars to the total corrosion levels were obtained from reinforcement bars fully extracted from concrete. Flexural strength, bond-slip, and moment-curvature relationships were examined for uncorroded and corroded reinforced concrete beams. A new model was developed to predict the flexural strength of corroded reinforced concrete beams. The proposed model for predicting the residual flexural strength of corroded beams was compared with test data published in previous studies. Furthermore, a novel model is presented for improved predictions between the actual and theoretically estimated corrosion mass losses, based on Faraday's law, with the aid of fully extracted reinforcement bars. The model used to predict the flexural strength of corroded reinforced concrete beams with large sizes demonstrated good agreement with current and previously published literature data. In the case of corroded beams comprising differing amounts of polypropylene fibers, the performance of the corroded beams was limited by a fiber volume fraction of 1.5% at low corrosion levels.

Keywords: Beam, Concrete, Corrosion, Flexural strength, Polypropylene fibers.

ÖZET

Poli-propilen liflerinin korozyonlu ve korozyonsuz betonarme kirişler üzerindeki etkilerini araştırmak için deneysel bir çalışma yapılmıştır. % 0, 0.5 ve % 1.5 olan üç farklı poli-propilen elyaf oranı, % 0 ve yaklaşık % 5, 7 ve % 9'lük dört korozyon seviyesinde test edilmiştir. Hızlandırılmış korozyon işlemi için tam-ölçekli bir hızlandırılmış korozyon havuzu kullanıldı. Betonarme kirişler monotonik bir eğilme deneyine tabi tutulmuşlardır. Enine ve boyuna donatı çubuklarının gerçek korozyon seviyelerinin toplam korozyon seviyelerine katkısı, betondan tamamen çıkarılan donatı çubuklarından elde edilmiştir. Korozyonsuz ve korozyona maruz kalmış betonarme kirişler için eğilme dayanımı, aderans-donatı kayma ilişkisi ve moment-eğrilik ilişkileri incelenmiştir. Korozyona maruz kalmış betonarme kirişlerin eğilme dayanımını tahmin etmek için yeni bir model geliştirilmiştir. Korozyonlu kirişlerin eğilme dayanımını tahmin etmek için önerilen model, önceki çalışmalarda yayınlanan test verileriyle karşılaştırılmıştır. Çalışmada ayrıca, beton içerisinden tamamen çıkarılmış donatı çubukları yardımıyla, Faraday yasasına dayanarak tahmin edilen gerçek ve teorik korozyon kütle kayıpları arasındaki gelişmiş tahminler için de yeni bir model sunulmaktadır. Büyük ölçekli korozyonlu betonarme kirişlerin eğilme dayanımını tahmin etmek için geliştirilen model, mevcut ve daha önce yayınlanmış literatür verileri ile iyi bir uyum göstermiştir. Farklı miktarlarda poli-propilen elyaf içeren korozyonlu kirişlerde, kirişlerin performansı, düşük korozyon seviyelerinde % 1.5'lik bir elyaf hacmi oranı ile sınırlandırılmıştır.

Anahtar kelimeler: Kiriş, Beton, Korozyon, Eğilme dayanımı, Polipropilen lifler.

Table of Content

ACKNOWLEDGEMENT	I
ABSTRACT	II
ÖZET.....	III
TABLE OF CONTENT	IV
LIST OF FIGURES	VII
LIST OF TABLES	VIII
LIST OF ABBREVAITONS.....	IX
CHAPTER 1: INTRODUCTION.....	1
1.1. Background	1
1.2. Scope and objective.....	5
1.3. Research questions and justifications	6
1.4. Methodology	7
1.5. Achievements.....	7
1.6. Problem statement	7
1.6.1. Problem statement of previously developed models for flexure strength of corroded RC beams	7
1.6.1.1. Used methods to obtain the corrosion levels	7
1.6.1.2. Structural approach	8
1.6.2. Problem statement of previous studies for plastic fibers.....	9

1.7. Structure of the Thesis	10
CHAPTER 2: LITERATURE REVIEW.....	11
2.1 Introduction.....	11
2.2 Literature.....	11
2.3 Developed empirical models for the prediction of strength capacity of corroded RC beams	16
2.4 Corrosion levels based on corrosion on cracks.....	18
2.5 Experimental studies on relationships between theoretical (Faraday's Law) and actual corrosion level	20
2.6 Fundamental.....	22
2.6.1 Reinforced concrete.....	22
2.6.2 Fiber	23
2.6.2.1 Properties of polypropylene fibers.....	23
2.6.2.2 Advantages of polypropylene fibers	23
2.6.3 Corrosion.....	25
2.6.4 Relationship between corrosion and steel bars.....	26
2.6.5 Types of Corrosion	29
2.6.6 Effects of Corrosion.....	29
2.6.7 Bond-Slip Relationships.....	30
CHAPTER 3: METHODOLOGY AND MATERIALS.....	31
3.1 Introduction.....	31
3.2 Experiment for Corroded Reinforced Concrete.....	31
3.3 The Construction of RC Beams.....	32
3.3.1 Formworks	32
3.3.2 Preparation of Reinforcement Bars.....	34
3.3.3 Utilization of Plastic Fibers.....	38

3.3.4 Mix Design.....	40
3.3.5 Workability of Concrete	42
3.3.6 Curing of Concrete	43
3.4 Accelerated Corrosion Test	46
3.5 Installation of Experimental Installation and Measurement Devices 49	
CHAPTER 4: RESULTS AND DISCUSSION	55
4.1. Introduction.....	55
4.2. Achieved Corrosion Levels	55
4.3. Residual Flexural Strength Test Results of Corroded RC Beams Without Polypropylene Fibers.....	61
4.4. Flexural strength test results of corroded and uncorroded reinforced concrete beams with polypropylene fibers.....	64
4.5. Bond-Slip Relationships	73
4.6. Moment-Curvature Relationships	74
CHAPTER 5: CONCLUSION.....	76
5.1. Conclusions Review.....	76
REFERENCES	79
APPENDIX A: EXAMPLE OF RECORDED CORROSION CURRENT DURING ACCELERATED CORROSION METHOD.....	88
APPENDIX B: CRACK PATENTS OF RC BEAMS	120
ÖZ GEÇMİŞ.....	130

LIST OF FIGURES

Figure 1.1: Demolished high school building (Yalciner et al., 2012a).	2
Figure 2.1: RC slabs without bond strength (Iefke high school).	27
Figure 3. 1: Reinforcement configuration of beams.	32
Figure 3. 2: Prepared plywood moulds.	33
Figure 3. 3: Strengthening of moulds.	34
Figure 3. 4: Cleaning phase of reinforcement.	35
Figure 3. 5: Weighting of reinforcement bars.	36
Figure 3. 6: Prepared reinforced concrete beams before concrete casting.	37
Figure 3. 7: Connection of copper wires to RC beams.	37
Figure 3. 8: Used polypropylene fibers.	39
Figure 3. 9: Homogeneously addition of fibers into concrete mixer.	40
Figure 3. 10: Poured concrete with fibers.	43
Figure 3. 11: Fine aggregate 0-5 mm	41
Figure 3. 12: Coarse aggregate 5-12 mm	41
Figure 3. 13: Coarse aggregate 12-22 mm	41
Figure 3. 14: Pouring and vibrating concrete process.	42
Figure 3. 15: Compacting the concrete in the cube moulds.	44
Figure 3. 16: Curing process of RC beams.	45
Figure 3. 17: Removal of the RC beams from the moulds.	46
Figure 3. 18: Accelerated corrosion method setup: (a) experimental test set up; (b) used balance; (c) schematic diagram.	47
Figure 3. 19: Copper wires used for transverse and longitudinal bars.	48
Figure 3. 20: Schematic view of bending test.	50
Figure 3. 21: Loading setup: (a) test setup, (b) schematic diagram.	52
Figure 3. 22: Application of strain gauges.	53
Figure 3. 23: Cleaning and repairing of support.	54
Figure 4. 1: Cleaning process: (a) extracted reinforcement bars, (b) mechanical cleaning, (c) chemical cleaning.	55

Figure 4. 2: Distribution of corrosion levels: (a) shear reinforcement bars; (b) longitudinal bars.	57
Figure 4. 3: Correlation between theoretical and actual mass losses.	59
Figure 4. 4: Load-displacement responses for the uncorroded and corroded beams at 0% V_f	61
Figure 4. 5: Validation of proposed model.	63
Figure 4. 6: Load-displacement relationships of uncorroded RC beams.	65
Figure 4. 7: Load-displacement relationships of corroded RC beams for group B.	68
Figure 4. 8: Load-displacement relationships of corroded RC beams for group C.	69
Figure 4. 9: Extracted reinforcement bars: (a) $C_{0.5}$ (V_f : 0.5%, C_I : 7.4%) and $C_{1.5}$ (V_f : 1.5%, C_I : 8.4%); (b) $D_{0.5}$ (V_f : 0.5%, C_I : 9.8%) and $D_{1.5}$ (V_f : 1.5%, C_I : 10.6%).	70
Figure 4. 10: Load-displacement relationships of corroded RC beams for group D.	71
Figure 4. 11: Damage levels at failure without releasing jack.	72
Figure 4. 12: Bond-slip relationships of uncorroded and corroded beams.	72
Figure 4. 13: Moment-curvature relationships: (a) V_f : 0%, (b) V_f : 1.5%.	75

LIST OF TABLES

Table 1. Gravimetric Test Results	58
Table 2. Comparisons of Theoretically Calculated and Experimentally Obtained Moment Capacities	62

LIST OF ABBREVAITIONS

RC: Reinforced Concrete

FRC: Fiber Reinforced Concrete

SFRC: Steel Fiber Reinforced Concrete

FL: Faraday's Law

V_f: Volume Fraction

C_L: Corrosion Level

P_f: Polypropylene Fiber

CHAPTER 1: INTRODUCTION

1.1. Background

In the 20th century, reinforced concrete (RC) which has a lot of development and application area is the most suitable building material that can be produced as desired, economical, and durable, with sufficient strength when it is planned and applied properly. However, deterioration of the RC structures has started to be seen in last decade. One of the most common reasons for this is thought to be the reinforcement corrosion in concrete and the construction industry loses millions of dollars each year due to corrosion (Zhu et al., 2014).

In the existing RC structures, reinforcement corrosion and strength and adherence losses caused by the earthquake are the major risk factors for earthquake safety. Corrosion may occur in RC structures due to various reasons and significant damage to the structural members. Over time, these damages reach significant levels and make expensive measures to be taken. Therefore, it is important to identify such damages as early as possible and to take precautions (Celep and Kumbasar, 2004).

In Turkey, 92% of which is in earthquake zones, it is known that 95% of the population live under the threat of earthquakes. During the last 58 years, 58,202 people lost their lives, 122,096 people were injured and approximately 411,465 buildings were destroyed or severely damaged (Coşkun, 2001). Therefore, the existing structures are constructed with old methods, the importance of which causes significant damage to the building elements such as corrosion increases.

In Turkey, August 17, 1999 Marmara earthquake after examining the RC buildings were found out to be one of the main causes of corrosion damage (Çağatay, 2005). According to research conducted by Çağatay (2005), it was determined that sea sand was used in the core samples taken to determine the compressive strength of concrete buildings after Marmara earthquake. The use of sea sand has led to the rapid development of corrosion in the RC structures. Considering the existing stock of RC structures, corrosion in almost all buildings

which have direct or indirect interaction with bridges, viaducts and water has become an international problem in recent years (Çağatay, 2005).

According to another study conducted by Yalciner et al. (2012) examined a 25-year-old high school building (Bekir Paşa High school) from the lightning point and analysed. Bond-slip relationships were considered as a function of corrosion rate in different time periods in nonlinear analysis (i.e., non-corroded (t: 0), existing (t: 25) and 50 years after construction). Therefore, they were used to ensure the effect of time-dependent slip rotation on the global structural behaviour by modifying the target post-yield stiffness of each structural member. As shown in Figure 1.1, one story of RC buildings was demolished without completing its economic life (Yalciner et al., 2012).



Figure 1.1: Damaged high school building which was demolish (Yalciner et al., 2012a).

In another study done by Yalciner et al. (2015) a 50-year-old high school building (Namık Kemal High School) was analysed to examine the effects of corrosion on time-dependent seismic performance levels. Based on the data obtained from the structure, it was used to estimate the performance level for different time intervals by combining the two main effects of corrosion. Deformation due to bond-slip relationships and loss in cross-sectional areas of reinforcing bars and corrosion rates for five corrosion levels were investigated. Plastic hinges were identified because of the corrosion effect and used to perform nonlinear thrust analyses. Then, increasing dynamic analysis was performed for 20 separate earthquake ground motion recordings to estimate the time-dependent performance levels of the structure as a function of the corrosion rate. As a result, it was found that corrosion had a significant effect on the performance levels of the school building by reducing the bond strength (Yalciner et al., 2015).

As it was explained above, the effects of corrosion and the results of corrosion on safety issues during earthquakes; such as Marmara earthquake happened in Turkey; and economic impacts of corrosion; such as demolished 25-year old building (Bekir Paşa High School) in North Cyprus require rapid decision making on corroded RC structures.

However, the structural assessment of RC buildings itself are complex and corrosion make such assessments more complex. Because of the complex structure of corrosion, the effects of corrosion are generally assumed as reduction in cross-sectional area of reinforcement bars during structural assessment and this problem come up to date in the available literature. The effects of corrosion is more than reduction in cross-sectional area of steel bars, such it effects bond-slip relationships, premature cracking of concrete, premature reduction in mechanical properties of concrete and reinforcement bars, strength reduction in earthquake indicators of structural members (i.e., energy absorption capacities, stiffness, lateral and axial displacement capacities, ductility ratios).

If an accurate flexural moment capacity of a corroded RC beam is evaluated; crack width, mechanical properties of concrete and reinforcement, bond-slip relationship due to corrosion are needed to be taken into account. However, on-site evaluation of a corroded structure with

all these parameters is not practical and not easy to be measured (e.g., not easy to estimate corrosion levels and types in each reinforcement for existing structures). Therefore, obtained empirical models are important for practical assessment of such structural members. Thus, in this thesis, series of experimental study was conducted to predict the flexural strength of corroded RC beams as a function of corrosion levels as a practical method. Moreover, the effect of corrosion on corroded RC beams with fibers were examined. An accelerated corrosion method was used to corrode the reinforcement bars embedment in concrete and to develop an empirical model for the prediction of flexural strength of corroded RC beams. RC beams were corroded for different degree of corrosion levels. Three points flexural strength tests were performed to investigate the structural behaviour of corroded RC beams. After accelerated corrosion method and flexural strength tests, all RC beams were broken and both tensile and stirrups were extracted from RC beams to determine the actual corrosion levels at each RC beam. The distribution of corrosion levels at both tensile and stirrups were considered for the developed model in this thesis. Moreover, the effect of fibers at different degree of corrosion levels on structural behaviour of corroded RC beams were investigated by flexural strength tests.

By performing this thesis, the following results were achieved and models were developed. With help of accelerated corrosion method and obtained actual corrosion levels provided to calculate the correlation between theoretically estimated corrosion levels (i.e., based on Faraday's Law) and the actual corrosion levels by considering the effect of the larger sizes of corroded RC beams. Develop empirical model provides to better predict the actual corrosion levels based on Faraday's Law for further studies. Experimental test results showed that predicted corrosion levels based on Faraday's Law were less compared to actual corrosion levels due to the resistance of concrete against the applied current. Investigated structural behaviour of corroded RC beams showed that the effect of corrosion was not only reduction in cross-sectional area of steel bars. As a result of cracking of concrete, reduction in mechanical properties of concrete and steel bars, reduced bond-slip relationships caused to reduce the structural performance of corroded RC beams. The ductility ratios, energy dissipation capacities, bond strength, initial and secondary stiffness, displacement and curvature capacities of corroded RC beams were reduced as the corrosion levels were

increased. An important result was obtained for the corroded RC beams in term of bending capacity. Not considered effect of stirrups on the flexural strength capacity of uncorroded RC beams showed that in the case of corrosion the effects of stirrups on the flexural strength capacity of corroded RC beams are needed to be considered. This was mainly because of significant effect of corrosion on stirrups compared to tensile bars. Since the diameter of stirrups are less than tensile bars; the effect of corrosion is more at stirrups compared to tensile bars at the same amount of corrosion levels. Therefore, develop empirical model in this thesis to predict the flexural strength of corroded RC beams consider the corrosion levels at both tensile bars and stirrups. Used different amount of fibers at both uncorroded and corroded RC beams increased the structural performance of RC beams. However, the performance of fibers at corroded RC beams were limited according to the corrosion levels. Mainly, used different amount of fibers increased the tensile strength of concrete thus ductility ratios and bond strength of corroded RC beams were regained.

1.2. Scope and objective

The scope of this thesis includes the comparison of structural behaviour of uncorroded and corroded RC beams at different degree of corrosion levels with used different amount of fibers.

The limitation of the thesis is as follows:

- The developed empirical model to predict the flexural strength of RC beams are only valid for RC beams due to the neglected axial loads,
- The obtained structural behaviour at corroded RC beams are limited for the following corrosion levels;
- The corrosion level of tensile bars are limited from 0 to 8.60% which are given in Table 1.
- The corrosion level at stirrups are limited from 0 to 15.80.
- The used amount of fibers and structural behaviour of corroded and uncorroded RC beams are limited for the volume fraction (V_f) of fiber at 0, 0.5, and 1.5%.

- The initial cracks during accelerated corrosion method may differ under sustained and absence of loads. For the current study, all RC beams were corroded under the absence of load.
- There was no any corroded inhibitor was used for the current study.

Within the scope of this thesis, the following items were aimed to be investigated:

- To investigate the structural behaviour of corroded RC beams,
- To develop an empirical model for the prediction of the flexural strength of corroded RC beams as a function of corrosion levels at tensile bars and stirrups,
- To investigate the structural behaviour of uncorroded RC beams with polypropylene fibers,
- To investigate the structural behaviour of corroded RC beams with polypropylene fibers,
- To correlate actual mass loss according to Faraday's law,

Within the aim of this thesis, the following earthquake indicators were also examined;

- The effect of corrosion on *flexural strength* of RC beams with and without fibers,
- The effect of corrosion on *bond-slip relationships* of RC beams with and without fibers,
- The effect of corrosion on the *energy absorption* capacity of RC beams with and without fibers,
- The effect of corrosion on *ductility ratios* of RC beams with and without fibers.

1.3. Research questions and justifications

The following questions can be asked as a research questions for the current thesis:

- Does Faraday's Law accurately predict the actual corrosion levels?
- What are the effects of corrosion on structural behaviour of corroded RC beams?
- Do stirrups effect the flexural strength capacity of corroded RC beams?
- Do plastic fibers provide to regain the structural performance of corroded RC beams?

Since there is no any code is available in earthquake codes to predict the seismic performance levels of corroded RC buildings, the justification for the subject of research stems from this requirement.

1.4. Methodology

An accelerated corrosion method was used to corroded reinforcement bars embedment in concrete. Actual corrosion levels were obtained by extracting all reinforcement bars from concrete and reweighting of each steel bars following flexural strength tests. Structural behaviour of uncorroded and corroded RC beams at different corrosion levels for different amount of fibers were investigated by performing three points of bending tests.

1.5. Achievements

An empirical model was developed for the prediction of the flexural strength of corroded reinforced concrete beams. The contribution of stirrups on bending capacity of corroded RC beams were considered for the develop model. Moreover, a novel model was presented for improved predictions between the actual and theoretically estimated corrosion mass losses, based on Faraday's Law. The limitation of the amount of fibers on corroded RC beams in term of structural performance were defined in the current study.

1.6. Problem statement

Within the scope of this thesis, two main problem statements were defined. First, one for the previous developed models to predict the flexure strength of corroded RC beams and second one for the corroded RC beams with fibers.

1.6.1. Problem statement of previously developed models for flexure strength of corroded RC beams

There are two main problem statements (e.g., methods to obtain the corrosion levels and structural approach for the developed models) can be counted in the developed models for the predicting of the flexural strength of corroded RC beams.

1.6.1.1. Used methods to obtain the corrosion levels

- The previously developed empirical models to predict the flexure strength of corroded RC beams were based on obtained theoretical corrosion levels (i.e., according to

Faraday's Law). In another word, obtained corrosion levels for the developed previous models were not based on actual corrosion levels.

- In addition to this statement, and contrast to theoretically obtained corrosion levels, other developed models (El Malumbela, 2010) were based on the corrosion levels obtained from steel coupons cut from the corroded bars to calculate the corrosion levels. Calculated corrosion levels from coupon tests may not represent the actual corrosion levels in a steel bar owing to the change in the original mass of the bars. This phenomenon was also demonstrated by Malumbela et al. (2010) on steel coupons. (El Malumbela et al., 2010)
- Very few studies have been performed on calculating the actual corrosion levels by extracting the corroded reinforcement bars from concrete (e.g., Ahmad, 2017 and Azad et al., 2010). However, the tested samples in those studies had a smaller size than those of the current study and may not represent the actual conditions of RC buildings due to size effect of structural members.

1.6.1.2. Structural approach

- The second problem statement for the prediction of residual flexural strength of previous developed models can be defined by the calculated moment-resisting capacities of corroded RC beams, considering only corroded tensile reinforcement bars. Although the theoretical calculation of moment resisting capacities of RC beams does not consider the effects of transverse reinforcement bars, these bars effect the load carrying, displacement, ductility and energy capacities, particularly in the case of corrosion.
- Theoretical flexural moment capacity which is calculated based on assumptions (i.e., plane section remains plane after bending, tensile strength of concrete and effects of transverse reinforcement bars on moment resisting capacity are neglected) of load carrying capacity is less than the actual capacity since strain hardening of reinforcing steel and confinement effects are neglected. Although transverse reinforcement bars resist the shear forces, they have effects on total displacement in a RC member that can

be obtained from displacements due to curvature, slip and shear. Previous studies also indicated this phenomenon (Higgins et al., 2012 and Wang et al., 2015).

- In the light of above sentences; an important result was obtained by Suffern et al. (2010). Suffern et al. (2010) indicated that the load-carrying capacity of uncorroded stirrups was better compared to beams without stirrups. However, the load-carrying capacity of the beams without stirrups was also greater than that of the corroded beams with stirrups. The results obtained by Suffern et al. (2010) indicated how corrosion effectively changes the failure mechanism of concrete members by considering the type of reinforcement bars. For the current study and considering the discussion explained above, a new model was proposed to predict flexural strength of full-scale corroded RC beams by revisiting previous models (e.g., Suffern et al., 2010).

Therefore, current study considers the corrosion levels not only at tensile bars, but also corrosion levels at stirrups.

1.6.2. Problem statement of previous studies for plastic fibers

Several studies that are detail explained in the section of literature survey of this thesis, have investigated the effectiveness of the use of steel, plastic, nylon or polyethylene terephthalate fibers in concrete members.

- Although considerable studies have been performed to take advantage of the use of plastic fibers, the effect of plastic fibers on full-scaled corroded RC beams has not been studied yet.
- Moreover, test results of previous studies on uncorroded RC beams with fibers have been limited based on load– displacement relationships, and the contributions of fibers to bond-slip relationships in full-scaled RC beams have not been investigated

Different from previous studies found in the available literature, the effect of fibers were investigated on full-scaled uncorroded and corroded RC beams for different earthquake indicators (e.g., load-displacement, ductility ratios, energy absorption capacities, and bond-slip relationships).

1.7. Structure of the Thesis

The thesis structured of the argumentation is presented five chapters and the contents are summarized as follows:

Chapter 1 begins with a background information on the research subject. The chapter identifies the research problem; this is followed by the aims, objectives, importance, and methodology of the study. The chapter concludes with the structure of the study.

Chapter 2 give information about the work done so far has been examined on two topics. The first topic, Corroded RC beams, slabs and columns on work is examined. Another issue examined the effects of plastic fibers on corroded reinforced concrete elements.

Chapter 3 explains accelerated corrosion method and bending tests. Requirements to determine the earthquake indicators obtained from experimental test results were also explained in this chapter.

Chapter 4 explains the experimental tests results of uncorroded and corroded RC beams at different amount of fibers. Obtained actual corrosion levels and developed models; prediction of flexural strength of corroded RC beams and correction factor to Faraday's Law were explained in this chapter.

Chapter 5 gives information about the summarized results obtained from experimental study and suggestions for further studies.

CHAPTER 2: LITERATURE REVIEW

2.1 Introduction

This chapter give information about the work done so far has been examined on two topics. The first topic, Corroded RC beams, slabs and columns on work is examined. Another issue examined the effects of plastic fibers on corroded reinforced concrete elements.

2.2 Literature

The following studies describe the experimentally and theoretically conducted literature studies on RC elements which are exposed to corrosion and reinforced concrete elements produced using fiber.

In 2012 Yalciner et al. (2012b) investigated the effect of corrosion on bond-slip relationships at different strength levels of concrete and concrete cover depths. The empirical models were developed by pull-out by using two different concrete mixes, three different cover depths and different rates of corrosion values. Bond-slip relationships were compared according to different corrosion rates. The main reason why the relationship between compressive strength and bond strength of noncorrosive specimens differs in the samples subjected to corrosion is the main reason that the element exhibits a brittle behaviour and sudden decreases in bond strength. According to this study, higher concrete strength levels and corroded reinforcements showed a higher percentage of bond strength deterioration because of concrete cracking during the pull-out tests (Yalciner et al., 2012b).

Yalciner and others (2012a) in their another study evaluated the effect of corrosion on 25-years olds RC building construct in north Cyprus. After modelling the structure with the findings, a study was conducted to estimate time-dependent seismic performance levels by applying time definition analysis. As a result, time-dependent fragility curves were developed for the 25-year-old reinforced concrete building, which showed that the effect of adherent force on the seismic performance level was quite high (Yalciner et al., 2012a).

According to Yalciner and Marar (2017) amprical models were developed for estimating the bond strength of corroded and non-corroded reinforcing bars at different geometry of reinforcement bars. In that study, they used an accelerated corrosion method to corrode reinforcing bars embedded in concrete specimens and performed pull-out tests to investigate

the ultimate bond strength of corroded cubic concrete samples. The effects of the geometry of two different reinforced concrete bars were discussed by considering two different concrete strength levels at different concrete cover depths. It has been found that the partially coated hook reinforcing bars increase the radial stress on the concrete surface and reduced the adhesion strength. Due to the increased roughness of the steel bar resulting from confined corrosion products, increases in bond strength were lower for hooked bars.

The one of the latest study was conducted by Yalciner et al. (2019) to correlate the initial corrosion crack widths with seismic performants levels of corroded 25 RC columns. In that study, RC columns were corroded by using accelerated corrosion method. After accelerated corrosion method and before cyclic loading tests, the crack widths due to corrosion were recorded. The recorded corrosion crack widths were then correlated with the energy absorption capacities and roof drift ratios of RC columns. Developed empirical models by Yalciner et al. (2019) provide to predict the seismic performance levels of RC columns based on non-destructive methods via initial corrosion crack widths (Yalciner, Kumbasaroglu, and Karimi, 2019).

Several models have been also performed by different researchers to estimate the corrosion rate of steel in concrete and its effects on structures, and it is possible to evaluate and define the seismic performance levels of reinforced concrete structures.

According to Junaid and Aboutaha (2016), the deteriorated concrete elements indicated that a strong assessment of their remaining strength is needed to develop a cost-effective reinforcement system. Unfortunately, there is a lack of reliable models for evaluating the residual strength of steel reinforced concrete beams, and it also suggests that there is no simplified analytical model that can reasonably estimate the final capacity of corroded reinforced concrete beams. In their analysis, the reduction in capacity for high corrosion grade beams was mainly due to the reduction in both steel reinforcement cross-section and corrosion resistance, the main cause of strength reduction in beams exposed to low corrosion grades was the loss of bond between steel and surrounding concrete. (Junaid and Aboutaha, 2016).

Campione et al. (2017) investigated the structural safety of RC beams exposed to corrosion by deriving moment curvature diagrams and moment-shear interaction diagrams. As a result, experimental results related to corrosion processes, steel rods, crack openings and bond formation due to corrosion formation were reviewed and an analytical model for cross-sectional analysis and shear strength prediction including the main effect of corrosion formation was developed and verified according to experimental data. Finally, they have also done a case study that includes moment-curvature diagrams and moment-shear interaction diagrams to illustrate the effects of different natural corrosion scenarios increasing over time on beam elements (Campione et al., 2017)

According to the study done by Stanish et al. (1999), the corrosion of reinforcing steel affects structural performance in two different ways: loss of steel and loss of steel-concrete bond. Therefore, the effects of corrosion products on the bond strength were investigated experimentally. This was done using accelerated corrosion management. As a result, the reduction in bond strength is proportional to the loss of steel mass, or alternatively, they are expressed by the reduction in bar diameter (Stanish et al., 1999).

The study conducted by Azad et al. (2016), 13 corroded and 4 non-corroded RC beams were examined in term of flexural strength capacity. In the scope of the study, accelerated corrosion method was applied for the corrosion of the beams. According to test results, the loss of shear strength of the beams is mostly associated with significant damage to the two factors, i.e., have revealed a reduction in the stirrup and concrete cover area is decreased due to corrosion of sadness corrosion cracking connected (Azad et al., 2016)

In the study conducted by Malumbela et al. (2009), previous studies conducted to investigate the effects of simultaneous load and steel corrosion on corrosion rates and behaviour of reinforced concrete structures were reviewed. The investigation showed contrasting results on the effects of loading on corrosion rate and corrosion crack widths. However, they have found that corrosion under load significantly increases sample deviations. (Malumbela et al., 2009)

Study conducted by Li et al. (2018) investigated the behaviour of RC beams under simultaneous loading and reinforcement corrosion experimentally. As a result, they found

that the corrosion of the supplements increased with continuous loading, but initially an increasing rate followed by a decreasing rate. They found that higher loading levels and longer corrosion time lead to brittle fractures of reinforced concrete beams. Continuously increasing the load lengthens the longitudinal crack, but found that the crack does not extend the width. At the same time, they found that continuous loading and corrosion time were more important in terms of joint effects, reinforcement corrosion, failure mode, final loading capacity and deformation ability of concrete beams compared to the single effect of a factor. At a higher continuous loading level, the final loading capacity and deformation ability of the beams are significantly reduced by corrosion times. They also found that a lower loading structure increases the bending stiffness of reinforced concrete beams, but a higher loading level decreases (Li, et al., 2018).

Following paragraphs summarizes the studies on fibers found in the available literature.

A study conducted by Lee et al. (2014), structural nano-synthetic and steel fibers were used to reduce the amount of steel rebar distributed in prefabricated reinforced concrete composite elements. According to the test results, it was found that hybrid fiber reinforced cement composites provide the necessary conditions for replacing the general reinforcing bars according to the RILEM standard when the mixture contains 0.4% by volume nano-synthetic fibers and 20 kg / m³ steel fibers. Furthermore, the flexural behaviour of the composite element reinforced with such a hybrid fiber blend and steel reinforcement was evaluated; maximum load 30% greater than the intended final load and 3.5% greater than that of a steel fiber reinforced composite element (Lee et al., 2014).

The aim of the study of Imran et al. (2015) was to investigate the effects of macro-synthetic fibers on the strength and ductility of the columns. As a result, the addition of macro-synthetic fibers has been found to increase ductility and strength (Imran et al., 2015)

According to the study of Bonacci et al. (2000), they conducted an experimental study on the simulation of corrosion in seven large-scale RC columns and their repair using carbon fiber reinforced polymer plates. In addition, they used accelerated corrosion method in this working capacity. As a result, it was found that carbon fiber reinforced polymer repair greatly increased the strength of the repair element and delayed the corrosion rate after

repair. Moreover, the repaired column extensive repair after exposure to corrosion, loss of strength or toughness and ductility of no repairs element was found to result in only a slight decrease (Bonacci et al., 2000).

In the study conducted by Rose et al. (2009), the results of an experimental research on reinforcing corrosion damaged reinforced concrete beams with unidirectional fabric glass fiber reinforced polymer laminates are shown. As a result, it has been found that glass fiber reinforced polymer laminates have beneficial effects even in the corrosion-damaged stage. (Rose et al., 2009)

Amin et al. (2017) investigated the post-cracking behaviour of macro synthetic polypropylene fiber-reinforced concrete through a series of paired tests that directly measure tension by uniaxial stress tests and indirectly detecting prism bending and indirectly round panel tests. As a result, the authors found that the analytical model developed by the authors to determine the residual tensile strength of steel fibers in prism bending tests were adapted to round panel tests and correlated well with the experimental data collected (Amin et al., 2017).

Al-Majidi et al. (2019) proposed a new reinforcement technique using additional high performance Fiber Reinforced Geopolymer Concrete layers and jackets reinforced with steel bars. The main objective of that technique was to improve the structural performance of the existing elements, as well as to improve the strength and corrosion resistance of the reinforcing layers. Reinforced concrete beams with reinforced concrete reinforcement were examined under standard and accelerated corrosion conditions. As a result, they achieved superior performance for fiber reinforced geopolymer reinforced concrete beams and improved performance of the interface between the additive layer and the first reinforced concrete beam (Al-Majidi et al., 2019).

In addition to the studies carried out on reinforced concrete beams and columns produced by using fiber, the relation of RC slabs produced by using fiber has been included in the literature.

Study Barros et al. (2015) showed that 1% volume of steel fibers bending collapse of slabs were converted to the ductility of the steel fibers and showed that contribute to the ductility of the floor (Barros et al., 2015).

Ju et al, (2015) investigated a semi-empirical model based on the prediction of tensile stresses generated by steel fibers around the punching cone. Critical shear crack theory, which is a semi-empirical method developed on the basis of the mechanism formed during punching, is one of the few model-based approaches that stand out in this field (Ju et al., 2015)

2.3 Developed empirical models for the prediction of strength capacity of corroded RC beams

According to an experimental study conducted by Azad et al. (2010), previous researchers have used small-scale reinforced concrete elements to ensure the accuracy of the test data. However, when the existing reinforced concrete building stock is examined, it is necessary to take full-scale attention into consideration during the design stage in the work to be done considering the size of the elements. In that study, small-scale RC members were revised and worked in full scale. A new experimental program was carried out using 48 beams with a width of 200 mm and a depth ranging from 215 to 315 mm, reinforced with tension bars of 16 and 18 mm in diameter. In the study done by Azad et al. (2010), 28 MPa concrete strength class was used in the model developed as a result of the study. Corrosion levels obtained in that study was based on Faraday's Law. Corrosion levels were varied from 0 to 12.76%. In the study done by Azad et al. (2010) the following Eq. (1a-1b) was develop to predict the flexural strength of corroded RC beams

$$\text{The residual flexural capacity } C_f = \frac{14.7}{D(I_{corr} T)^{0.15}} \leq 1.0 \quad (1a)$$

$$\text{Values of moment capacity } M_{res} = C_f \cdot M_{thc} \quad (1b)$$

In Eq. (1a-1b) the developed model by Azad et al. (2010) considers the corrosion at only tensile bars.

In Eq. (1a and 1b), D is a diameter of rebar in mm, I_{corr} represents corrosion current density in mA/cm² and T is a duration of corrosion in days, M_{thc} is theoretical values of the flexural capacity of corroded beam and C_f is correction factor.

Another experimental study done by Ahmed (2017) investigated the residual bending strength of RC beams subjected to reinforcement corrosion and to improve previous model. In that experimental study, 28 RC beams of 150 x 150 x 1100 mm dimensions were casted. Four of the RC beams were un-corroded and 24 of them were corroded using accelerated corrosion method. In addition, the compressive strength of the concrete using beam samples varies between 33 and 47 MPa. Later, the flexure test was performed on the corroded RC beams. According to the test results of the non-corroded and corroded beams, an experimental model was obtained to estimate the flexural strength of the beams considering the given corrosion current density, corrosion time and diameter of the reinforcing bars. In the study done by Ahmad (2017) the following Eq. (2a-2b-2c) was developed to predict the flexural strength of corroded RC beams.

The values of percentage residual flexural strength of corroded beam calculated as:

$$R = \frac{M_c}{M_{uc}} \times 100, \quad (2a)$$

The residual flexural strength an empirical model was set, as given by equation,

$$R = 100 - A(I_{corr} \cdot T)^m (D)^n, \quad (2b)$$

In Eq. (2) the developed model by Ahmad (2017) considers the ideal equation for the residual flexural strength of corroded RC beams is as follows:

$$R = 100 - 0.23(I_{corr} \cdot T)^{1.3} (D)^{0.5}, \quad (2c)$$

where, R is residual flexural strength of corroded beam, I_{corr} , T is degree of corrosion, D is diameter of rebar (mm), and A , m and n are empirical constants. Lastly, M_c and M_{uc} are corroded and un-corroded concrete beams moment capacity (Ahmad, 2017).

Another study conducted by Suffern et al. (2010) investigated how the stirrups in the concrete beams affect the structural performances. In the study, the dimensions of the

reinforced concrete beams were 350 mm deep, 125 mm wide and 1850 mm long. In the experimental study, the average compressive strength of the unsalted and salted concrete for 28 days was 40 and 32 MPa. The RC beams were tested in three-point bending under a simple supported range of 1500 mm. In that study, nine RC beam with stirrups were corroded by accelerated corrosion method and the corrosion damage level, and the shear span-to-depth ratio. As a result, corrosion RC beams have lower shear strength compared to un-corroded RC beams. Another result was the shear strength reduction of reinforced concrete beams up to 53%. In addition, another important result was found that the reduction in shear strength due to corrosion was greater at smaller shear depth ratios. In the experimental study, reinforced concrete elements were corroded controlled by using Faraday's Law. Then, a model was developed according to Faraday's Law by evaluating the actual mass losses.

An experimental study done by O'Flaherty et al. (2008) investigated effect of flexural strength corroded RC beams and to determine the detail parameters. In the experimental study, twelve RC beams of 100x150x910 mm were used. In the experimental study, the compressive strength of concrete used for RC beams is 40 N/mm². In addition to this experimental study, accelerated corrosion method was applied to RC beams and evaluated according to Faraday's Law. The corrosion rates used in this study ranged from 0.1 mA / cm² to 2 mA / cm². In the study done by O'Flaherty et al. (2008) the following Eq. (3) was developed to model, the residual tensile strength moment of corroded concrete beams is estimated.

$$M_{t(corr)} = \frac{M_c \alpha(Corr\%)}{100} + M_{t(0)}/\gamma_c, \quad (3)$$

where, $M_{t(corr)}$ is Moment of resistance of the corroded beam in the tensile zone, M_c is maximum moment of resistance of the concrete in the compression zone, $M_{t(0)}$ is moment of resistance of the control beam in the tensile zone, and γ_c is partial safety factor for the strength of concrete (O'Flaherty et al., 2008).

2.4 Corrosion levels based on corrosion on cracks

In this thesis, the obtained corrosion levels were actual corrosion levels. Moreover, the developed models in this thesis require to know actual corrosion levels. However, in the case

of non-destructive methods; in other word, rather than extracting the reinforcement bars, the corrosion levels can be also obtained based on non-destructive methods (based on actual corrosion crack widths). Therefore, previously developed crack models were also explained in the following paragraph to be used for the developed model in this thesis as a non-destructive method.

An experimental study done by El Maaddawy et al. (2006) investigated the results of previous studies on the effects of corrosion and sustained loads on the structural performance of reinforced concrete beams. In the experimental study, nine RC beams of 152 x 254 x 3200 mm were used. In addition, the compressive strength of the concrete using beam samples varies between 40 and 41 MPa. Within the scope of the study, one RC beam was subjected to corrosion and the other eight RC beams were subjected to accelerated corrosion method for 310 days. Accordingly, corrosion levels ranged from 4.12 to 25.04%. Later, the four RC beams are corroded under the sustained load beam, corresponding to about 60% of the yield load of the virgin beam. The other four remaining RC beams were kept un-loaded during the corrosion exposure. According to the test results of the research, the presence of a sustained load and associated flexural cracks during the exposure to corrosion significantly reduced the duration of corrosion cracking and slightly increased the corrosion crack width. Flexural cracks during exposure to corrosion reduced the steel mass loss ratio in proportion to the beam strength. However, as the strength of the reinforced concrete beams decreased, the effect of flexural cracks was observed depending on the time. In the study done by El Maaddawy (2006) the following Eq. (4) was developed to determine the crack widths.

$$W_{min} = 0.05m_t$$

$$W_{avg} = 0.08m_t$$

$$W_{max} = 0.11m_t \tag{4}$$

where, w_{min} is defined as the minimum measured corrosion crack width, w_{avg} is defined as the average measured corrosion crack width, and w_{max} is defined as the maximum measured corrosion crack width. Finally, m_t is the percentage of the steel mass loss due to corrosion (El Maaddawy, 2006).

The aim of a study conducted by Vidal et al. (2004) was to investigate the relationship between the reinforcement corrosion distribution and the corrosion crack width. In that study, longitudinally reinforced 14 and 17 years old RC beams were investigated in the experimental direction. In that study, two reinforced concrete beams were used and the size of the reinforced concrete beams was 150x280x 3000 mm. In addition, the compressive strength of the concrete using beam samples were varied between 32 and 45 MPa. According to their experimental results, they compared the existing models that link the crack width and attack penetration. Accordingly, they developed a new model using the reinforcing cross-section loss parameter, stating that it partially predicted actual experimental data. In the study done by Vidal et al. (2004) the following Eq. (5) was developed to the empirical linear expression predicting crack propagation.

$$W = K(\Delta A_s - \Delta A_{s0}), \quad (5)$$

where, W is the crack width (mm), ΔA_s is the steel loss of cross-section in mm^2 , ΔA_{s0} is the expression of the local steel cross-section loss (mm^2) and K is the slope of the curve (Vidal et al., 2004).

2.5 Experimental studies on relationships between theoretical (Faraday's Law) and actual corrosion level

An experimental study done by Yalciner et al. (2012) investigated samples with compressive strength of 23 MPa and 51 MPa concrete were used at three different concrete cover depths as 15, 30 and 45mm. Yalciner et al. (2012) obtained corrosion values between 0% and 18.75% in his experimental study. Yalciner et al. proposed Eq. (6) to calculate the actual mass loss according to the Faraday's Law.

$$\text{Actual mass loss} = 0.703F - 0.15 \quad (6)$$

In Eq. (7) is the corrosion level was predicted based on Faraday's Law. An experimental study done by Auyeung et al. (2000) was a proposed a model to correlate the actual mass loss with Faraday's Law. The corrosion levels obtained used in that experimental study were between 0% and 5.91%. In that experimental study, Auyeung et al. (2000) proposed Eq. (7) to calculate the actual mass loss.

$$\text{Actual mass loss} = 0.4651xF - 0.5624 \quad (7)$$

Another experimental study was done by El Maaddawy et al. (2006) investigate the effect of fiber-reinforced polymer windings on corrosion activity and fracture of chloride contaminated concrete rollers. In the experimental study, the compressive strength of concrete used for RC beams is 35 N / mm^2 . Three different diameters (11.3, 16 and 19.5 mm) were placed on concrete cylinders with two different (102 mm and 204 mm) heights and obtained corrosion rates between 0 and 39.3%. El Maaddawy et al. (2006) propped Eq. (8).

$$\text{Actual mass loss} = 0.44F \quad (8)$$

An experimental study done by Paul et al. (2016) investigated correlation between corrosion levels based on Faraday's Law and actual corrosion levels. In that study, two different concrete compressive strengths (28 and 26 MPa) were used. The following Eq. (9) was proposed by Paul et al. (2016) to predict the actual corrosion levels based on Faraday's Law.

$$\text{Actual mass loss} = 1.0939F - 8.2744 \quad (9)$$

The samples used in all of the models obtained from the experimental studies presented above were small-scale in size. Therefore, it is difficult to estimate the actual mass loss values obtained from accelerated corrosion method to be applied in full-scale reinforced concrete element.

According to Apostolopoulos et al. (2006), in order to simulate natural abrasion in the study made by salt spray sprayed in an experimental study aimed at evaluating the mechanical behaviour of the reinforcing bars. In the sample observed a mass loss in the samples in parallel with the corrosion exposure time. In addition, it indicates that the tensile strength and tensile ductility value shows a significant decrease with increasing corrosion rate. To calculate the reduction in diameter due to the increased rate after the corrosion tests Eq. (10).

$$d_r = d\sqrt{1 - a} \quad (10)$$

In the given equation, the d_r final diameter d and a are the first diameter and percentage of corrosion rate, respectively.

2.6 Fundamental

2.6.1 Reinforced concrete

Concrete is a building material obtained from the mixing of sand, gravel, cement, and water. The tensile strength of this homogeneous and inelastic material is very low compared to the compressive strength. Therefore, it is difficult and uneconomical to create structural systems with low tensile strength such as concrete.

The first solution that comes to mind is to give the element or system a form that will only create pressure in the sections, similar to the use of stone in ancient times. However, in many cases such construction geometries may not be functional and economical.

The second solution that comes to mind is that another material, which is placed in the concrete and has high tensile strength and ductility, meets the tensile stresses. This second solution is much more suitable for engineering. For this purpose, steel reinforcement is used to meet tensile stresses in concrete.

Composite material consisting of steel reinforcement and concrete is called reinforced concrete. In order for the steel reinforcement and concrete material to be reinforced, they must work together as a whole.

In other words, the reinforcement must be firmly clamped to the surrounding concrete mass so that the deformation of the reinforcement and the surrounding concrete does not differ. This phenomenon, which enables concrete and steel to work together, is called docking or adherence (Ersoy and Özcebe, 2004). The pH of fresh concrete is around 12.5-13. The high alkalinity in the concrete is provided by the calcium hydroxides resulting from the hydration of the C_3S and C_2S main components in the Portland cement. The concrete with high pH is a very good material that can protect the steel bars embedded in it against corrosion. With the water leaking into concrete, the pH in the concrete may be reduced cause of the salts in the water and carbonation. By decreasing the pH value of the concrete to 9-10, the protective oxide film on the steel is broken and it can't protect the steel in the concrete against corrosion (Erbil, 1996).

2.6.2 Fiber

The use of fiber as concrete admixture has been increasing in recent years in order to improve the structural behaviour of reinforced concrete structures (Banthia, 2010). Steel or synthetic fibers that allow the tensile stresses to be transported in cracked concrete increase the tensile and shrinkage strength of concrete significantly (Murathan and Karadavut, 2014).

2.6.2.1 Properties of polypropylene fibers

- Resistant to water, alkali and acids.
- Stainless.
- Resistant to abrasion.
- It is not affected by atmospheric gases, chemicals, mould and microorganisms.
- It adapts to the mixture and distributes properly.

2.6.2.2 Advantages of polypropylene fibers

- It prevents the plastic shrinkage which occurs with the loss of water in fresh concrete by increasing the tensile strength.
- Resistance to impact increases.
- It provides 5-10 times more strength than normal concrete in ACI (American Concrete Institute) standards tests.
- Concrete fiber does not form a micro-crack in concrete because it is three-dimensional.
- Prevents concrete dusting.
- The tendency to crack is low
- Minimizes concrete wear.
- Reduces rusting speed of equipment
- Prevents segregation in concrete and connects aggregates.
- Ductile concrete is obtained.

- Also no need for labour due to easy operation

There are many types of fibers used, but the most commonly used are steel, glass, polypropylene and carbon fibers. Fibrous concrete generally exhibits very good deformation and high strength compared to fiber-free concrete. The positive effect of fiber on concrete; fiber type (length / diameter ratio, fiber quantity), type, shape, size of aggregate, sample size and preparation depends on factors such as.

Concretes, a brittle material, have weak properties in terms of tensile strength, fatigue strength, abrasion resistance and post-crack load carrying capacity. Significant improvements in these properties of concrete have been achieved with the incorporation of fibers into concrete (Ünal et al., 2013; Yıldırım et al., 2015). Fiber additive also makes significant contributions to the shear strength of reinforced concrete elements (Dinh et al., 2014).

In another study by Tezel (2010), the effects of steel and polypropylene fiber additive on workability and mechanical behaviour in self-compacting concrete were investigated. As a result of the experimental research, it was stated that there should be an optimum fiber additive, otherwise the excess fiber additive would lead to segregation. In addition, it was observed that fiber additive reduced workability, did not have a significant effect on modulus of elasticity but increased compressive strength (Tezel, 2010)

According to the experimental study conducted by Furlan and Hanai (1997), the shear strength and bending tensile strength of reinforced concrete beams having different volumetric polypropylene and steel fiber ratio were investigated. It has been found that polypropylene and steel fiber additive increase shear strength and increase ductility considerably (Furlan and Hanai, 1997).

In the study performed by Al-lami (2015), the effect of fibers on the behaviour and mechanical properties of reinforced concrete beams produced by adding polypropylene and steel fibers was investigated. As a result of the experiment, it has been observed that fiber additive increases the shear strength capacity of the beams and polypropylene additive at the

rate of 1% increases the tensile strength of the bending, which causes cracking by creating a bridge between micro cracks (Al-lami, 2015).

According to the study conducted by Sahoo et al. (2015), where the effects of polypropylene and steel fiber additive on bending tensile behaviour were observed, the effect of fiber additive on the behaviour of reinforced concrete beams under monotonic load was investigated. It was observed that the use of 1% steel and polypropylene fibers prevent crack development and increase bending strength. (Sahoo et al., 2015)

İpek et al.(2015), in the study comparing the mechanical properties of steel fiber and polypropylene fiber concretes, it was stated that the use of polypropylene fibers would be more appropriate where steel fibers contribute more to the mechanical properties of concrete than polypropylene fibers, but where the corrosion risk is high (İpek et al., 2015).

2.6.3 Corrosion

In existing reinforced concrete structures, reinforcement corrosion, strength, and adherence losses caused by the major risk factors for earthquake safety are observed in the press. Corrosion occurs in reinforced concrete structures due to various reasons and significant damage to the elements occurs. Over time, these damages reach significant levels and make expensive measures to be taken. Therefore, it is important to identify such damage as early as possible and to take precautions (Celep and Kumbasar, 2004).

Corrosion is the name given to the physical and chemical events occurring in metal elements. One of the most common causes of corrosion in the reinforced concrete element is the first of atmospheric corrosion penetration for the reinforced concrete element is to reduce the alkalinity of the environment. A second reason is the regional loss of section due to the presence of chlorides (Çakır, 1994).

The progress of the corrosion process adversely affects the performance level of the reinforced concrete structural element. Although the mechanical properties of the reinforcement change due to the corrosion of the reinforcement, the first volume of the reinforced concrete reinforcement, which has lost the cross section, increases by 2-4 percent compared to the final volume and causes the concrete to crack (Bažant, 1979).

The existing reinforced concrete structures in our country are highly affected by corrosion due to the low concrete strength frequently encountered. Moreover, Turkey's earthquake line in take place and not configured well the existing building stock, engineering services never seen, to be composed of the structure been built with the old methods, the importance of significantly damaging situation to the structural elements such as corrosion is further increased.

Considering the loss in the cross-sectional area, which will only occur as a result of corrosion, many parameters that are caused by corrosion have been neglected. Moreover, it is complex to model the response of a concrete structure exposed to corrosion.

It is known that the most common types of corrosion in reinforced concrete structures are generally pitting corrosion caused by chlorine and uniform corrosion caused by carbonation (Tuutti, 1982). When observing the cavities in the reinforcement due to corrosion, although the cavities are small in shape, they may have a larger and diffuse gap inside. Corrosion products are formed in the reinforcement due to corrosion. As a result of the increase in the volume caused by corrosion products, the stresses in the concrete around the reinforcement lead to the formation of cracks in the concrete after the tensile strength of the concrete is suspended. As a result of cracks, the adherence between reinforcement and concrete weakens. In addition, section loss caused by cavitation on the reinforcement surface adversely affects the tensile and deformation capacity of the reinforcement.

Total Flexural strength capacity of the corroded reinforced concrete beam; crack width, mechanical properties of concrete and reinforcement and bond slip relationship. All these parameters need to be taken into account in order to make an accurate assessment. On-site evaluation of a corroded structure with all these parameters is not practical. In addition, it is not easy to estimate corrosion levels and types (homogeneous and regional) of each reinforcement in existing structures.

2.6.4 Relationship between corrosion and steel bars

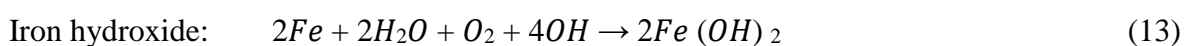
Corrosion materials in the nature of the most stable state in the event of the transition to oxide (Baradan, Yazici and Un, 2002). Most metals found in nature are not stable in the form of elements. They try to return to the old compound states in nature by giving back the energy

they carry on in a suitable environment. Figure 2.1 shows the corroded reinforced concrete beam. Corrosion reactions always result in a reduction in free energy. The susceptibility of metals to corrosion is directly related to this free energy exchange.



Figure 2.1: RC slabs without bond strength (Lefke high school).

The steel used in the existing reinforced concrete structures is damaged by atmospheric and aqueous effects in plain form. In a reinforced concrete building element, it can partially protect itself against the effects of corrosion due to the basic properties of the surrounding concrete. Corrosion of steel in aqueous media is an electrochemical event. There are some conditions for this to happen, otherwise the corrosion stops. In order to continue the process; anodic reactions, cathodic reactions and ion and electron exchange between these reactions.



The electrical resistance of the concrete and the current ion content directly affect the steel reinforcement corrosion. The resistance of concrete decreases corrosion and the ion ratio increases corrosion. Environmental factors affecting the formation of corrosion can be described in two main categories. The first one is carbonization and the other one is chloride attack.

In a reinforced concrete structural member, carbonation has a structure starting from the outermost fiber of the concrete layer to the inner parts of the sample. The mechanism of formation is that carbon dioxide in the atmosphere reacts with cement in an aqueous environment to form calcium hydroxide product. Basically, the formation of carbonation requires moist medium carbon dioxide and calcium hydroxide. The rapid carbonation rate on the surface slows down as it progresses to the interior of the sample (Baradan et al. 2002). As a result of the carbonation, the reinforcement becomes open to the atmosphere and the corrosion process will be started. Carbonation equation is given in Equation 14.



In the given equation, Ca(OH)_2 formed in the concrete combines with CO_2 in the atmosphere to form CaCO_3 . The pH level drops as a result of this event. The most harmful event occurring in the reinforcement is triggered by chloride ions. The protective film layer on the reinforcement is degraded by the presence of chloride ions. The interaction of chloride ions with the reinforcement increases the ion transfer between the anode and cathode. Chloride ions, which reduce the pH of the medium, increase the acidic value. Corrosion mechanism due to the continuous presence of iron ions and hydroxide ions in the chloride reaction continues. Equation 15 shows the chloride reaction.



The most common form of chloride ions penetration into the reinforcement is that it penetrates through the cracks in the concrete and reaches the reinforcement. Chloride content in concrete mixture is controlled according to TS EN 206-1 standards. (Baradan et al., 2003)

2.6.5 Types of Corrosion

Corrosion process generally depends on the distribution of anodes and cathodes. Changes in the physical structure of the metals due to corrosion are different. The main corrosion types are uniform, crack, galvanic and pitting corrosion.

Uniform corrosion is a type of corrosion that occurs evenly across the reinforcement surface. Corrosion speed is equal at every point of the reinforcement as a result of the same speed at each point of the reinforcement. In damaged structures, metal in direct contact with the atmosphere is often exposed to this type of corrosion. The least harmful type of corrosion. Because the metal can be used for a long time without perforation and breakage (Onaran, 2009).

Another type of corrosion is pitting corrosion. Formation usually occurs when cavities and holes occur in the reinforcement. The pit takes different names according to the state of the shape formed corrosion. In general, the occurrence of pitting corrosion is caused by the introduction of chloride (Gulikers, 2005).

Galvanic corrosion is the type of corrosion seen by the appropriate electrolyte effect of two different types of metal. In this way, the anodic of metals causes the other to corrode.

The type of corrosion occurring in the crack formed on the outer surface of the metal is called crack corrosion. The main cause of crack corrosion is the difference in oxygen density of the cracked metal on the inner and outer surfaces.

2.6.6 Effects of Corrosion

Corrosion in reinforced concrete reinforcement has two main negative effects for the construction sector. The first of these causes serious damages to the economy of the countries by giving results ranging from the completion of the service life of the structure to the demolition of reinforced concrete structures. The other impact is structural safety, which is more important than the impact of corrosion on the economy, and plays an important role for reinforced concrete buildings in earthquakes.

The cost of corrosion is important for the construction industry. However, cost is just an issue. Safety is the most important issue. As the reinforcement wears out, there is cracking,

pouring of concrete, reduction in reinforcement cross-section and bonding strength between concrete and reinforcing bars. As is known, reinforced concrete structures have a limited service life.

As long as the reinforcing bars are protected against corrosion, the service life of the structure can be increased. In terms of structural safety, it is important for corrosion to prevent the life of corroded concrete structures, to prevent premature damage during earthquakes or to decide on the correct repair and strengthening of corroded structures. (A.K. Choe, 2008).

With corrosion occurring, the decrease in the cross-sectional area of the reinforcement has negative effects such as the volumetric increase of the corrosion product and the decrease in the bonding force between the concrete and the reinforcement. With these results, bearing capacity, bending and torsional strength of reinforced concrete elements are reduced and targeted building performance is reduced.

2.6.7 Bond-Slip Relationships

In order for a structural element consisting of concrete and reinforcement to act as reinforced concrete, the reinforcement must be clamped to the concrete. The shear stresses between the steel bar and the concrete that provide the clamping are called adherence (Karakoç, 1985). Due to these bond forces between the reinforcement and concrete, the tension in the reinforcement increases or decreases in parallel with the moment change. Due to adherence, concrete-specific deformations such as shrinkage and creep also affect the reinforcement (Ersoy, 1985).

CHAPTER 3: METHODOLOGY AND MATERIALS

3.1 Introduction

This chapter in detail explains accelerated corrosion method and bending tests. Requirements to determine the earthquake indicators obtained from experimental test results were also explained in this chapter.

3.2 Experiment for Corroded Reinforced Concrete

In this study, plastic fibers dispersed in concrete were used at different corrosion levels. The test samples were divided into four main groups: A, B, C and D. Group A represents 0% corrosion level, while B, C and D groups represent 5, 7 and 9% corrosion levels, respectively. Each main group was then divided into three subgroups based on the volume (V_f) of 0, 0.5 and 1.5% of the poly-propylene fibers (P_f). As shown in Figure 3.1, the depth and width of a reinforced concrete beam produced are 400 and 250 mm, respectively, while the aperture length of the beam is 2500 mm. The concrete cover depth from the concrete surface to the middle of the transverse reinforcement bars was taken as 25 mm. Fabricated reinforcing bars were used for each sample. All reinforced concrete beams are designed to withstand the beam capacity of 118 kN.m according to the beam theory. Diameters of the lower tensile reinforcement bars are taken as 16 mm and the upper pressure reinforcement bars are taken as 12 mm. The transverse reinforcing bar spacing's are set to 130 mm in the beam clamping zone and 180 mm in the apertures.

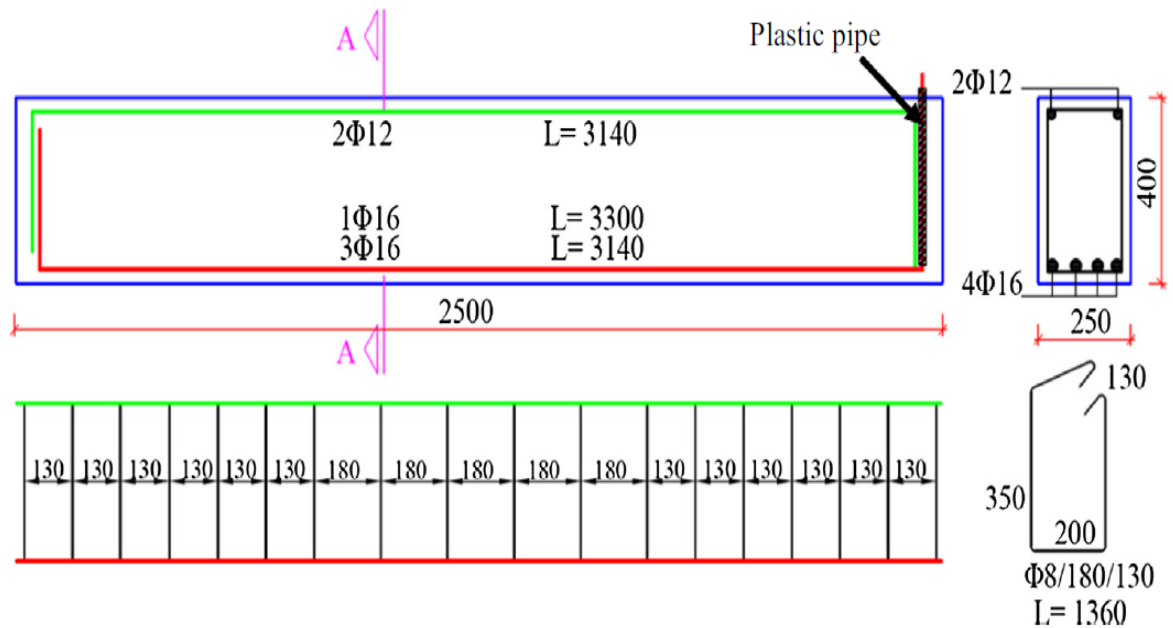


Figure 3. 1: Reinforcement configuration of beams.

3.3 The Construction of RC Beams

3.3.1 Formworks

The moulds, which were prepared for the placement of reinforced concrete beams used in experimental studies, were made of plywood material to obtain a smooth surface. Before the concrete beam samples were placed into the prepared plywood moulds, the plywood moulds were lubricated with oil in order to prevent damage to the concrete beam samples during mould removal. Figure 3.2-3.3 shows the moulds made ready for concrete pouring.

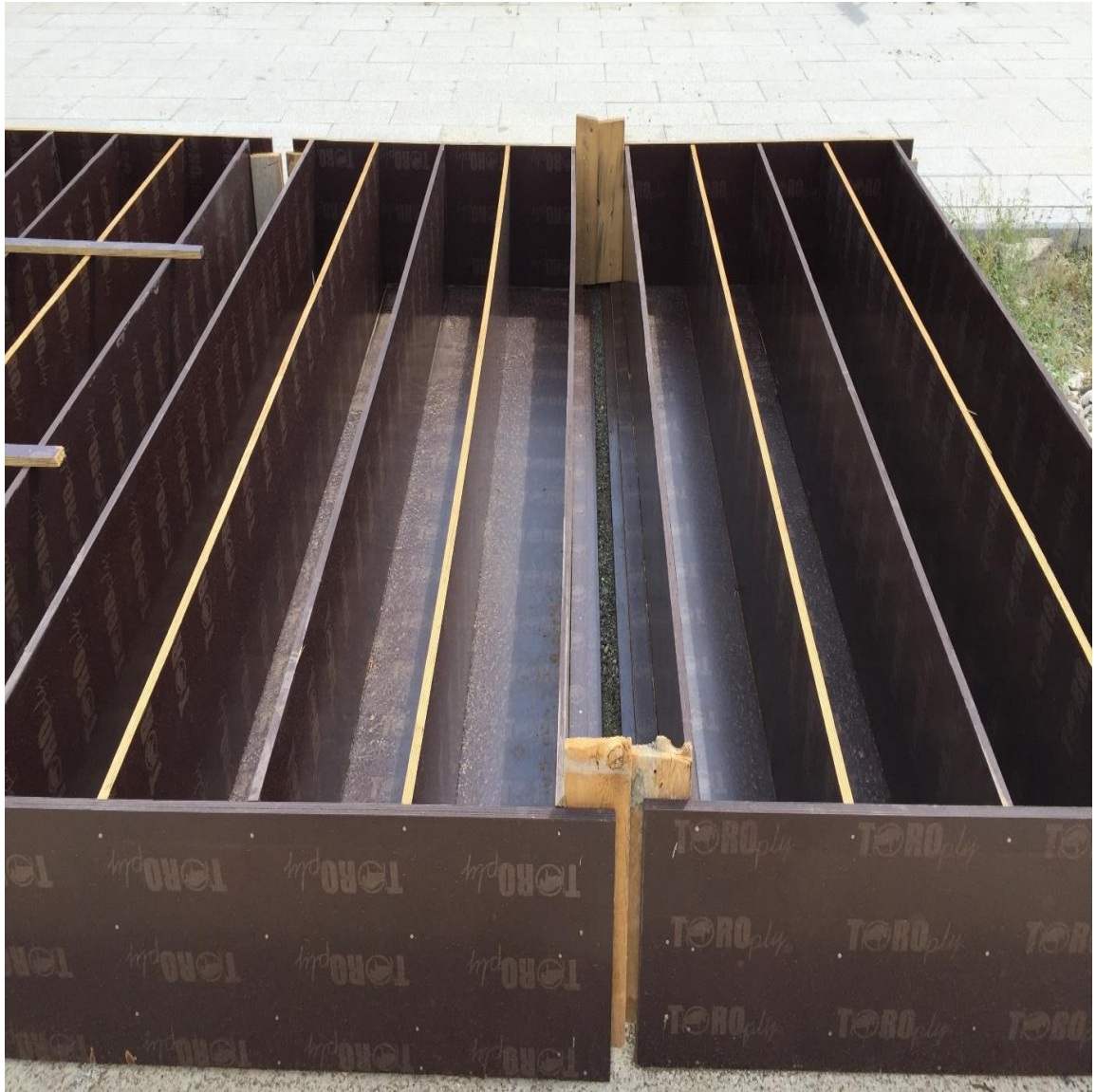


Figure 3. 2: Prepared plywood moulds.



Figure 3. 3: Strengthening of moulds.

3.3.2 Preparation of Reinforcement Bars

In this study, the recorded mechanical properties of the reinforcement bars were as follows: yield strength at 490 MPa, rupture strength at 600 MPa, and strain at yielding and rupture at 0.00245 and 0.0115, respectively. The calculated elastic modulus of the reinforcement bars was 2×10^5 MPa. The reinforcement of the reinforced concrete beams were cut according to the theoretically calculated values and the assembly operations were started. All kinds of elements that may affect the results of the experiment were kept at the minimum level and the reinforcement works of the reinforced concrete beams were carried out in the laboratory. Prior to the installation of the reinforcement, the longitudinal and stirrup reinforcement was cut to the same length according to the project and supplied from a single company.

All dust, rust and similar dirt products that affect the initial weights of the reinforcements were first mechanically cleaned in accordance with ASTM G1-03 (2003) standards as figure 3.4 show. After the cleaning process was completed, the initial weights of all transverse

(stirrups) and longitudinal (tensile) reinforcement were recorded using a two-point load cell with a precision of 0.01 g as figure 3.5 show.



Figure 3. 4: Cleaning phase of reinforcement.



Figure 3. 5: Weighting of reinforcement bars.

Figure 3.6 shows the details of the selected and connected reinforcement of the reinforced concrete beam before pouring the concrete. In Figure 3.6, S indicates the number of 18 transverse reinforcing bars, while T and C show the number of tensile and compression-reinforcing bars used for gravimetric test results.

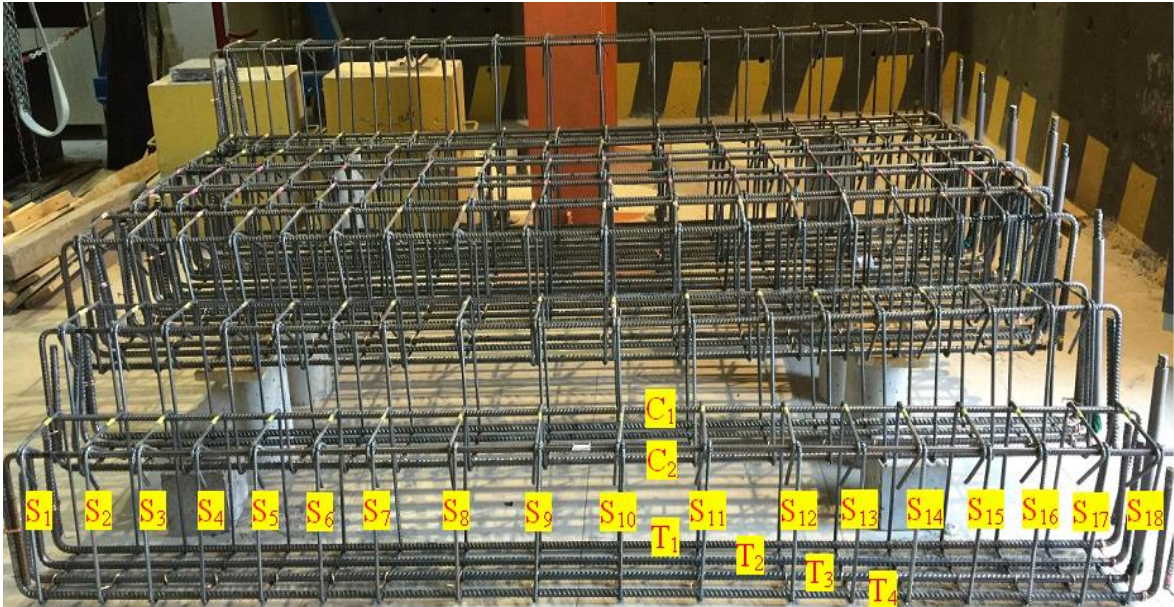


Figure 3. 6: Prepared reinforced concrete beams before concrete casting.

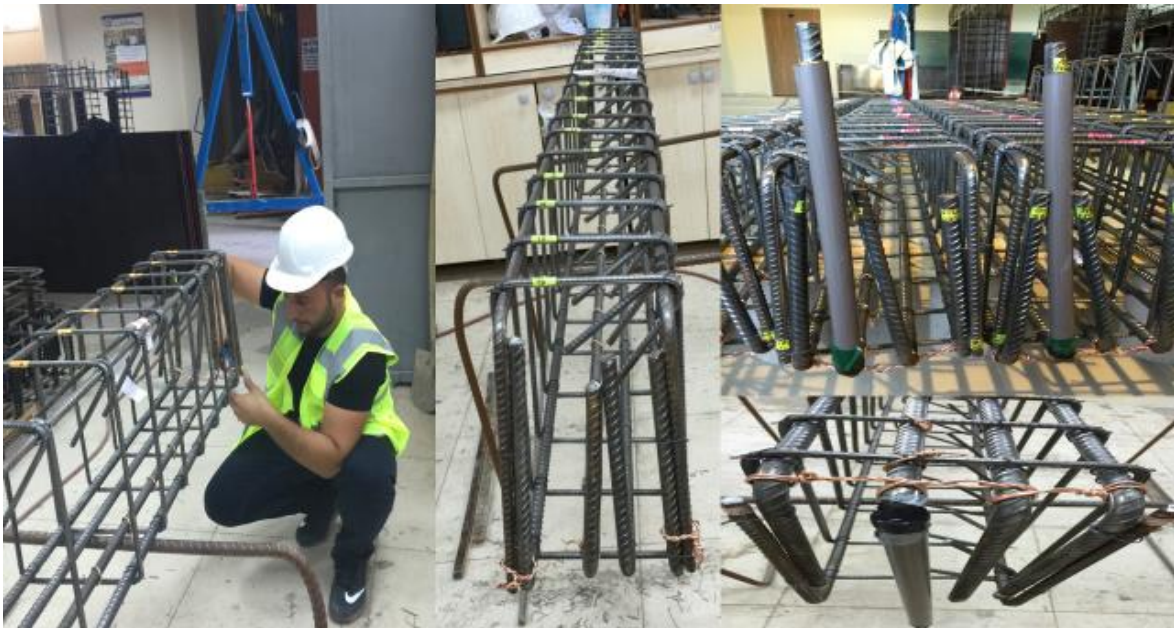


Figure 3. 7: Connection of copper wires to RC beams.

3.3.3 Utilization of Plastic Fibers

The plastic fibers used within the scope of the study were packaged in special bags for use in 1 m³ concrete. Since these packages were special packages which were water soluble, they were thrown into the concrete mixer. Polypropylene fibers were produced in a wide range of sizes. Its raw material was 100% polypropylene. In this study, the length of polypropylene fibers used varies between 54 mm and 60 mm and the density is 0.91 g / cm³. The diameters of the fibers used in the research varied between 0.44 mm and 0.48 mm. Thus, the calculated average aspect ratio was 124. Figure 3.8 shows the used fibers in this study.

When the concrete fibers were incorporated in concrete, fibers were dispersed well and no balling of fibers was observed. It increases the strength of the concrete and serves as a micro-crack defender by scattering three-dimensionally as a homogeneous body. After the concrete is poured, the concrete undergoes shrinkage as it loses moisture and during this shrinkage, the concrete starts to crack due to the tension in the concrete.

The addition of fibers to concrete increases the tensile capacity of concrete due to its distribution within the concrete and cuts the fiber front before the crack starts and a ductile more flexible concrete can be obtained. As fibers are used in concrete, it prevents concrete from segregation.



Figure 3. 8: Used polypropylene fibers.

Within the scope of the study, plastic fibers were homogeneously added into the mixer. Figure 3.8 shows the mixture of fibers with concrete.



Figure 3. 9: Homogeneously addition of fibers into concrete mixer.

3.3.4 Mix Design

In the scope of this study, ready mixed concrete was used. The Portland Cement (CEM I 42.5 N) type was used. No any admixtures was used. After three months of curing, the calculated concrete compressive strength was 30 MPa based on cubic tests. The ultimate strain for the concrete was assumed to be as 0.003.

Grouped amounts of fibers were gradually added into the concrete mixers before pouring the concrete. In this study, mechanical properties of concrete (i.e., compressive and splitting tests) with fibers as a function of corrosion levels were not tested. Further studies are required by considering the mechanical properties of corroded samples with additive materials to be used for analytical analyses.

The amounts of concrete used in ready-mixed concrete are as follows: Cement (CEM 1 42.5 R) was 280 kg/m^3 , w/c ratio was 0.60, total fine aggregate was 33 %, total coarse aggregate was 66 % and total amount of material: 2340 kg/m^3 . Material sieve analysis results are shown in Figures 3.10-3.12.

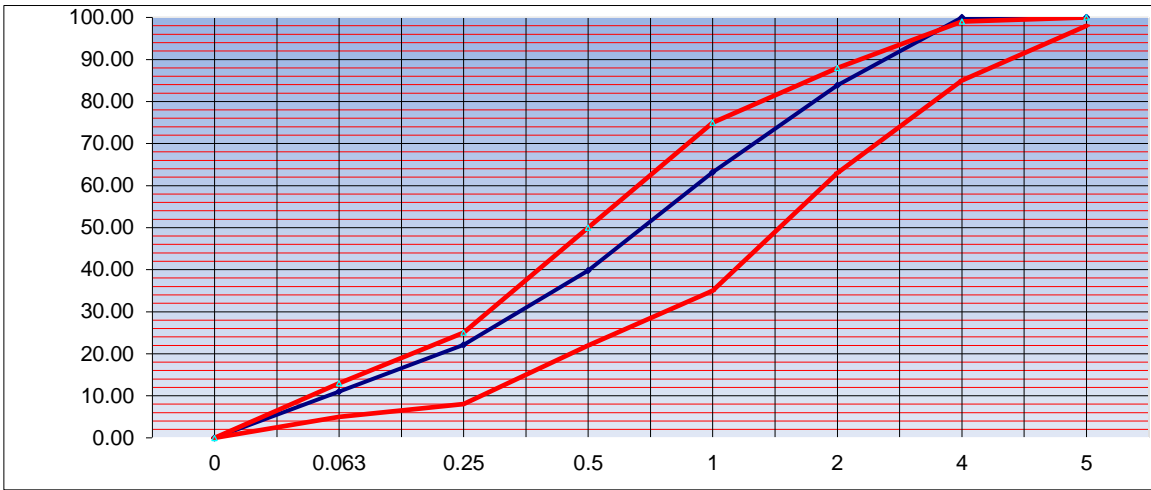


Figure 3.100: Fine aggregate 0-5 mm

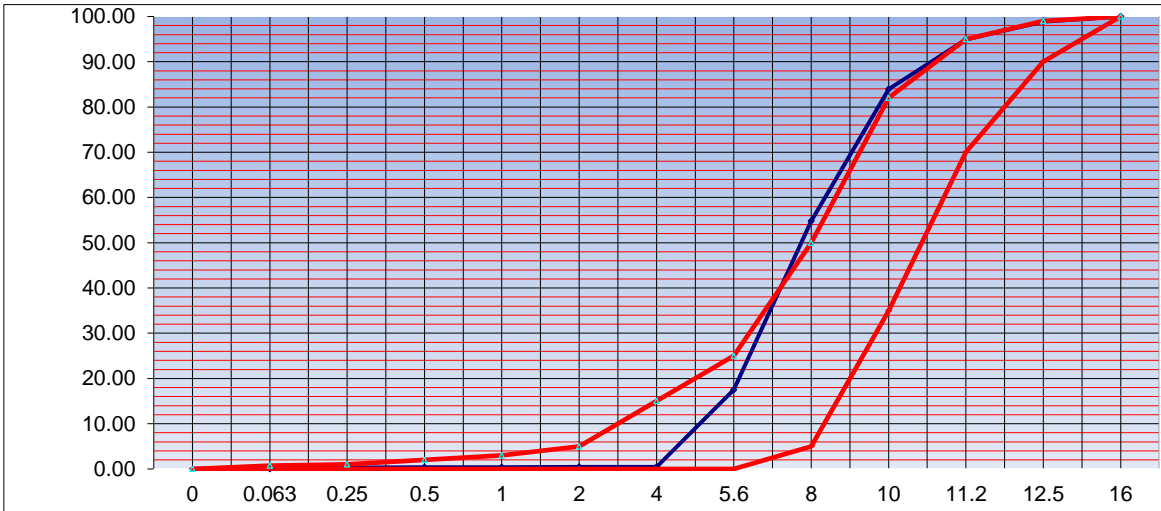


Figure 3.111: Coarse aggregate 5-12 mm

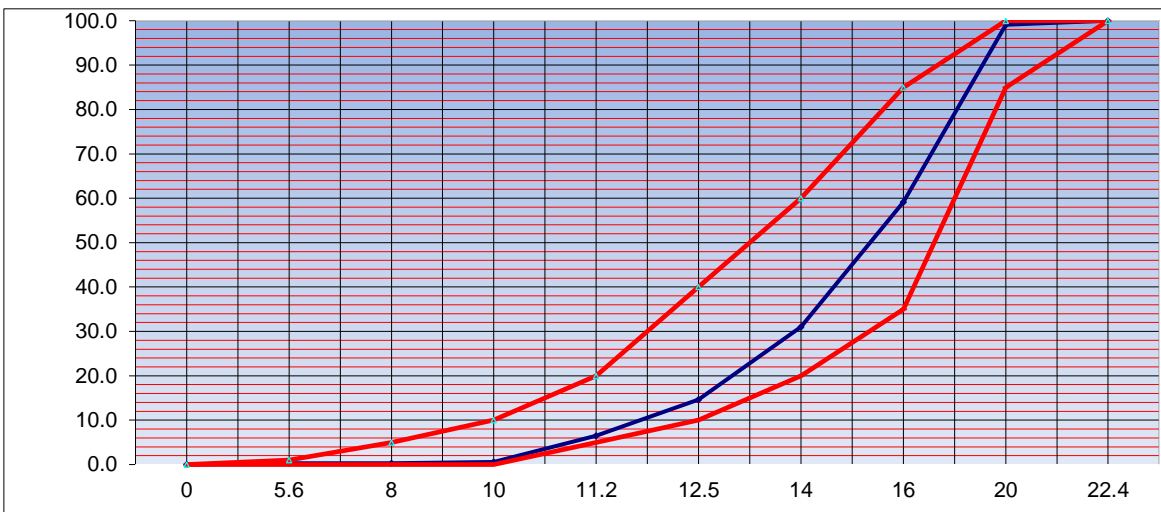


Figure 3.12: Coarse aggregate 12-22 mm

3.3.5 Workability of Concrete

Firstly, the concrete of RC beams without adding any polypropylene fibers were poured. After that 0.5 and 1.5% of polypropylene fibers were poured. The usage concrete vibration generator during concreting supports for the experimental studies were applied. Pouring works with removal air bubbles for maximum strength and consistency in concrete is shown in Fig. 3.14.



Figure 3. 12: Pouring and vibrating concrete process.

In the study, the vibrator was immersed vertically in the concrete and the immersion range was made not to exceed 45–50 cm depending on the radius of action of the vibrators.



Figure 3. 14: Poured concrete with fibers.

The distance between the concrete production site and the laboratory is approximately 5 minutes. There was no change in the effect of slump in concrete.

In this study, Slump test according to polypropylene fiber ratios was examined. Slump test results according to 0, 0.5 and 1.5% polypropylene fibers ratio are 23 cm, 20 cm, 16 cm respectively. The results obtained are as follows:

- With the increase in fiber content, significant reductions in the consistency of fresh concrete occur.
- Difficulties arise in the workability of concrete as a result of the incorporation of fiber into the concrete. This phenomenon has a first-degree effect on the mixing, placing and compacting of the concrete and is not related to the transport, separation and homogeneity of the concrete.

3.3.6 Curing of Concrete

The concrete once poured into the RC beam moulds remained there for 5 days then with the use of a crane were taken out of the moulds. The sample concrete RC beams were left outside

in natural conditions to gain durability. RC beams were kept for 3 months of curing. As shown in Fig. 3.15 the cubic samples were taken in order to obtain the compressive strength of concrete.



Figure 3. 13: Compacting the concrete in the cube moulds.

Water curing is the best method of curing as it satisfies all the requirements of curing, namely, promotion of hydration, elimination of shrinkage and absorption of heat of hydration. Therefore, RC beams shown in figure 3.16 were irrigated every 4 hours.

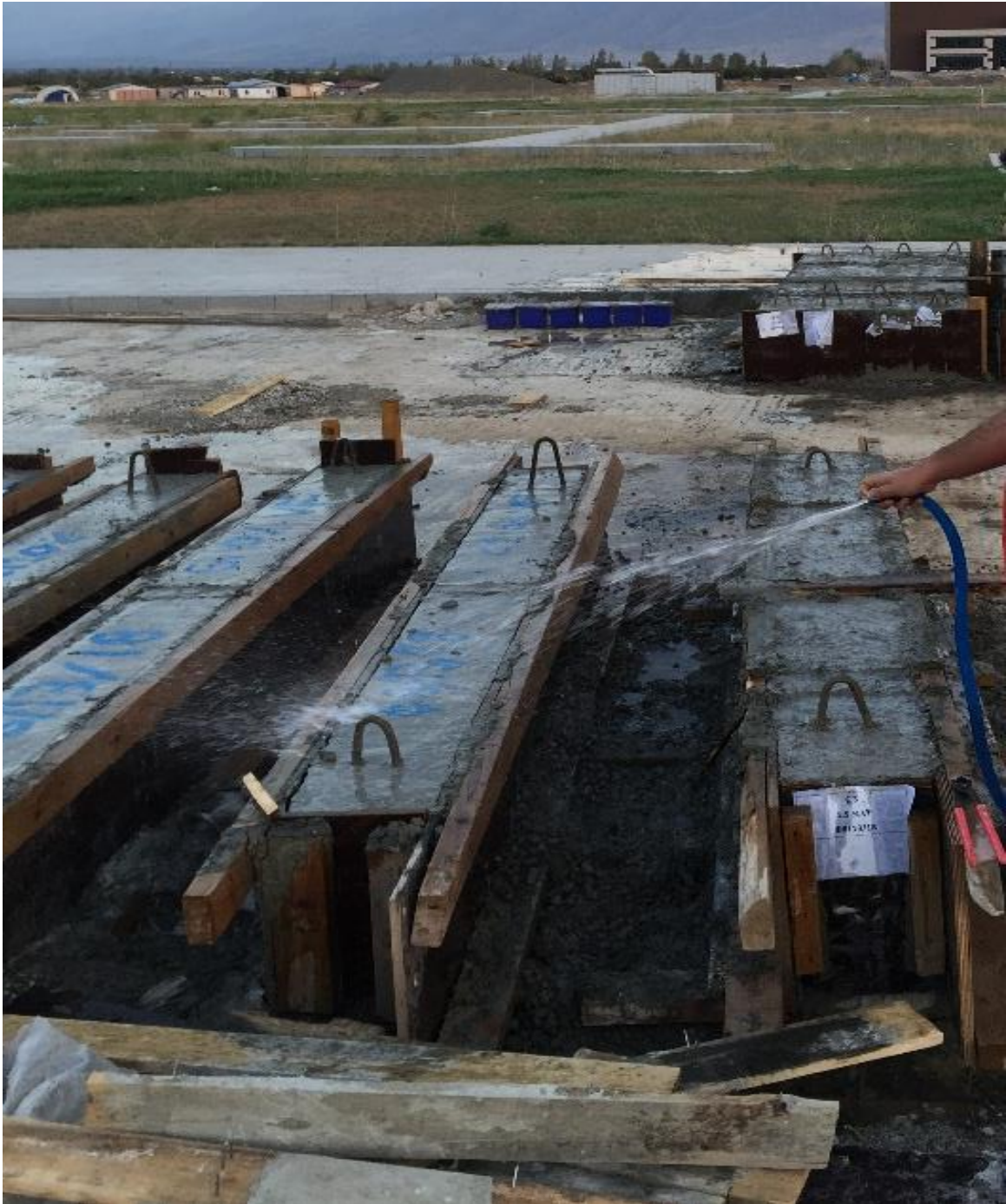


Figure 3. 14: Curing process of RC beams.



Figure 3. 15: Removal of the RC beams from the moulds.

3.4 Accelerated Corrosion Test

Since it would take years for noticeable corrosion to occur naturally, corrosion was accelerated for testing purposes. Faraday's Law was used to determine the amount of metal loss resulting from a constant current over a controlled time period. Following three months of curing, the specimens were subjected to an accelerated corrosion method. Fig. 3.18 illustrates the accelerated corrosion method setup.

The concrete pool was isolated with a plastic membrane to prevent any loss of current flow, and the copper plates that surrounded the concrete pool acted as a cathode. One of the bending reinforcement bars was extended by 160 mm beyond the concrete top face, and was planned to be used as an anode. The extended bars were surrounded with polyvinyl chloride pipes to prevent pitting corrosion on the concrete's top surface. As shown in Fig. 3.19, copper tie wires were used in the shear reinforcement bars to provide improved conductivity in the extended bending reinforcement bar.

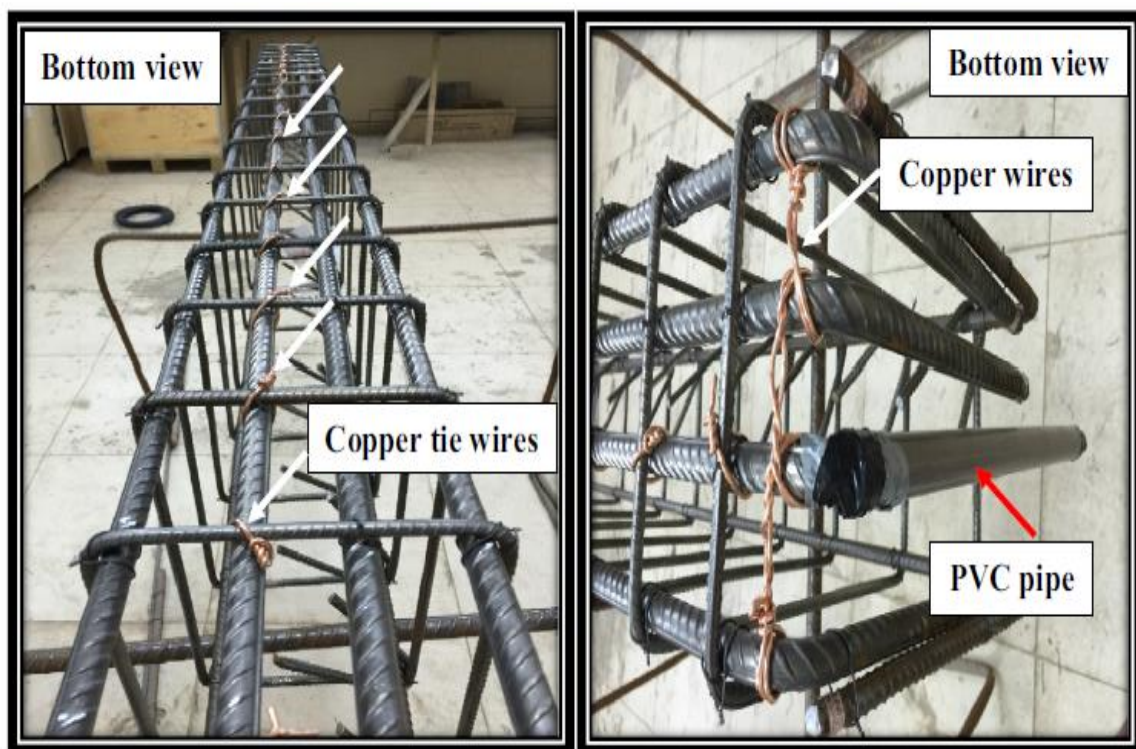


Figure 3.17: Copper wires used for transverse and longitudinal bars.

An adjustable, direct current power supply at a rated voltage of 60 V and a rated current within the range of 0–10 A was used. In order to shorten the corrosion process, 3.5% sodium chloride by the mass of water was added to the corrosion pool. Voltmeters were connected to each specimen to record the current at one-minute intervals, in order to monitor and achieve the designed corrosion levels. An example of a recorded current-time is given in Appendix A. The time required for achieving the estimated corrosion levels was calculated based on Faraday's Law for steel reinforcement in accordance to the following Eq. (16):

$$mass\ loss = \frac{t(s)*I(A)*55.847}{2x96487} \quad (16)$$

where t is the time and I is the current. In this case, Faraday's law was used only to monitor the designed corrosion levels. The actual corrosion level for each specimen was calculated based on Eq. (17):

$$C_L = \frac{W_i - W_f}{W_i} \times 100 \quad (17)$$

where W_i is the original mass of the reinforcement bars before corrosion and W_f is the mass of the reinforcement bars following removal of the corrosion products. The actual corrosion levels were calculated by crushing the concrete and extracting all reinforcement bars following the flexural strength tests, and reweighting each of the longitudinal and transverse reinforcement bars. A balance having two points of load cells was used to record the original reinforcement bar mass before pouring concrete, and the mass of each reinforcement bar after removing corrosion products was achieved by mechanical and chemical cleaning carried out according to the ASTM standards (ASTM, 2013).

3.5 Installation of Experimental Installation and Measurement Devices

Corrosive and control beam samples were planned to be subjected to displacement-controlled bending tests by applying the incremental load (monotonic charge) from a single point in order to evaluate the parameters declared within the scope of the study after accelerated corrosion processes.

A schematic view of the bending test to be performed on beam samples is shown in Fig. 3.20.

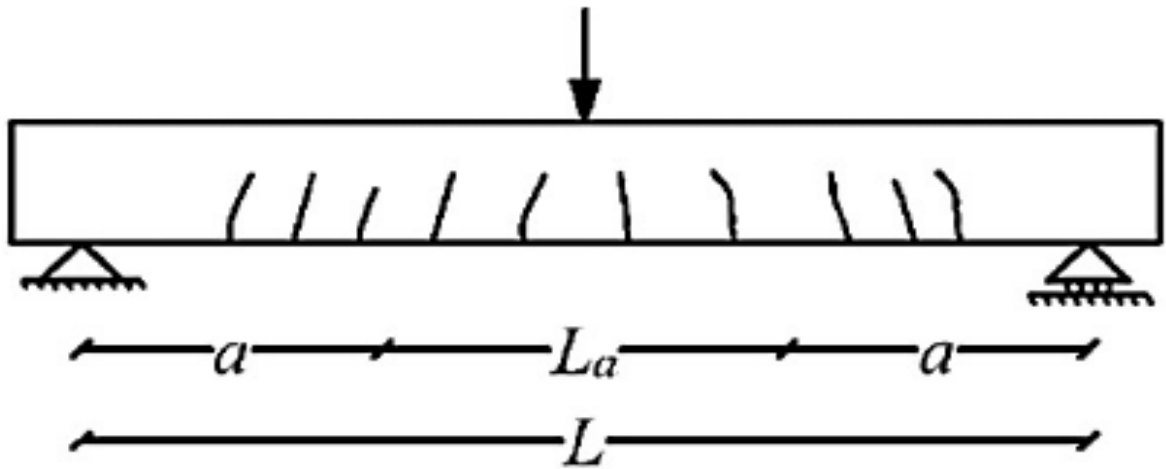


Figure 3. 18: Schematic view of bending test.

In all samples, the loading was increased incrementally until the failure mode. For this purpose, a hydraulic cylinder driven by a hydraulic jack with a capacity of 600 kN, suspended in the vertical direction, was used in the steel loading frame in the laboratory. Flexural strength tests were performed for each uncorroded and corroded RC beams after accelerated corrosion process. Test set up for the loading is shown in Fig. 3.21. RC beams were loaded as three points loading directly on the top compressive face of the beams. RC beams were loaded until failure mode. 600 kN capacity of a hydraulic jack was used that were suspended from a steel loading frame. Vertical displacement at the mid span of the beams was measured by a linear variable differential transformer (LVDT). Two LVDT were placed on each right and left side of the bottom and the top region of the beams to calculate the rotations. The critical locations and the length of the plastic hinges were taken based on Inel et al. (2006) and Park et al. (1975) respectively to install the rotation LVDT. Two strain gauges were installed on the bending reinforcement bars at the mid span of the beams. Strain gauges that could be damaged during aging process were bonded after the accelerated corrosion process. Small holes at the bottom of the RC beams were opened to bond the strain gauges to the bending reinforcement bars. Opened holes then repaired with epoxy concrete patch with a sand aggregate. The silica sand was mixed in with the epoxy to act as a filler. All instruments were connected to the data-acquisition unit to record their readings. Recorded strain values were used to calculate the bond stress by using equilibrium of forces in bar as given by Eq. (18) (Inel et al., 2006; Park et al., 1975).

$$u_b = \frac{f_s d_b}{4l_d} \quad (18)$$

Where u_b is the bond stress, f_s is the stress in the reinforcement bars, l_d is the development length of bar and d_b is the bar diameter. In order to calculate the bond stress after elastic region modest strain hardening was adopted for the current study according to the study done by Sezen et al. (2008). Recorded strain values were used to calculate the changes in the development length of the bar and to calculate slippage of reinforcement bars by integrating the strains along the development length: (Sezen et al., 2008)

$$slip = \int_0^{l_d+l'_d} \varepsilon(x) dx \quad (19)$$

In Eq. (19), $\varepsilon(x)$ is the strain along the length of the bending reinforcement bar; l_d is the development length of the bar in elastic region and l'_d is the development length of the bar in inelastic region.

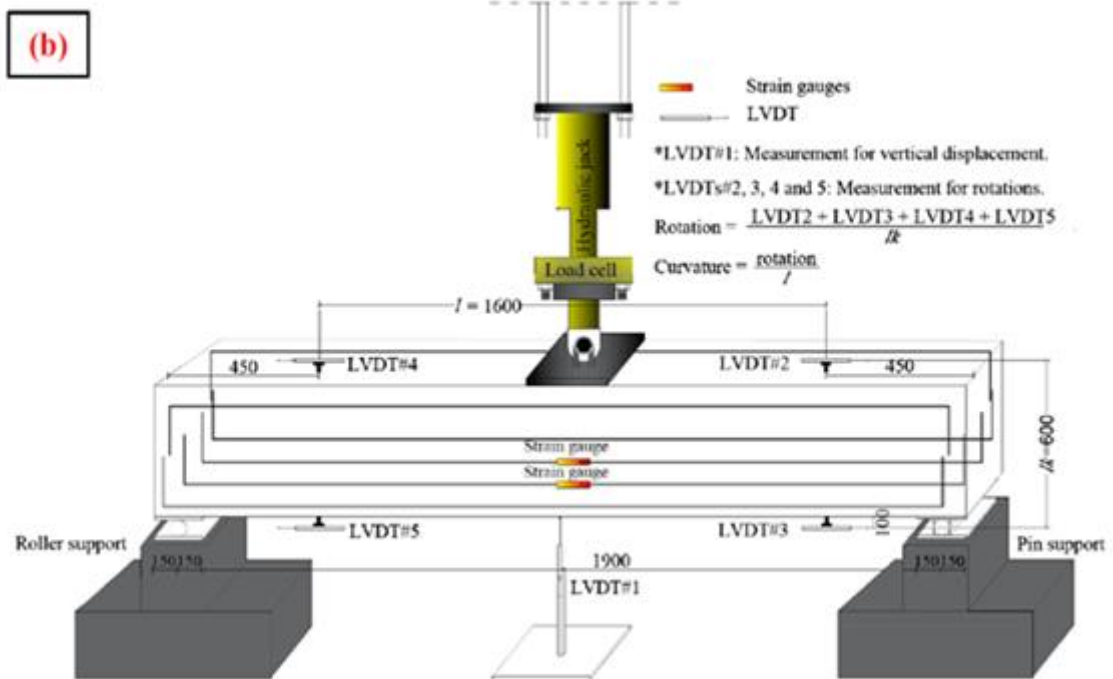
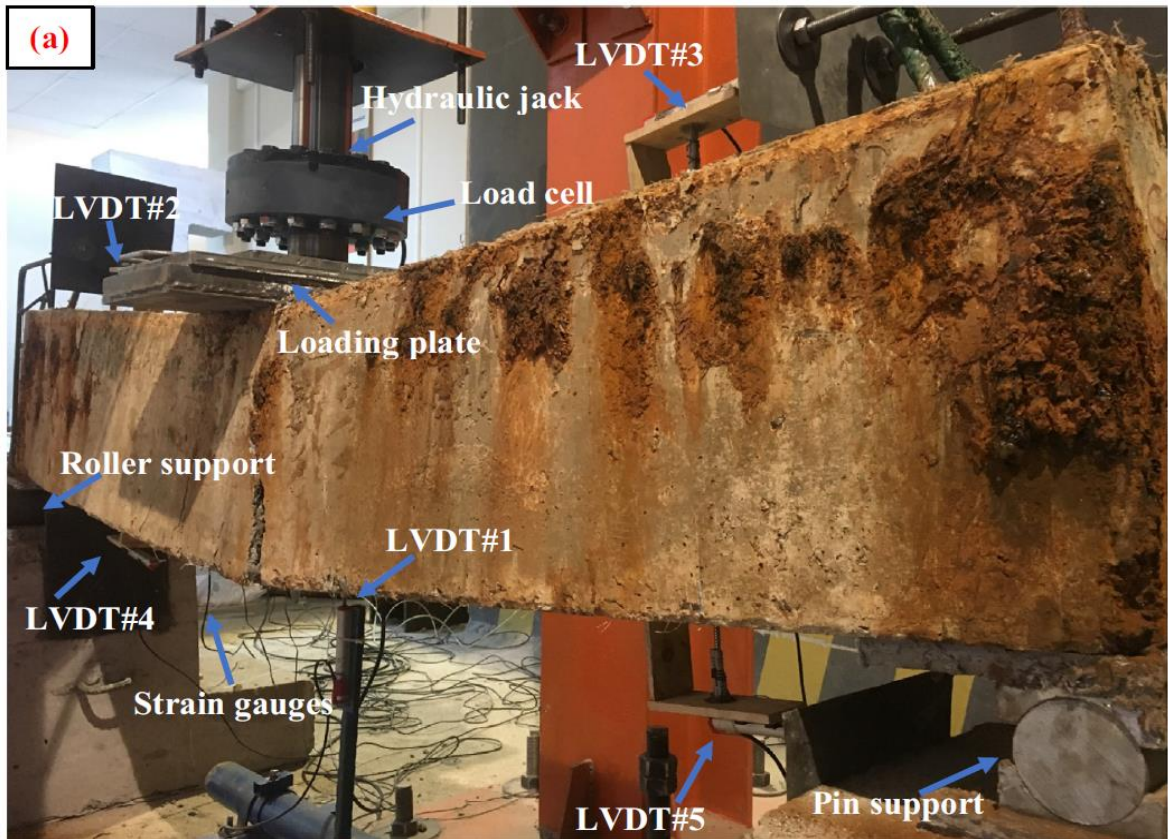


Figure 3. 19: Loading setup: (a) test setup, (b) schematic diagram.

In order to be able to correctly discuss the relationship between adherence of reinforcement bars, strain gauges were bonded on tensile reinforcements bars before loading tests and after accelerated corrosion method. Figure below shows the application of strain gauges.



Figure 3. 20: Application of strain gauges.

Before loading tests the concrete cover depths for the length and width of support regions of the corroded RC beams were removed. As showed in Fig. 3.23, also polypropylene fiber were burn with help of blowtorch. After that, the concrete cover depths of the support regions were repaired by same strength level of concrete.



Figure 3. 21: Cleaning and repairing of support.

CHAPTER 4: RESULTS AND DISCUSSION

4.1. Introduction

Explains the experimental tests results of uncorroded and corroded RC beams at different amount of fibers. Obtained actual corrosion levels and developed models; prediction of flexural strength of corroded RC beams and correction factor to Faraday's Law were explained in this chapter.

4.2. Achieved Corrosion Levels

Corroded all RC beams were broken to extract the reinforcement bars after flexural strength tests. Extracted all transverse and longitudinal bars were reweighted to calculate the actual corrosion levels based on Eq. (17). Fig. 4.1 shows some of the extracted reinforcement bars and cleaning process based on ASTM standards (ASTM, 2003).

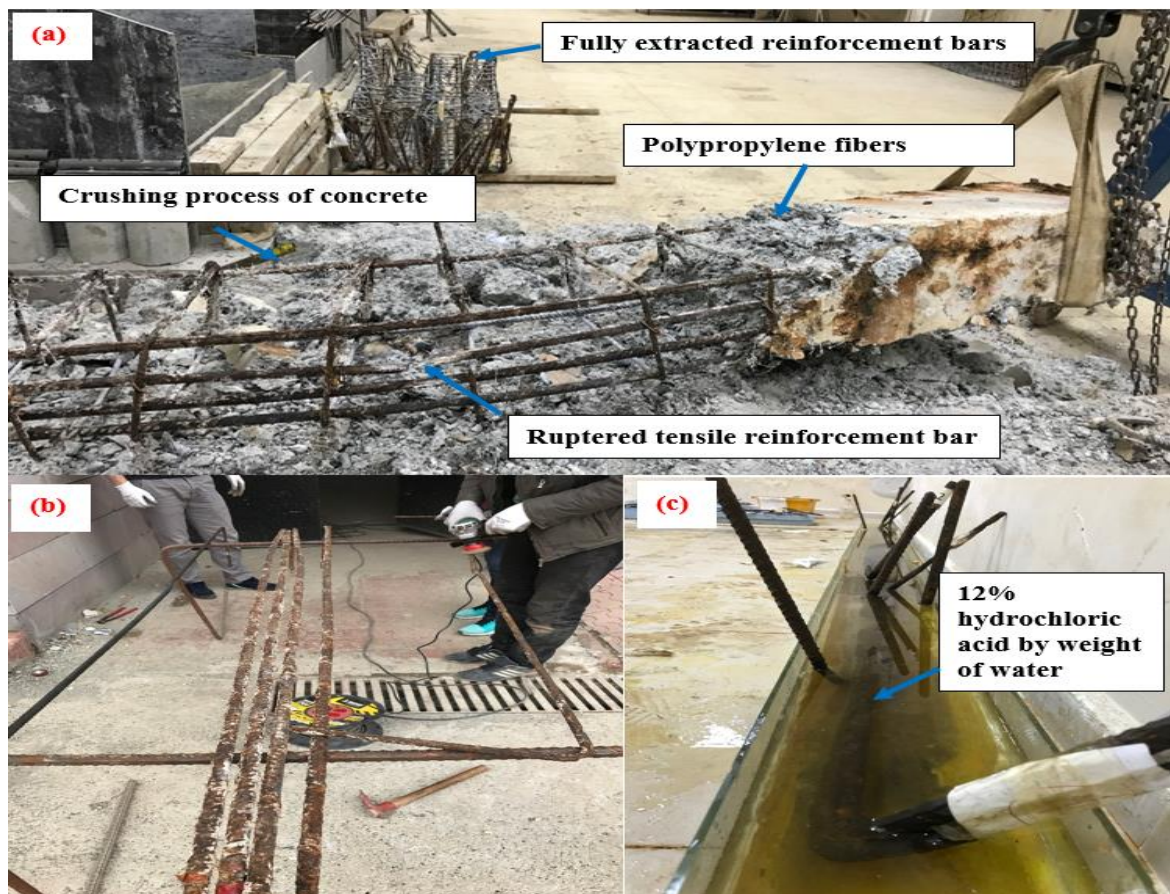


Figure 4. 1: Cleaning process: (a) extracted reinforcement bars, (b) mechanical cleaning, (c) chemical cleaning.

Since all reinforcement bars were reweighted, and there are currently very less studies are available for the fully extracted reinforcement bars, the distribution of corrosion levels for each specimen shown in Figs 4.2. Given distribution data of corrosion levels may be then used for the developing of other corrosion models for further studies especially for probabilistic corrosion models. Previously indicated problem for the assumed uniform corrosion levels after accelerated corrosion method can be also seen in Fig. 4.2. As shown in Fig. 4.2 accelerated corrosion method yields to have different corrosion levels based on the location of the bars because of the resistance of concrete. Corrosion levels of tensile reinforcement bars at the closer side of the concrete (T1 and T4) and transverse reinforcement bars at densification were generally more compared to inner tensile and transverse reinforcement bars at the mid span of the beams, respectively.

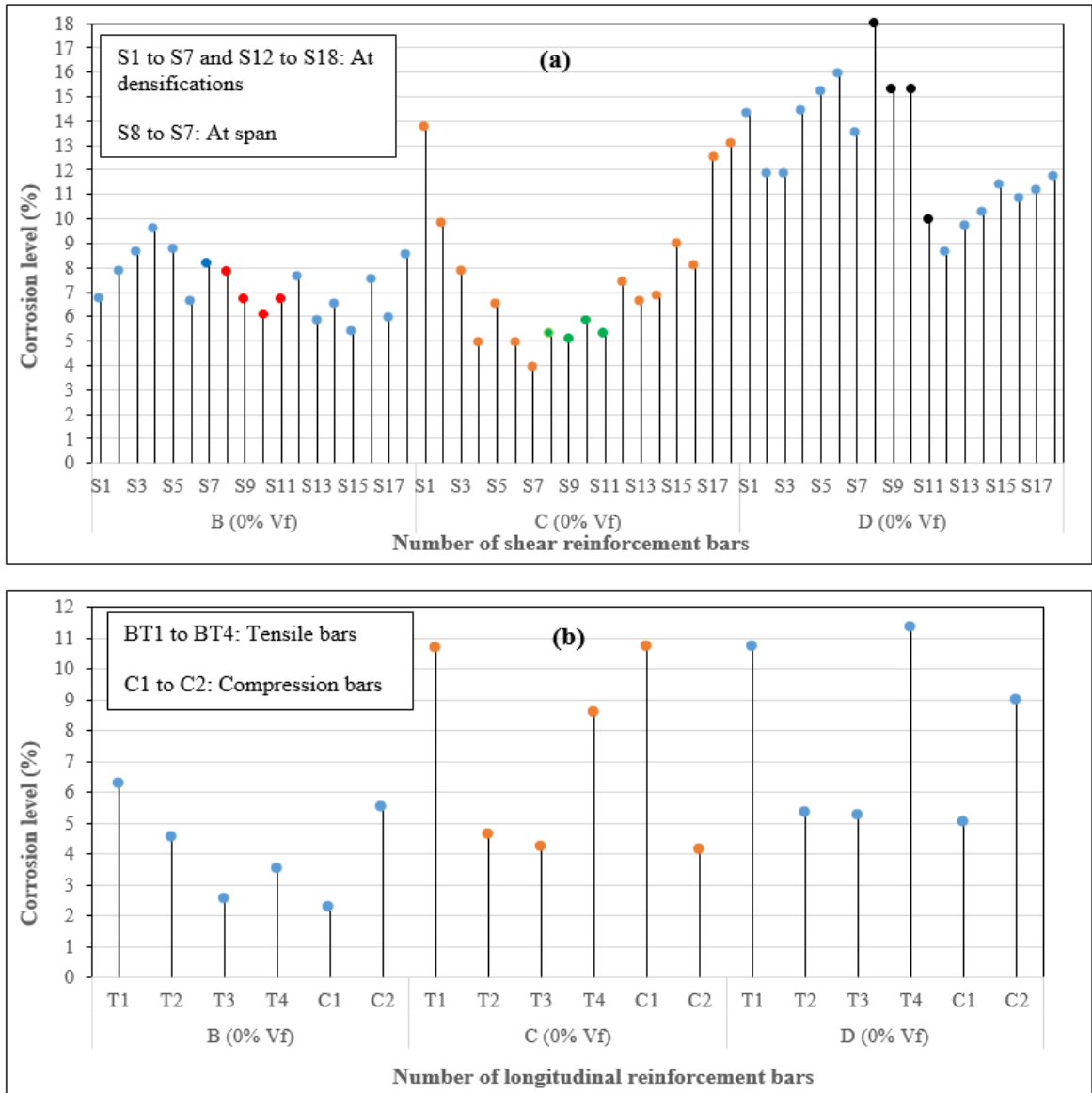


Figure 4. 2: Distribution of corrosion levels: (a) Shear reinforcement bars; (b) Longitudinal bars.

Table 1 shows the gravimetric tests results. In Table 1, S indicates the total weight of eighteen transverse reinforcement bars and L indicates the total weight of four tensile and two compression reinforcement bars. In Table 1, total achieved corrosion level of a beam by considering the all reinforcement bars turned into a single bar (S+L) and total achieved corrosion levels at shear and longitudinal bars were separately given in Table 1.

Table 1. Gravimetric test results

Specimen	V_c (%)	Sound Mass (g)		Faraday's mass loss (g)	Actual mass loss (g)		Faraday's corrosion level (%)	Achieved corrosion level (%)		Applied current-time (A.h)
		S	L	S+L	S	L	S+L	S	L	
Group B	0	9247	23461.5	3256.2	671.5	974.5	9.96	7.3	4.2	3125.4
		Total: 32708.5			Total: 1646			Total: 5		
	0.5	9063	23270.5	3155.6	663	1166	9.76	7.3	5	3028.8
		Total: 32333.5			Total: 1829			Total: 5.7		
	1.5	9121.5	23528.5	3307.8	813.5	1117	10.13	8.9	4.7	3174.9
		Total: 32650			Total: 1930.5			Total: 5.9		
Group C	0	9225.5	23234	4488.8	703	1648	13.83	7.6	7.1	4308.5
		Total: 32459.5			Total: 2351			Total: 7.2		
	0.5	9182	23467.5	4635.4	1150	1253.5	14.20	12.5	5.3	4449.2
		Total: 32649.5			Total: 2403.5			Total: 7.4		
	1.5	9172	23280	4609.6	1034.5	1678.5	14.20	11.3	7.2	4424.5
		Total: 32452			Total: 2713.0			Total: 8.4		
Group D	0	9054.5	23471.5	5214.3	1153.5	1844	16.03	12.7	7.9	5004.9
		Total: 32526			Total: 2997.5			Total: 9.2		
	0.5	9102.5	23430	5216.2	1294.5	1887.5	16.03	14.2	8.1	5006.6
		Total: 32532.5			Total: 3182			Total: 9.8		
	1.5	9061.5	23279.5	5232	1434	2005.5	16.18	15.8	8.6	5021.8
		Total: 32341			Total: 3439.5			Total: 10.6		

S: Eighteen shear reinforcement bars

L: Longitudinal bars (tensile + compression bars)

As shown in Table 1, there were differences between theoretically estimated corrosion levels based on Faraday's Law and calculated actual mass losses. Previous studies were also explained the reason of such occurred differences by using Faraday's Law for accelerated corrosion method. Theoretically calculated mass losses were greater than actual mass losses due to resistance of concrete against to current and effect of different concrete strength levels against to corrosion was detail explained by Yalciner et al. (2012). Yalciner et al. (2012) investigated the relationships between concrete resistivity and corrosion time for both the

low and high strength concrete levels. Trial tests of this experimental study showed that below the almost 5% of obtained corrosion levels based on Faraday's Law (FL) did not let the corrosion process begin for large scale of RC beams. Fig. 4.3 shows the comparisons between theoretically calculated mass loss (FL) and actual mass losses from obtained current experimental data and revisited previous developed models.

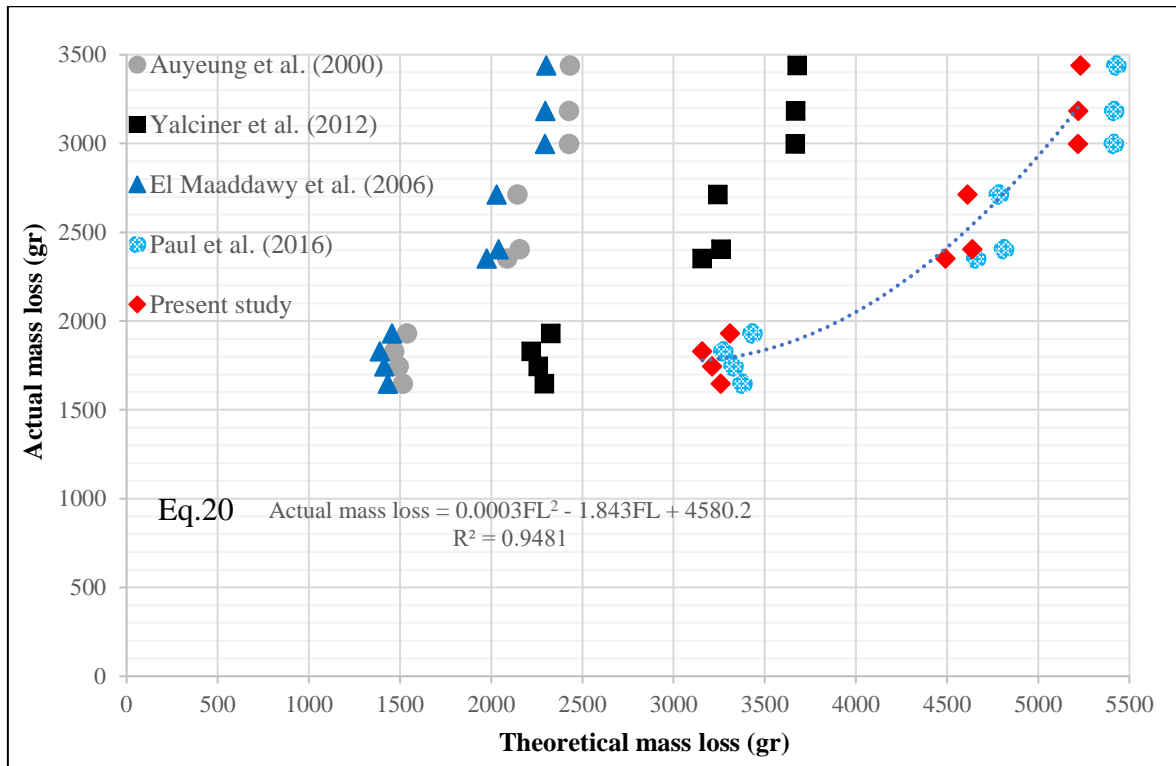


Figure 4. 3: Correlation between theoretical and actual mass losses.

In Fig. 4.3, among the developed models to predict the actual mass losses Auyeung (Auyeung, 2000) and Yalciner et al. (Yalciner et al., 2012b) reasonably better predicts the actual corrosion mass losses. Ratios of theoretically calculated mass losses to the actual mass losses based on the developed model by Auyeng et al. (2000) were ranged between 0.71 (C_L : 10.6%) and 0.92 (C_L : 5%). In contrast to under estimated values by Auyeng et al. (2000) and El Maaddawy et al. (2006), developed model by Yalciner et al. yielded over estimated values where the ratios of theoretically calculated mass losses to actual mass losses were ranged between 1.07 (C_L : 10.6%) and 1.39 (C_L : 5%). While Auyeng et al. (2000) better predicted the actual mass losses at lower corrosion levels Yalciner et al. (2012) better predicted the actual mass losses at higher corrosion levels. Developed model by El Maaddawy et al.(2006)

was also showed closer results at lower corrosion levels compared to Auyeng et al. (2000) Two models at the highest corrosion levels (C_L : 10.6%) caused to have more than one thousand gr mass losses than actual mass losses. Developed models considerably well predicts the actual corrosion levels based on Faraday's Law when the smaller size effect and other many parameters (e.g., concrete strength level, concrete cover depth, applied current) were considered. Developed model by Paul et al. (2016) Provided the lowest performance when it was compared to other three developed models. Ratios of theoretically calculated mass losses to the actual mass losses based on the model developed by Paul et al. (2016) Significantly over estimated having the ratios between 1.58 and 2.55. Since all reinforcement bars were reweighted for the current study, the given Eq. (20) on Fig. 4.3 was developed for further studies to be used for the correlation between theoretically estimated corrosion levels and actual corrosion levels by considering larger size effect of corroded RC beams. Study done by Ahmad (2017) indicated that if the gravimetric tests were conducted on the rebar after application of the external current following Eq. (21) can be used to calculate the actual corrosion current density (I_{corr}):

$$I_{corr} = \frac{(W_i - W_f)F}{\pi DLWT} \quad (21)$$

Where, F is the Faraday's constant (96487 Amp-sec), D is the steel bar diameter (cm), L is the length of the bar (cm), W is the equivalent weight of steel (27.925 g), T is the induced corrosion time (sec). Calculated actual corrosion current densities were used to calculate the penetration rates (P_r) based on proposed model by Ijsselin (1986). Once the penetration rate is calculated it yields to calculate the metal loss factor ($a = 2P_r T/D$) according to Azad et al. (Azad et al., 2007), for the calculation of reduced net diameter of corroded bars by considering the gravimetric test results. Calculated reduced net diameters (D') of tensile reinforcement bars were used to calculate the theoretical moment capacities (M_{thc}) of corroded RC beams.

4.3. Residual Flexural Strength Test Results of Corroded RC Beams Without Polypropylene Fibers

Fig. 4.4 shows the total applied load and mid-span displacement responses for the uncorroded and corroded specimens without using P_f .

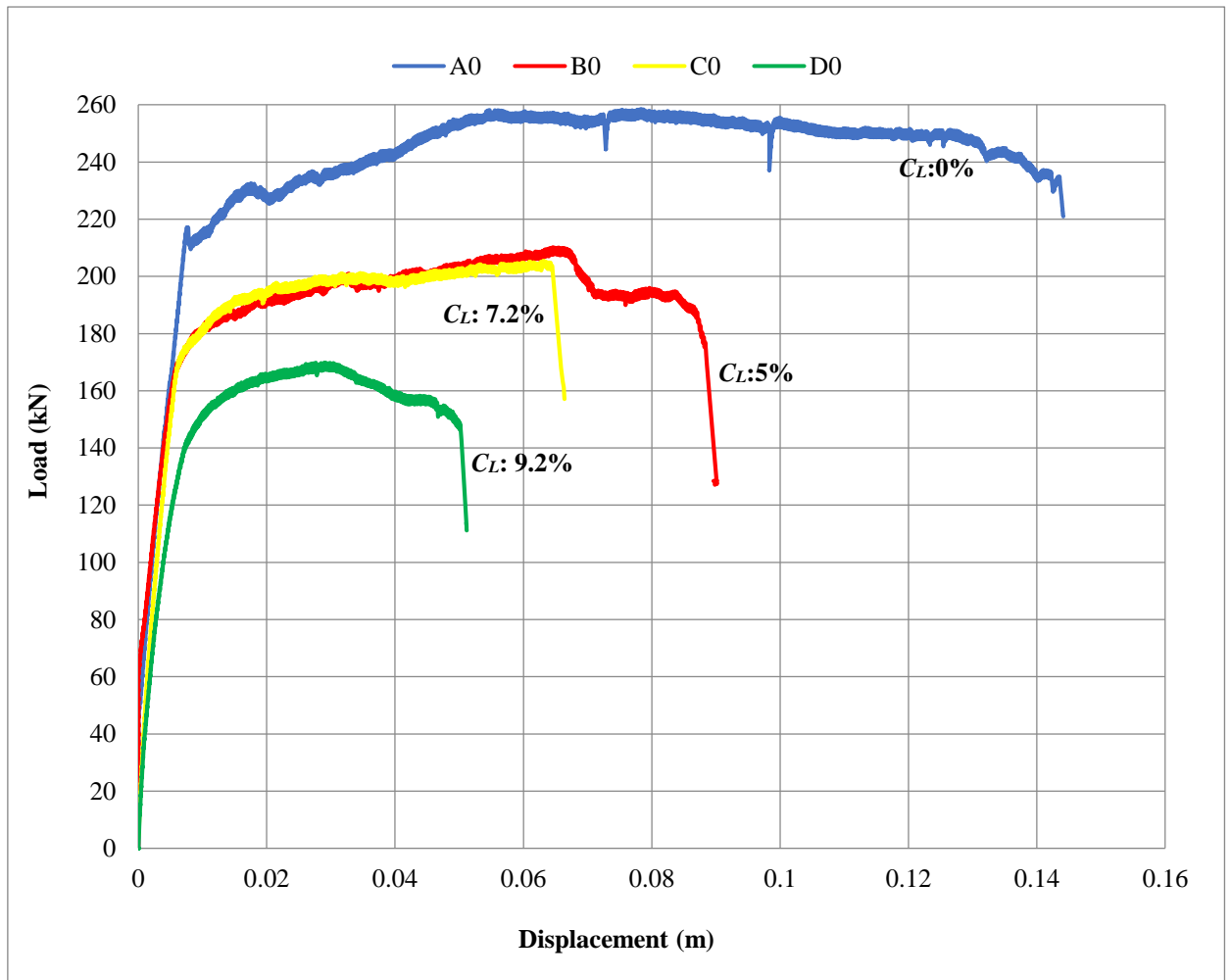


Figure 4. 4: Load-displacement responses for the uncorroded and corroded beams at 0% V_f .

Emphasized first bully point in the problem statement of this research (considered uniform corrosion levels by using Faraday's Law, used steel coupons cut off from the corroded bars) for the prediction of residual flexural strength was shown in Table 1. As shown in Table 1, obtained total corrosion level in a beam based on Faraday's Law differed corrosion levels at longitudinal and shear reinforcement bars. Obtained actual corrosion levels were generally more for the transverse reinforcement bars due to the closer side of the concrete. Metal loss

factor and then reduced net diameters of each corroded tensile reinforcement bar were calculated to obtain the M_{thc} and to develop a model for the prediction of residual flexural strength. Table 2 shows the actual corrosion density values of tensile reinforcement bars and comparisons between M_{thc} and experimentally obtained moment capacities of corroded RC beams (M_{cexp}). As shown in Table 2, since the calculation of M_{thc} considers only the reduced net diameters D' of tensile reinforcement bars due to corrosion it causes to yield different moment resisting capacities compared to experimentally obtained values.

Table 2. Comparisons of theoretically calculated and experimentally obtained moment capacities

Specimen	Number of tensile bars	W_i (g)	W_f (g)	L (cm)	T (s)	I_{corr} (mA/cm ²)	D (cm)	D' (cm)	A_{Stotal} (cm ²)	M_{thc} (kN m)	M_{cexp} (kN m)	$R = \frac{M_{cexp}}{M_{thc}} \times 100$
B	B _{T1}	4510.5	4227	300	3,208,741	0.202	1.6	1.552	7.725	113.415	131.362	115.82
	B _{T2}	4459.5	4257.5	300	3,208,741	0.144	1.6	1.566				
	B _{T3}	4648	4529	300	3,208,741	0.080	1.6	1.581				
	B _{T4}	4471.5	4313	300	3,208,741	0.113	1.6	1.573				
C	C _{T1}	4418.5	3947	300	4,970,701	0.217	1.6	1.520	7.525	110.689	128.408	116.01
	C _{T2}	4434	4228.5	300	4,970,701	0.095	1.6	1.565				
	C _{T3}	4651.5	4454	300	4,970,701	0.085	1.6	1.569				
	C _{T4}	4419	4040	300	4,970,701	0.175	1.6	1.536				
D	D _{T1}	4435.5	3961	300	3,907,021	0.278	1.6	1.520	7.443	109.560	106.146	96.88
	D _{T2}	4482.5	4244	300	3,907,021	0.140	1.6	1.560				
	D _{T3}	4640	4396	300	3,907,021	0.134	1.6	1.561				
	D _{T4}	4434	3932.5	300	3,907,021	0.294	1.6	1.515				

Corrosion current densities which were obtained from fully extracted reinforcement bars were used to propose a new model for the prediction of flexural strength of corroded RC. Developed new model for the prediction of the moment resisting capacities of corroded (M_c) RC beams is given in Eqs. (22) and (23) by considering the contribution of corrosion levels at shear and longitudinal bars. In Eq. (23) the contribution of transverse reinforcement bars on the flexural strength was taken as 0.37 based on the calculated theoretical experimentally obtained moment capacities of uncorroded RC beams.

$$M_c = \exp(0.01862\beta + 0.08323\alpha + 0.02046M_{thc} - 1.4995) \quad (22)$$

$$\beta = (100 - T_{I_{corr}}) \times 0.63; \alpha = (100 - S_{I_{corr}}) \times 0.37 \quad (23)$$

Where, $T_{I_{corr}}$ (mA/cm²-day) and $S_{I_{corr}}$ (mA/cm²-day) are the corrosion current density in tensile and shear reinforcement bars, respectively. Proposed new model was compared with previous developed models in Fig. 4.5. Firstly, obtained experimental corrosion values from the current study were inserted into the previous developed models and predicted moment resisting capacities were divided to the obtained M_{cexp} .

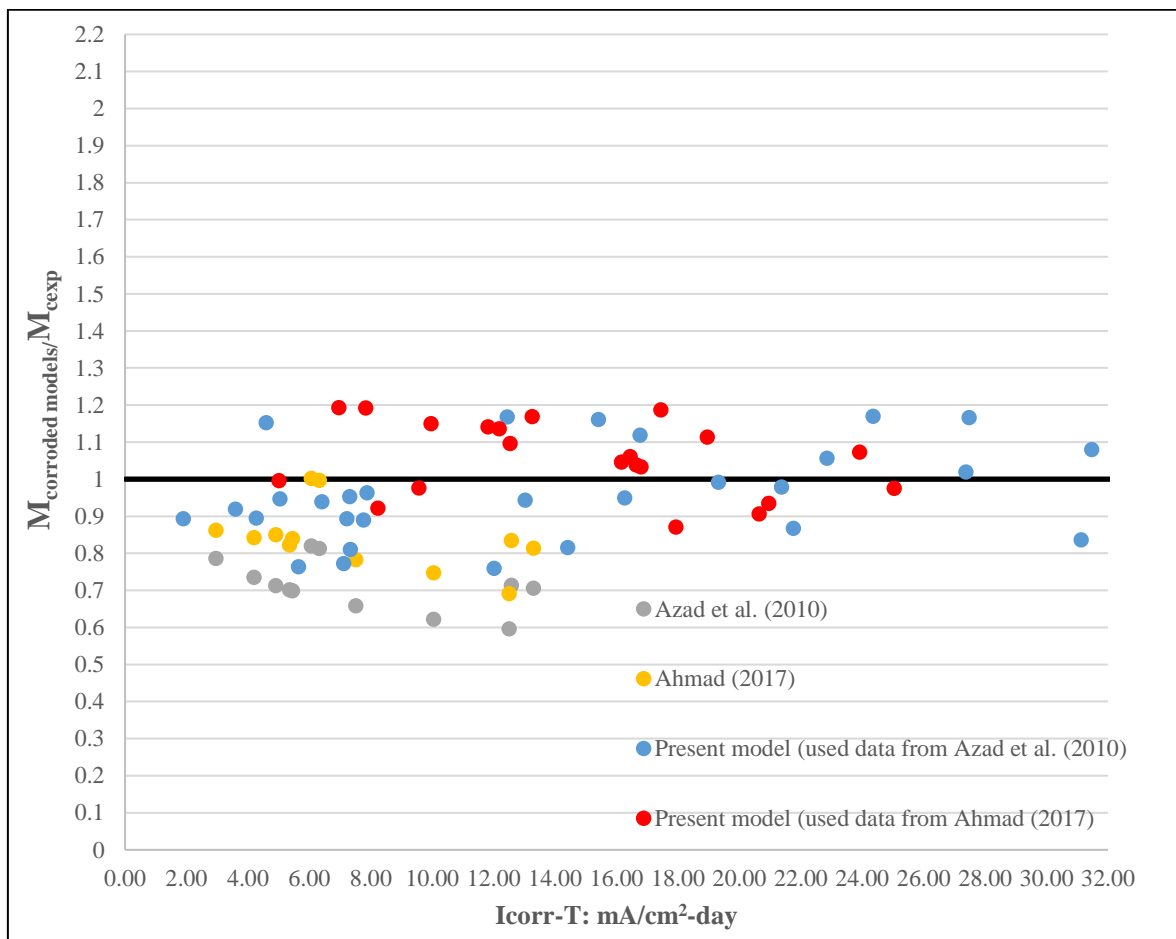


Figure 4. 5: Validation of proposed model.

Even the developed model by Azad et al. (2010), coated the stirrups and the contribution of corrosion levels by stirrups were not taken into account, predicted flexural strength of corroded RC beams were lower than experimentally obtained values. This might be

explained by the smaller size effect of RC beams where the effect volumetric expansion by corrosion products was more. Stirrups were uncoated by the study done Ahmad (2017). Therefore given model by Ahmad (Ahmad, 2017) showed better performance compared to the model developed by Azad et al. (2010) However, in both models the moment resisting capacities of uncorroded and corroded RC beams were ten times (i.e., Azad et al., 2010) and four times (i.e., Ahmad, 2017), less than the current study due to the size effect of the samples which may not generally reflect the real condition of RC structures. Secondly to validate the proposed model, given corrosion current densities by Azad et al. (Azad, 2010) and Ahmad (Ahmad,2017), were inserted into the new model and predicted moment values divided to experimentally obtained own corroded moment values by Azad et al. (2010) and Ahmad (Ahmad,2017). Since the stirrups were coated in the study done by Azad et al. (2010) in Eq. (23) $S_{I_{corr}}$ was taken zero for the collected data from Azad et al. (2010). In the study done by Ahmad (2017), stirrups were not coated and corrosion current densities were given at each specimen. Therefore, given corrosion current densities by Ahmad (2017) was taken same as for $S_{I_{corr}}$ and $T_{I_{corr}}$. As shown in Fig. 4.5 , by considering the many uncertainties due to corrosion, proposed new model better predicts the flexural strength of corroded RC beams that can be used for both smaller and larger sizes of corroded RC beams (Ahmad, 2017).

4.4. Flexural strength test results of corroded and uncorroded reinforced concrete beams with polypropylene fibers

Uncorroded reinforced concrete beams of group A were discussed at three different volume of fractions (0%, 0.5% and 1.5%) to examine the effect of fibers on flexural strength. Fig. 4.6 shows the load-displacement relationships of uncorroded RC beams at three different V_f .

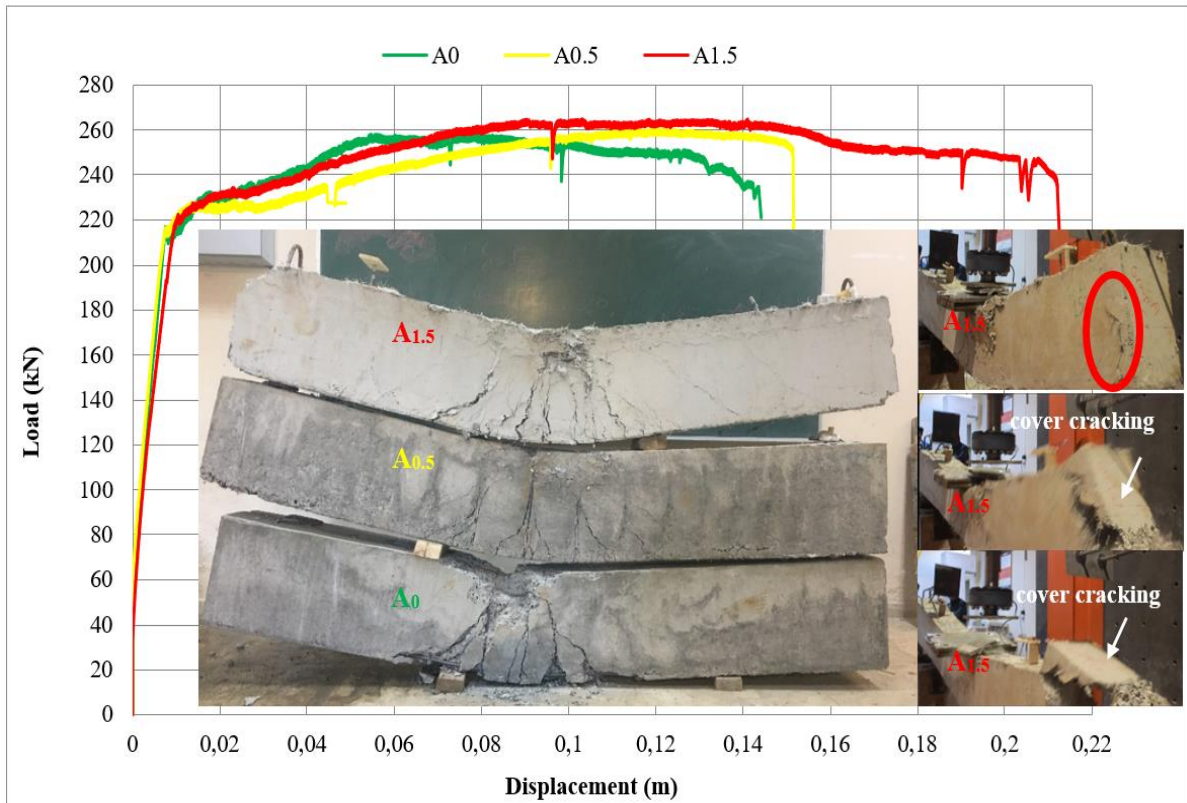


Figure 4. 6: Load-displacement relationships of uncorroded RC beams.

The detail cracking pattern of uncorroded and corroded RC beams were given in Appendix B. Failure of all three uncorroded reinforced concrete beams was ductile. Theoretically calculated resisting moment capacity (M_{th}) of A₀ (0% V_f , C_L : 0%) well obtained during flexural strength tests by considering the effect of transverse reinforcement bars on load carrying capacities. Theoretically calculated 188 kN load carrying capacity (M_{th} : 118 kN.m) of A₀ was increased by 38% with the contribution of the transverse reinforcement bars. In Fig. 4.6 the ultimate load carrying capacity of A_{0.5} was not change and almost equal to A₀. At 1.5 of V_f , the ultimate load carrying capacity of A_{1.5} was increased by only 2%. Although there were no significant increases about the ultimate load carrying capacities with the help of fibers, the displacement ductility significantly improved by fibers. This behaviour can be explained by failure mechanism. In group A, failure mechanism was flexural failure combined with top crushing of concrete. Main differences between three specimens were regarding with delayed top crushing of concrete with the help of fibers. As shown in Fig. 4.6 once the initial cracking has occurred, the stresses have been redistributed by the Pf additive which strengthened the adherence, tensile and deformation compliance mechanisms of

reinforced concrete members with the help of other cracks to form. Appearance of the additional cracks conforms to the slope of the experimentally measured load-displacement curve and the increased ratio of polypropylene additive material. By considering load-displacement and crack forms in Fig. 4.7 less cracks were occurred in the elastic zone up to the yielding where the less displacement was also measured against to the increased load. Meanwhile, the cracks were more and scattered in the plastic region where the displacement was measured more for the less increased load. Reduction in the applied load was realized faster which was resisted by the samples using of 0%, 0.5% and 1.5% polypropylene additive material, respectively. The presence of the polypropylene additive material allows the transverse reinforcement bars to be subjected to less stress that provided more favourable contribution to the bending behaviour of the RC members. At 0% of fibers of pure sample, there was a risk of punching with the crushing of concrete in the pressure zone where the load was applied. However, punching safety was provided for samples of 0.5% and 1.5% polypropylene additive materials used because of the crushing was relatively less in these samples. If polypropylene additive material is used at more ratios (1.5%), paying attention to the workability feature, it increases the load carrying capacity with resistance to tensile cracking even after final loading and even after rupturing of the reinforcement bars. The resistance of the polypropylene additive materials to tensile cracking was gained by bridging properties of aggregates where the polypropylene additive materials provided for the cracks to be dispersed in the bending zone of the specimens. This status provided more ductile behaviour with the help of preserving their post-cracking strength. The failure mechanism at the specimen of 1.5% of fiber ($A_{1.5}$) occurred by cover cracking of sample which caused the deboning of the steel plate at the pin support. Due to the extreme bending behaviour and the applied forces by the anchorage bars of tensile reinforcement bars cracked the concrete cover (see Fig. 4.6) due to the limited tensile strength of concrete. Even at that stage, $A_{1.5}$ maintained the bending behaviour and spalling of concrete at the compression zone of the beam were not as much as at the specimens A_0 and $A_{0.5}$. Fig. 4.7 shows the total applied load and mid-span displacement responses for the specimens of group B at three different used amount of P_f and at different corrosion levels. As shown in Fig. 4.7 increased amount of P_f provided increased bending capacities at group B. At 0% of fiber (B_0) recorded ultimate load carrying capacity of B_0 was 210 kN and increased to 242 kN and 234 kN at $B_{0.5}$ and $B_{1.5}$,

respectively. Although ultimate load carrying capacity of B_{0.5} was more than B_{1.5} but not obvious, the main effect of fibers was on ductility behaviour. The calculated displacement ductility ratio of B₀ was increased from 8.07 to 16.97 at B_{0.5} and to 19.86 at B_{1.5}. The displacement ductility ratio of B_{0.5} was very close to uncorroded specimen of A_{0.5} with reduced ultimate load carrying capacity. By neglecting 18 kN ultimate load carrying capacity, energy absorption and stiffness capacities between A_{0.5} and B_{0.5}, used 0.5% of P_f with 5.7% of corrosion level almost showed same behaviour of uncorroded specimen of A_{0.5}. Among the group B, the displacement ductility ratio at 1.5% of P_f of B_{1.5} was more than A₀ and A_{0.5}. At 5.9% of corrosion level (B_{1.5}), when the highest used amount of fibers was compared to uncorroded specimens with lower amount of used fibers, P_f provided adequate displacement ductility but having lower ultimate load carrying capacity due to effect of corrosion. The reduction in the ultimate load carrying capacity of uncorroded specimen of A_{1.5} was reduced by 13% at B_{1.5}. Calculated displacement ductility ratio of A_{1.5} was 24.27 and reduced to 20.31 at B_{1.5}. When the reduction in displacement ductility ratio of A₀ and B₀ was compared which was almost two times, it is clear to indicate that up to a certain value of corrosion level, P_f provided to regain the lost shear capacities of corroded RC beams by considering the percentage in reduction of calculated values (A_{0.5}-B_{0.5}, A_{1.5}-B_{1.5}). This might be explained by stress transfer capability by fibers for the obtained lower corrosion level. Micro cracks at lower corrosion levels due to the volumetric expansion by corrosion products were prevented to become larger by the stress transfer capability of fibers during the bending behaviour corroded RC beams at group B. As shown by the photo in Fig. 4.7, with the increased used amount of fibers more tensile cracks were distributed at the tension zone of the beam.

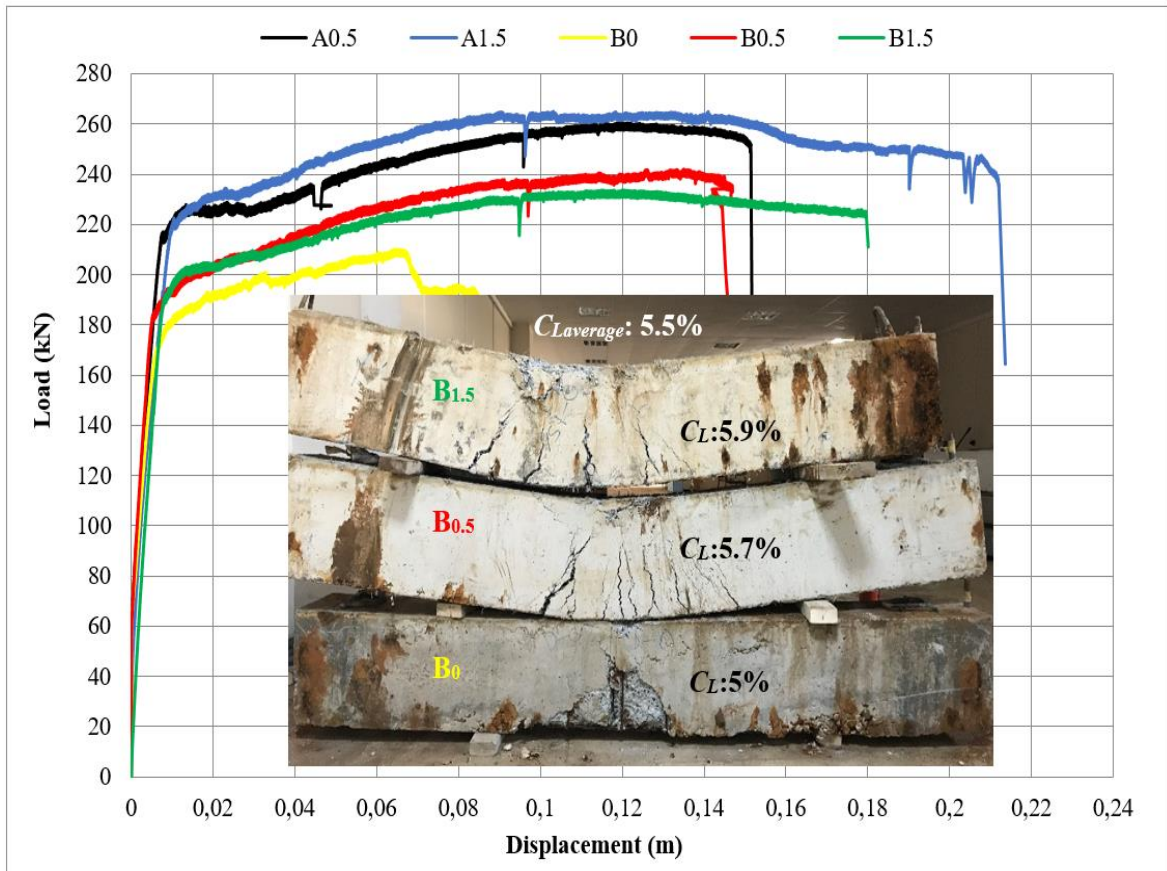


Figure 4. 7: Load-displacement relationships of corroded RC beams for group B.

Fig. 4.8 shows the total applied load and mid-span displacement responses for the specimens of group C at three different amounts of used fibers. With increased corrosion level stiffness, degradation in the corroded beams become more visible. Thus, contribution of P_f on the shear capacity become more important. The ultimate load carrying capacity of uncorroded specimen A_0 at 0% and $A_{0.5}$ at 0.5% of fibers were reduced by 26% and 19% with C_0 and $C_{0.5}$, respectively. Calculated displacement ductility ratios of A_0 and $A_{0.5}$ compared to C_0 and $C_{0.5}$ were reduced from 16.37 to 7.27 and 17.11 to 9.66, respectively. Up to a certain value of applied load the initial stiffness of the specimens given in Fig. 4.7 showed similar behaviour. With the increased applied load and after the yielding capacity of the member secondary stiffness showed significant differences due to the effect of corrosion. As shown in Fig. 4.8, after the yielding of the member and at the same applied load more deflection occurred due to the reduction in secondary stiffness of the members. When the corrosion level increased to 8.4%, only 1.5% of polypropylene specimen ($C_{1.5}$) tried to challenge to have the similar displacement ductility ratio of the lowest used amount of fiber A_0 ($C_L: 0\%$).

However, when the displacement ductility ratio $C_{1.5}$ was compared to $A_{1.5}$, reduction in the ductility ratio was 51% (see Fig. 4.8).

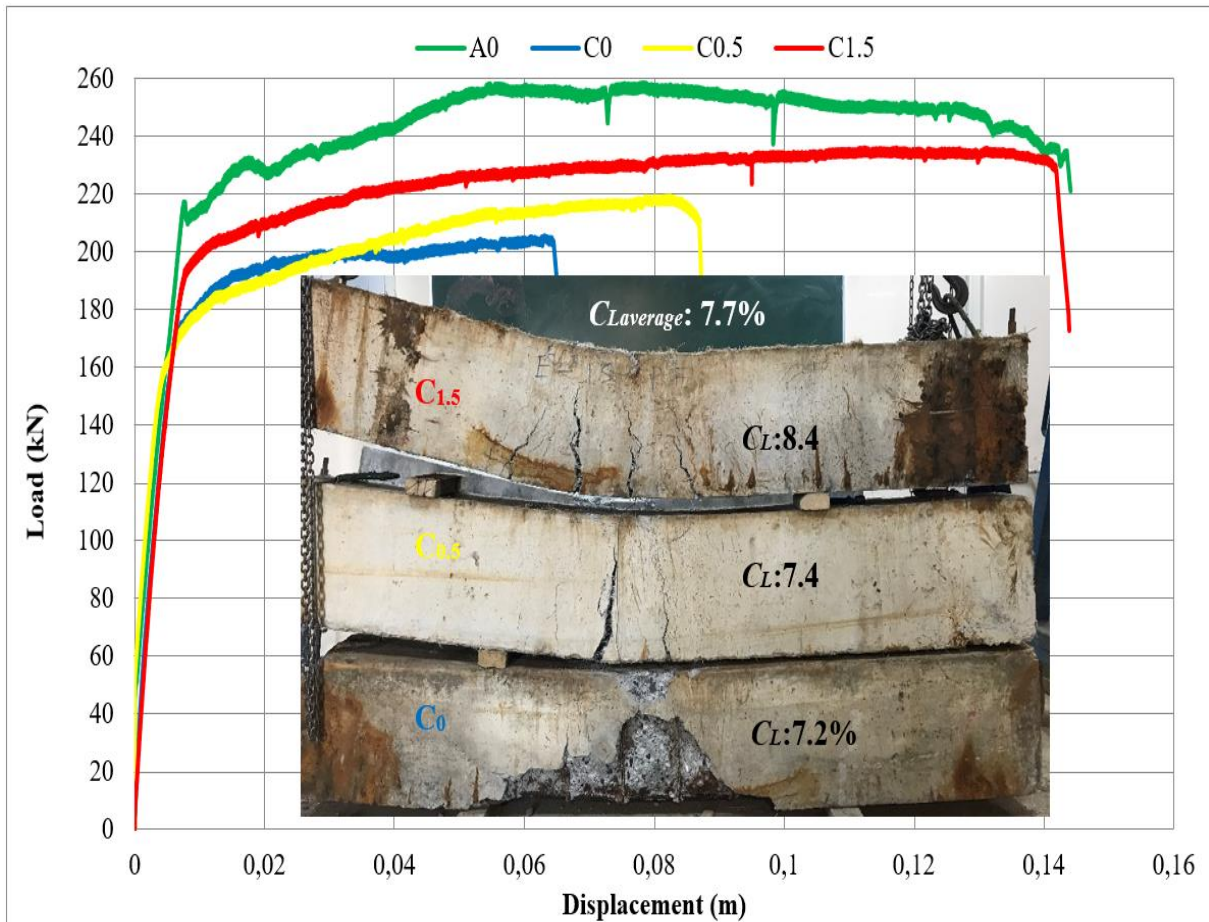


Figure 4. 8: Load-displacement relationships of corroded RC beams for group C.

Better ductility behaviour and load carrying capacity of $C_{1.5}$ compared to C_0 and $C_{0.5}$ can be explained from fully extracted reinforcement bars from the concrete in Fig. 4.8. As shown in Fig.4.9 (a-b) shows the fully extracted reinforcement bars and visual observations for $C_{0.5}$, $C_{1.5}$, $D_{0.5}$ and $D_{1.5}$. Ruptured numbers of transverse reinforcement bars were changed with the stress contribution by fibers. At higher corrosion levels (e.g., group C and D) localized sectional losses were occurred. In Fig. 4.9(a) even the corrosion level of $C_{1.5}$ was more than the corrosion level of $C_{0.5}$, number of ruptured stirrups were nine at $C_{0.5}$ (CL: 7.4%) which was five at $C_{1.5}$ (CL: 8.4%). Same results regarding with the stress contribution by fibers can be seen in Fig. 4.9 (b) for group D. In Fig. 4.9(b), while the number of ruptured stirrups at $D_{0.5}$ (CL: 9.8%) was twelve, it was nine at $D_{1.5}$ (CL: 10.6%). Ruptured transverse

reinforcement bars were generally concentrated at densification regions of the beams. Rather than $D_{1.5}$ transverse reinforcement bars of $D_{0.5}$ at the mid span of the beam was also ruptured. All these results clearly define the contribution of amount of used Pf on shear and tensile strength for the members.



Figure 4. 9: Extracted reinforcement bars: (a) $C_{0.5}$ (V_f : 0.5%, C_L : 7.4%) and $C_{1.5}$ (V_f : 1.5%, C_L : 8.4%); (b) $D_{0.5}$ (V_f : 0.5%, C_L : 9.8%) and $D_{1.5}$ (V_f : 1.5%, C_L : 10.6%).

None of the corroded specimens with the help of fibers had a capability to challenge with the uncorroded specimens when the corrosion level reached to around 9% and 10% for the group D. Fig. 4.10 shows the total applied load and mid-span displacement responses for the specimens of group D at three different amounts of used fibers. As shown in Fig. 4.10 at a corrosion level of 10.6% with the highest used amount of fiber at D_{1.5} could not reach to the displacement ductility capacity of uncorroded specimen of A₀ at 0% of fiber. Based on the obtained overall test results it is clear to indicate that the performance of the Pf were limited by corrosion levels. In Fig.4.10 the unexpectedly displacement ductility ratio of D_{0.5} was less than D₀. This can be explained by provided initial stiffness by P_f . At 0.5% of used Pf with a corrosion level of 9.8% tried to increase the initial stiffness of D_{0.5}. However, because of the inadequate shear strength and with the increased ultimate load carrying capacity caused to have lower ductile behaviour compared to D₀. Final cracking failure modes of group D without releasing the loads were illustrated in Fig. 4.11. As shown in Fig. 4.11 exception of D_{1.5} exerted stresses by corrosion products and limited tensile strength of concrete resulted in cover cracking and splitting of reinforcement bars at D₀ and D_{0.5}.

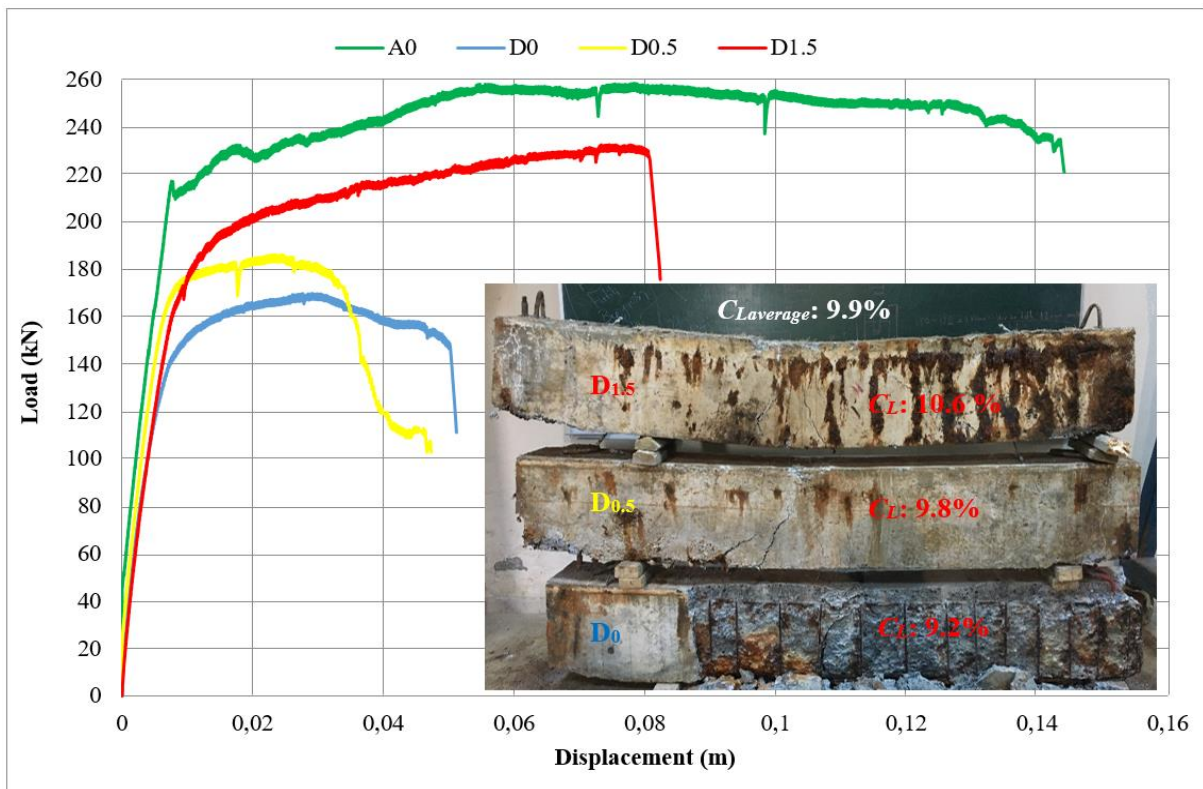


Figure 4. 10: Load-displacement relationships of corroded RC beams for group D.



Figure 4.11: Damage levels at failure without releasing jack.

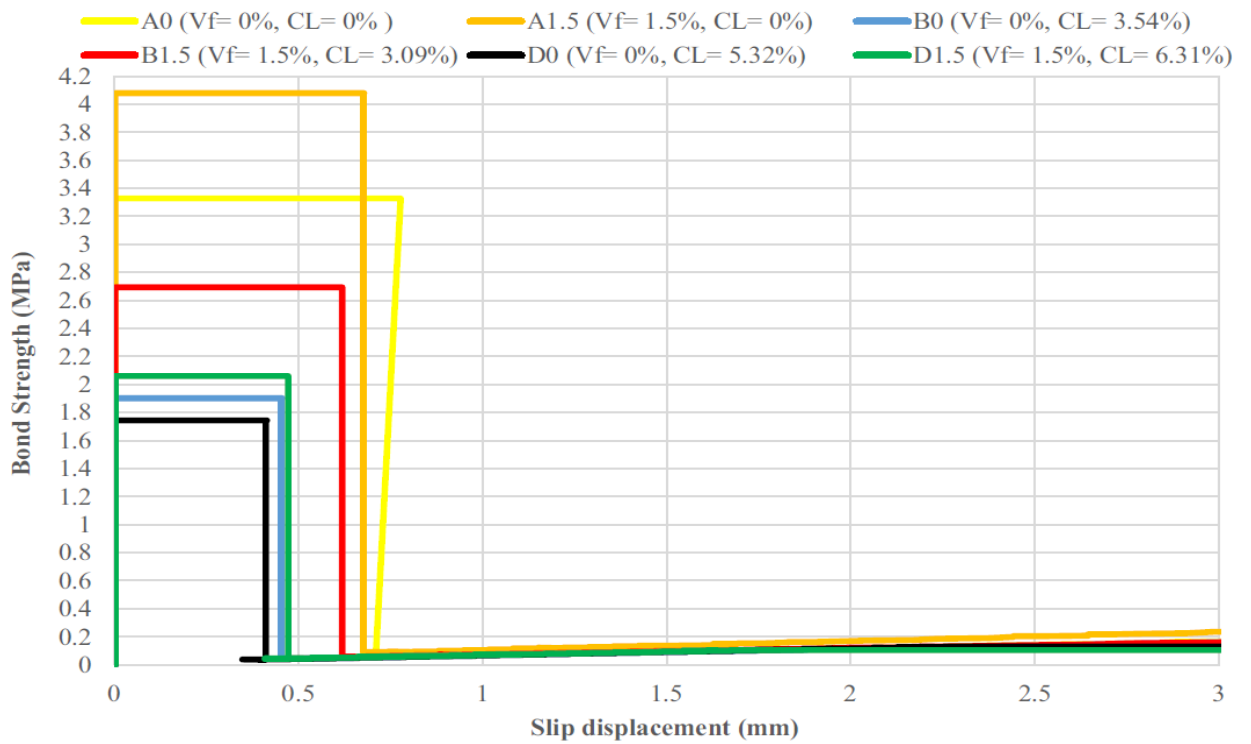


Figure 4.12: Bond-slip relationships of uncorroded and corroded beams.

4.5. Bond-Slip Relationships

Fig. 4.12 shows the bond-slip relationships of uncorroded and corroded reinforcement bars at different used amount of fibers by using Eqs. (18) and (19). In Eq. (18) changes in the diameter of tensile reinforcement bars were considered based on the gravimetric test results at which strain gauge was bonded on tensile reinforcement bars. Reduction in elastic modulus of reinforcement bars as a function of corrosion levels were also considered according to the proposed model by Lee et al. (2009). Given corrosion levels on Fig. 4.12 indicates corrosion levels of a single reinforcement bars from a specimen. Test results of uncorroded and corroded RC beams showed that there were no significant changes in the bond strength at 0.5% of V_f (Lee et al., 2009).

The calculated bond strength of uncorroded specimen A_0 increased by 23% with the help of using 1.5% V_f at $A_{1.5}$. Reduction in the calculated bond strength values of B_0 (C_L : 3.54%) and D_0 (C_L : 5.32%) compared to A_0 (C_L : 0%) were 75% and 91%, respectively. Even the highest amount of fibers was used at $B_{1.5}$ (C_L : 3.09%), calculated bond strength of $B_{1.5}$ could not reach to the bond strength performance provided at the lowest used amount of fibers at uncorroded specimen of A_0 . Same results were also obtained for other specimens at different corrosion levels. Even if corroded specimens with the help of fibers could not reach to the bond strength values of uncorroded specimen, up to a certain value of corrosion fibers provided significant increases in bond strength. The bond strength value of B_0 was increased by 42% with the help of used highest amount of fibers at $B_{1.5}$.

The calculated bond strength value of $D_{1.5}$ at 6.31% corrosion level was very close and more than B_0 having a corrosion level of 3.54%. Previous indicated limited performance of fibers on load-displacement relationships and regained shear strength by fibers up to a certain value of corrosion levels was also valid for the bond strength. Once the corrosion level was become more, particularly damaged lugs of the reinforcement bars decreased the transfer stress from the corroded reinforcement bars to the concrete. Obtained slip values can be used to calculate the slip rotation, which provides to modify the plastic hinge properties of RC members for further structural analyses.

4.6.Moment-Curvature Relationships

Fig. 4.13(a) and (b) illustrate the experimentally measured moment-curvature relationships along the beam length for uncorroded (A_0) and corroded (B_0 , C_0 , and D_0) specimens. As expected, the curvature ductility ratio of the uncorroded beam was higher than that of the corroded beams.

The yield strength and ductility ratios were decreased gradually, while the rate of corrosion was increased. According to Fig. 4.13(a) and (b), when a comparison is made regarding the increased polypropylene ratio, it can be observed that the shear capacity of the beams depending on the increased polypropylene ratio improves.

The decrease in the yielding capacity of the sections as a result of the corrosion effect was improved with the aid of an increased ratio of fibers. Even at the highest corrosion level for group D, polypropylene fibers recalled the lost yielding moment capacity of the section under the corrosion effect. As shown in Fig. 4.13, the curvature ductility ratios of corroded RC beams were improved with the aid of fibers. The calculated curvature ductility ratio of A_0 was 8.54, which was reduced to 6.48, 6.01, and 5.45 at B_0 , C_0 and D_0 , respectively.

The curvature ductility ratios of $B_{1.5}$ and $C_{1.5}$ at 1.5% of P_f were greater than uncorroded beam A_0 and equal to 18.97 and 11.73, respectively. At a corrosion level of 10.6%, and with the highest amount of fiber used at $D_{1.5}$, the curvature ductility ratio of the uncorroded specimen of A_0 with a 0% fiber composition could not be reached. However, the calculated ductility ratio of $D_{1.5}$ which was 6.55 was also greater than B_0 , C_0 and D_0 . Accordingly, it is understood that the confinement effect of the polypropylene fibers in RC beams subjected to corrosion demonstrated its efficiency, particularly at 1.5% of V_f .

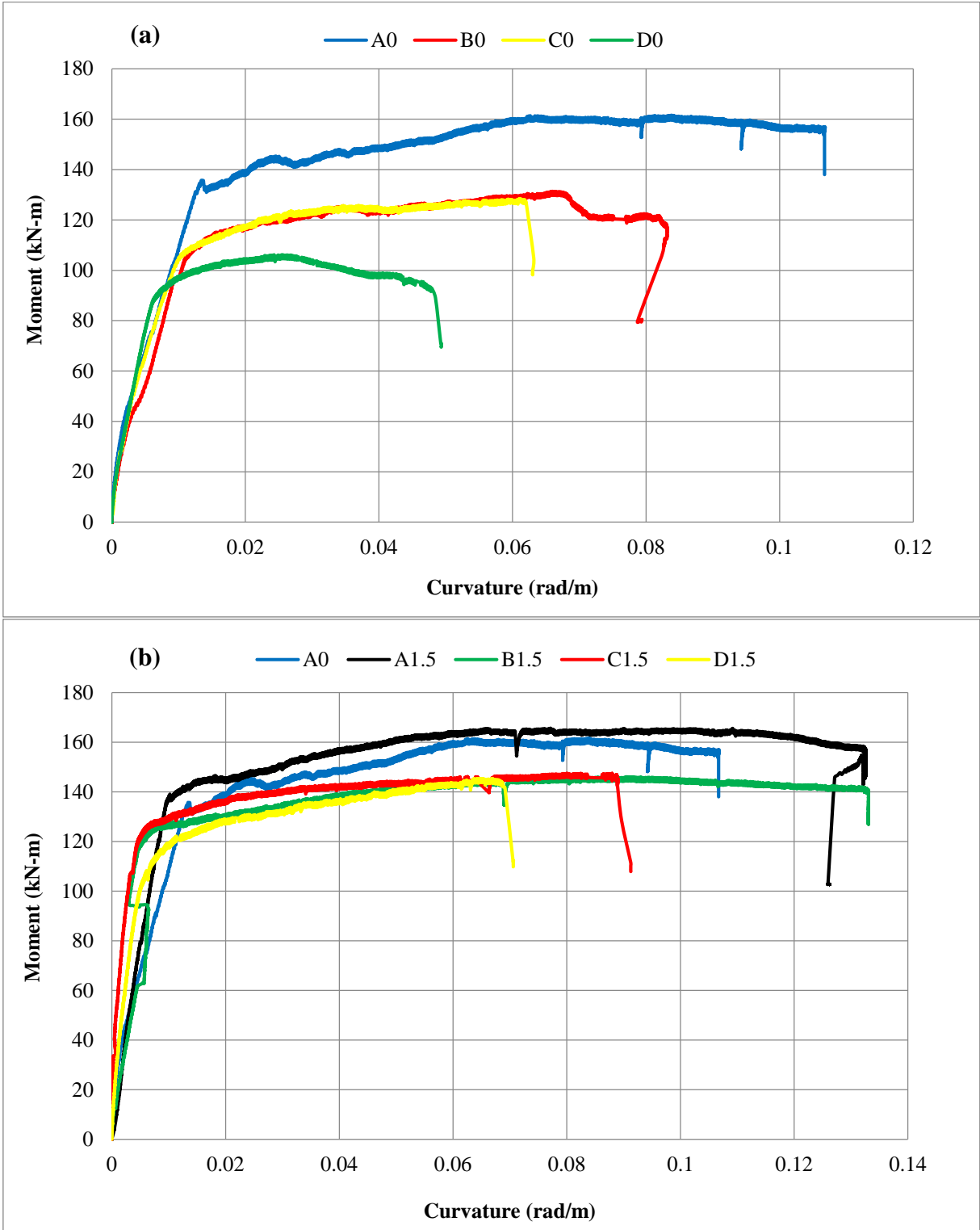


Figure 4. 13: Moment-curvature relationships: (a) $V_f : 0\%$, (b) $V_f : 1.5\%$.

CHAPTER 5: CONCLUSION

5.1. Conclusions Review

An experimental study was performed to investigate the effect of polypropylene fibers on corroded reinforced concrete beams by considering bond-slip relationships and to develop a new model for the prediction of moment resisting capacities of corroded beams.

Based on the test results, the following conclusions were summarized.

Previously developed models to predict the actual mass losses based on Faraday' Law were limited with lower levels of corrosion for smaller reinforced concrete beams.

Based on the obtained corrosion levels from fully extracted reinforcement bars showed that corrosion levels by using accelerated corrosion method show significant differences based on the location of the bars.

If the assumed corrosion levels based on the Faraday's Law or steel coupons cut off from the corroded bars is preferred to be used to define the corrosion level in a member by using accelerated corrosion method, it may be suggested for further studies to increase the two times of the corrosion levels for outer face of the bars compared to inner face of the bars.

Obtained test results indicated that polypropylene fibers had a significant effect to provide ductile behaviour for reinforced concrete beams. In the case of corrosion up to a certain value of corrosion levels polypropylene fibers provided to regain the lost shear capacities of corroded reinforced concrete beams.

Corrosion levels obtained at groups B and C with the used highest amount of fibers provided to regain the displacement ductility's compared to the lowest used amount of fibers at uncorroded specimens. However, the performance of fibers limited with corrosion levels for group D. Up to a certain value corrosion levels while the regained ductility provided with the help of fibers, none of the corroded specimens with the help of fibers provided better or closer bond strength compared to uncorroded specimens.

The results of the present study may provide valuable information regarding with the effectiveness of fibers for the service life and seismic performance levels of reinforced concrete structures subjected to corrosive environmental conditions.

Proposed model to predict the flexural strength of corroded reinforced concrete beams still require further studies. Developed model in this study to predict the flexural strength of corroded reinforced concrete beams was limited by the obtained experimental tests results for the contribution of uncorroded stirrups on moment resisting capacities from uncorroded beams. Studies including the combination of uncorroded stirrups with corroded tensile reinforcement bars and corroded stirrups with uncorroded tensile reinforcement bars at different corrosion levels may be performed for the better prediction of actual resisting capacities of corroded reinforced concrete beams. Experimental test result were also summarized as below:

The punching safety was provided for the samples containing 0.5 and 1.5% polypropylene additive materials; because the crushing was relatively lower in these samples.

At a corrosion level of 5.9% ($B_{1.5}$), Pf demonstrated adequate displacement ductility when the highest amount of fibers used was compared to the uncorroded specimens.

When the corrosion levels reached approximately 7 and 8% for group C, only the polypropylene specimen with 1.5% of fiber ($C_{1.5}$) had a similar displacement ductility ratio to that of the specimen that contained the lowest amount of fiber, namely A_0 .

None of the corroded specimens aided by fibers had the capability to challenge the uncorroded specimens when the corrosion level reached approximately 9 and 10% for group D. The reductions in the calculated bond strength values of B_0 (CL = 3.54%) and D_0 (CL = 5.32%), and compared to A_0 were 75 and 91%, respectively.

The bond strength value of B_0 was increased by 42% with the aid of the highest amount of fibers used at $B_{1.5}$. The calculated bond strength value of $D_{1.5}$ at a corrosion level of 6.31% was greater than B_0 .

The calculated curvature ductility ratio of A_0 was 8.54, which was reduced to 6.48, 6.01, 5.45 at B_0 , C_0 and D_0 , respectively.

The curvature ductility ratios of $B_{1.5}$ and $C_{1.5}$ at 1.5% of P_f were greater than uncorroded beam A_0 and equal to 18.97 and 11.73, respectively. At a corrosion level of 10.6%, and with the highest amount of fiber used at $D_{1.5}$, the curvature ductility ratio of the uncorroded specimen of A_0 with a 0% fiber composition could not be reached.

REFERENCES

- Ahmad, S. (2017). Prediction of residual flexural strength of corroded reinforced concrete beams. *Anti-Corrosion Methods and Materials*, 64(1), 69-74.
- Ahmad, S., (2017), "Prediction of Residual Flexural Strength of Corroded Reinforced Concrete Beams," *Anti-Corrosion Methods and Materials*, V. 64, No. 1, pp. 69-74.
- Al-lami. K.. (2015). "Experimental Investigation of Fiber Reinforced Concrete Beams" Master of Science Degree. Portland State University.
- Al-Majidi, M. H., Lampropoulos, A. P., Cundy, A. B., Tsioulou, O. T., & Alrekabi, S. (2019, June). Flexural performance of reinforced concrete beams strengthened with fibre reinforced geopolymer concrete under accelerated corrosion. In *Structures*(Vol. 19, pp. 394-410). Elsevier.
- Altun, F., Haktanir, T., & Ari, K. (2007). Effects of steel fiber addition on mechanical properties of concrete and RC beams. *Construction and Building Materials*, 21(3), 654-661.
- Amin, A., Foster, S. J., Gilbert, R. I., & Kaufmann, W. (2017). Material characterisation of macro synthetic fibre reinforced concrete. *Cement and Concrete Composites*, 84, 124-133.
- Apostolopoulos, C. A., Papadopoulos, M. P., & Pantelakis, S. G. (2006). Tensile behavior of corroded reinforcing steel bars BSt 500s. *Construction and building Materials*, 20(9), 782-789.
- Auyeung, Y., Balaguru, P., & Chung, L. (2000). Bond behavior of corroded reinforcement bars. *Materials Journal*, 97(2), 214-220.
- Auyeung, Y., Balaguru, P., & Chung, L. (2000). Bond behaviour of corroded reinforcement bars. *Materials Journal*, 97(2), 214-220.
- Azad, A. K., Ahmad, S., & Azher, S. A. (2007). Residual strength of corrosion-damaged reinforced concrete beams. *ACI Materials Journal*, 104(1), 40.

Azad, A. K.; Ahmad, S.; and Al-Gohi, B. H. A., (2010), "Flexural Strength of Corroded Reinforced Concrete Beams," Magazine of Concrete Research, V. 62, No. 6, pp. 405-414.

Azad, K., Ahmad, S., & Al-Gohi, B. H. A. (2010). Flexural strength of corroded reinforced. Magazine of Concrete Research, 62(6), 405-414.

Banthia, N. (2010). Report on the physical properties and durability of fiber-reinforced concrete.

Baradan, B. Yazıcı H., 2003. Betonarme Yapılarda Durabilite ve TS EN 206-1 Standardının Getirdiği Yenilikler.

Baradan, B., Yazıcı, H., ve Ün, H. (2002) "Betonarme Yapılarda Kalıcılık (Durabilite)", İzmir: Dokuz Eylül Üniversitesi Mühendislik Fakültesi Yayınları, 1. Baskı.

Bazant, Z. P. (1979) "Physical Model for Steel Corrosion in Sea Structures Theory", Journal of the Structural Division, pp. 1137-1153.

Bentur, A. (1990). S. Mindess 'Fiber reinforced cementitious composites'.

Bicer, K., Yalciner, H., Pekrioglu, BA., ve Kumbasaroglu, A. (2018) "Effect of corrosion on flexural strength of reinforced concrete beams with polypropylene fibers", *Construction and Building Materials*, 185, 574-588.

Çağatay, İ. H. (2005) "Experimental Evaluation of Buildings Damaged in Recent Earthquakes in Turkey", *Engineering Failure Analysis*, 12, 440-452.

Çakır, A. F. (1994) "Türkiye'nin Metalik Korozyon Kaybı", IV.Korozyon Sempozyumu, 25-27 Ekim, İTÜ İstanbul, s.1-8.

Campione, G., Cannella, F., & Cavaleri, L. (2017). Shear and flexural strength prediction of corroded RC beams. *Construction and Building Materials*, 149, 395-405.

Campione, G., Cannella, F., & Cavaleri, L. (2017). Shear and flexural strength prediction of corroded RC beams. *Construction and Building Materials*, 149, 395-405.

- Cavaco, E. S., Bastos, A., & Santos, F. (2017). Effects of corrosion on the behaviour of precast concrete floor systems. *Construction and Building Materials*, 145, 411-418.
- Celep, Z., & Kumbasar, N. (2004). İstanbul: Deprem Mühendisliğine Giriş ve Depreme Dayanıklı Yapı Tasarımı.
- Choe, D.E., Gardoni, P., Rosowsky, D., & Haukaas, T. (2008). Probabilistic capacity models and seismic fragility estimates for RC columns subject to corrosion. *Reliability Engineering and System Safety*, 93(3), 383–393.
- Çoşgun, T. (2001). İstanbulda Deprem Sonrası Yapılan İncelemelerde Karşılaşılan Korozyon Hasarı Üzerine Bir İnceleme. İÜ MF, İnşaat Mühendisliği Bölümü.
- DE LA FUENTE, A. N. T. E. Q. U. E. R. A., & Armengou, J. (2007). Aplicaciones estructurales del HRFA: Tubos de saneamiento, paneles de cerramiento y placas de suelo reforzado. *Aplicaciones estructurales del HRFA, Jornada Técnica*.
- De la Fuente, A., Pujadas, P., Blanco, A., & Aguado, A. (2012). Experiences in Barcelona with the use of fibres in segmental linings. *Tunnelling and Underground Space Technology*, 27(1), 60-71.
- Di Prisco, M., Plizzari, G., & Vandewalle, L. (2009). Fibre reinforced concrete: new design perspectives. *Materials and structures*, 42(9), 1261-1281.
- Dinh, H. H., Parra-Montesinos, G. J., & Wight, J. K. (2010). Shear strength model for steel fiber reinforced concrete beams without stirrup reinforcement. *Journal of Structural Engineering*, 137(10), 1039-1051.
- El Maaddawy, T., Chahrour, A., & Soudki, K. (2006). Effect of fiber-reinforced polymer wraps on corrosion activity and concrete cracking in chloride-contaminated concrete cylinders. *Journal of Composites for Construction*, 10(2), 139-147.
- El Maaddawy, T.; Soudki, K.; and Topper, T., (2005), “Long-Term Performance of Corrosion-Damaged Reinforced Concrete Beams,” *ACI Structural Journal*, V. 102, No. 5, pp. 649-56.

El, Maaddawy, T., Chahrour, A. and Soudki. K. (2006) "Effect of fiber-reinforced polymer wraps on corrosion activity and concrete cracking in chloride-contaminated concrete cylinders", *Journal of Composites for Construction*, 10(2), 139-147.

Ersoy, U. (1985). *Betonarme: temel ilkeler ve taşıma gücü hesabı*. İnşaat Mühendisleri Odası.

Furlan. S. ve Hanai. J. (1997). "Shear Behavior of Fiber Reinforced Concrete Beams". *Cement and Concrete Composites* .19(4):359-366.

Gouveia, N. D., Fernandes, N. A., Faria, D. M., Ramos, A. M., & Lúcio, V. J. (2014). SFRC flat slabs punching behaviour–Experimental research. *Composites Part B: Engineering*, 63, 161-171.

H.S. Lee, Y.S. Cho, Evaluation of the mechanical properties of steel reinforcement embedded in concrete specimen as a function of the degree of reinforcement corrosion, *Int. J. Fract.* 157 (1) (2009) 81–88.

Higgins, C., Farrow III, W. C., & Turan, O. T. (2012). Analysis of reinforced concrete beams with corrosion damaged stirrups for shear capacity. *Structure and Infrastructure Engineering*, 8(11), 1080-1092.

Imam, A., & Azad, A. K. (2016). Prediction of residual shear strength of corroded reinforced concrete beams. *International Journal of Advanced Structural Engineering*, 8(3), 307-318.

Imran, I., Sugiri, S., & Pane, I. (2015). Behaviour of macro synthetic fiber reinforced concrete columns under concentric axial compression. *Procedia Engineering*, 125, 987-994.

Inel, M., & Ozmen, H. B. (2006). Effects of plastic hinge properties in nonlinear analysis of reinforced concrete buildings. *Engineering structures*, 28(11), 1494-1502.

İpek M., Canbay M. Ve Yılmaz K., (2015) "Çelik ve Polipropilen Liflerin Yalın ve Kombinasyonlu Olarak Kullanılmasının Sifconun Mekanik ve Fiziksel Özelliklerle Etkisi " *SAU Fen Bilimleri Dergisi* 19(1) : 41-52.

- J, Gulikers. (2005) “Theoretical considerations on the supposed linear relationship between concrete resistivity and corrosion rate
- Jnaid, F., & Aboutaha, R. S. (2016). Residual flexural strength of corroded reinforced concrete beams. *Engineering Structures*, 119, 198-216.
- Ju, H., Cheon, N. R., Lee, D. H., Oh, J. Y., Hwang, J. H., & Kim, K. S. (2015). Consideration on punching shear strength of steel-fiber-reinforced concrete slabs. *Advances in Mechanical Engineering*, 7(5), 1687814015584251.
- Karakoç, C. (1985). Aderansta mekanik etkileşim olayı (Doctoral dissertation, Fen Bilimleri Enstitüsü).
- Lee, C., Bonacci, J. F., Thomas, M. D., Maalej, M., Khajehpour, S., Hearn, N., & Sheikh, S. (2000). Accelerated corrosion and repair of reinforced concrete columns using carbon fibre reinforced polymer sheets. *Canadian Journal of Civil Engineering*, 27(5), 941-948.
- Lee, S. J., & Won, J. P. (2014). Flexural behaviour of precast reinforced concrete composite members reinforced with structural nano-synthetic and steel fibers. *Composite Structures*, 118, 571-579.
- Li, H., Li, B., Jin, R., Li, S., & Yu, J. G. (2018). Effects of sustained loading and corrosion on the performance of reinforced concrete beams. *Construction and Building Materials*, 169, 179-187.
- Malumbela, G., Alexander, M., & Moyo, P. (2009). Steel corrosion on RC structures under sustained service loads—A critical review. *Engineering Structures*, 31(11), 2518-2525.
- Malumbela, G., Alexander, M., & Moyo, P. (2010). Variation of steel loss and its effect on the ultimate flexural capacity of RC beams corroded and repaired under load. *Construction and Building Materials*, 24(6), 1051-1059.
- Malumbela, G., Moyo, P., & Alexander, M. (2009). Behaviour of RC beams corroded under sustained service loads. *Construction and Building Materials*, 23(11), 3346-3351.

Murathan, a., Murathan, A., & Karadavut, s. (2014). Yüksek Yoğunluklu Polipropilen Tekstil Atıklarının Kompozit Malzeme Üretiminde Kullanılabilirliği. Journal of The Faculty of Engineering & Architecture of Gazi University, 29(1).

O’Flaherty, F. J.; Mangart, P. S.; Lambert, P.; and Browne, E. H., (2008), “Effect of under- Reinforcement on the Flexural Strength of Corroded Beams,” Materials and Structures, V. 41, No. 2, pp. 311-321.

Park, R., & Paulay, T. (1975). Reinforced concrete structures. John Wiley & Sons.

Paul, S. C., Babafemi, A. J., Conradie, K., & van Zijl, G. P. (2016). Applied voltage on corrosion mass loss and cracking behavior of steel-reinforced SHCC and mortar specimens. Journal of Materials in Civil Engineering, 29(5), 04016272.

Paul, SC., Babafemi, AJ., Conradie, K., and van, Zijl, GP. (2016) “Applied voltage on corrosion mass loss and cracking behavior of steel-reinforced SHCC and mortar specimens”, Journal of Materials in Civil Engineering, 29(5), 1-9.

Rose, A. L., Suguna, K., & Ragnath, P. N. (2009). Strengthening of corrosion-damaged reinforced concrete beams with glass fiber reinforced polymer laminates. *Journal of Computer Science*, 5(6), 435.

Saatci, S., Yaşayanlar, S., Yaşayanlar, Y., & Batarlar, B. (2019). Effects of steel fibers on the punching behavior of reinforced concrete slabs with different longitudinal reinforcement ratios. Journal of the Faculty of Engineering and Architecture of Gazi University, 34(2), 1046-1059.

Sahoo. D.R.. Solanki. A. ve Kumar. A. (2015). “Influence of Steel and Polypropylene Fibers on Flexural Behavior of RC Beams” Journal of Meterials in Civil Engineering . 27(8)

Sezen, H., & Setzler, E. J. (2008). Reinforcement slip in reinforced concrete columns. ACI Structural Journal, 105(3), 280.

Shah, S. P., Daniel, J. I., Ahmad, S. H., Arockiasamy, M., Balaguru, P. N., Ball, C. G., & Casamatta, D. (1993). Guide for specifying, proportioning, mixing, placing, and finishing steel fiber reinforced concrete. *ACI Materials Journal*, 90(1), 94-101.

Sofi, A., & Phanikumar, B. R. (2015). An experimental investigation on flexural behaviour of fibre-reinforced pond ash-modified concrete. *Ain Shams Engineering Journal*, 6(4), 1133-1142.

Standard, A. S. T. M. (2003). G1-03. Standard practice for preparing, cleaning and evaluating corrosion test specimens", American Society for Testing and Materials.

Stanish, K. D. (1999). Corrosion effects on bond strength in reinforced concrete (Doctoral dissertation, National Library of Canada= Bibliothèque nationale du Canada)

Suffern, C., El-Sayed, A., & Soudki, K. (2010). Shear strength of disturbed regions with corroded stirrups in reinforced concrete beams. *Canadian Journal of Civil Engineering*, 37(8), 1045-1056.

Suffern, C.; El-Sayed, A. K.; and Soudki, K., (2010), "Shear Strength of Disturbed Regions with Corroded Stirrups in Reinforced Concrete Beams," *Canadian Journal of Civil Engineering*, V. 37, No. 8, pp. 1045-1056.

Tezel. O. (2010). "Farklı Tiplerdeki Çelik ve Polipropilen liflerin Kendinden Yerleşen Betonlarda İşlenebilirliğe ve Mekanik Davranışa Etkisi". Yüksek Lisans Tezi. İstanbul Teknik Üniversitesi.

Torres-Acosta, A. A., Navarro-Gutierrez, S., & Terán-Guillén, J. (2007). Residual flexure capacity of corroded reinforced concrete beams. *Engineering structures*, 29(6), 1145-1152.

Tuutti, K. (1982). Corrosion of steel in concrete. *Cement-och betonginst.*

Ünal, B., Köksal, F., ve Eyyubov, C., (2003). "Polipropilen ve Çelik Liflerin Betonun Donma-Çözülme ve Asınma Direncine Ortak Etkisi" TMMOB Insaat Mühendisleri

Odasi 5. Ulusal Beton Kongresi – Betonun Dayanıklılığı (Durabilite), Harbiye – İstanbul, (345-353)

Vidal, T., Castel, A., & Francois, R. (2004). Analyzing crack width to predict corrosion in reinforced concrete. *Cement and concrete research*, 34(1), 165-174.

Wang, L., Zhang, X., Zhang, J., Ma, Y., & Liu, Y. (2015). Effects of stirrup and inclined bar corrosion on shear behaviour of RC beams. *Construction and Building Materials*, 98, 537-546.

Wang, L., Zhang, X., Zhang, J., Ma, Y., & Liu, Y. (2015). Effects of stirrup and inclined bar corrosion on shear behavior of RC beams. *Construction and Building Materials*, 98, 537-546.

Yalciner, H, Kumbasaroglu, A., & Karimi, A., (2019). Prediction of Seismic Performance Levels of Corroded Reinforced Concrete Columns as a Function of Crack Width. *Advances in Civil Engineering Materials*, 8(3).

Yalciner, H., & Marar, K. (2017). Experimental study on the bond strength of different geometries of corroded and uncorroded reinforcement bars. *Journal of Materials in Civil Engineering*, 29(7), 05017002.

Yalciner, H., Eren, O., & Sensoy, S. (2012b). An experimental study on the bond strength between reinforcement bars and concrete as a function of concrete cover, strength and corrosion level. *Cement and Concrete Research*, 42(5), 643-655.

Yalciner, H., Sensoy, S., & Eren, O. (2012a). Effect of corrosion damage on the performance level of a 25-year-old reinforced concrete building. *Shock and Vibration*, 19(5), 891-902.

Yalciner, H., Sensoy, S., & Eren, O. (2015). Seismic performance assessment of a corroded 50-year-old reinforced concrete building. *Journal of Structural Engineering*, 141(12), 05015001.

Yildirim, S. T., Ekinci, C. E., (2005).“Karışık Lif Kullanımının Betonun Bazı Mekanik Özelliklerine Etkisinin İncelenmesi”, TMMOB İnşaat Mühendisleri Odası 6. Ulusal Beton Kongresi – Yüksek Performanslı Betonlar, Maslak – İstanbul, (327-336)

Zhu, W., & François, R. (2014). Corrosion of the reinforcement and its influence on the residual structural performance of a 26-year-old corroded RC beam. *Construction and Building Materials*, 51, 461-472.

Appendix A: Example of recorded corrosion current during accelerated corrosion method

Second	Hour	Current	Faraday's mass loss	Second *	Hour *	Day
1	0.72383 1	0.05	1.45E-05	0.05	1.38889E-05	1.16E-05
60	12:38	3.23	0.056086	193.8	0.053833333	0.000694
60	12:39	3.23	0.056086	193.8	0.053833333	0.000694
60	12:40	3.23	0.056086	193.8	0.053833333	0.000694
60	12:41	3.23	0.056086	193.8	0.053833333	0.000694
60	12:42	3.23	0.056086	193.8	0.053833333	0.000694
60	12:43	3.23	0.056086	193.8	0.053833333	0.000694
60	12:44	3.23	0.056086	193.8	0.053833333	0.000694
60	12:45	3.23	0.056086	193.8	0.053833333	0.000694
60	12:46	3.23	0.056086	193.8	0.053833333	0.000694
60	12:47	3.23	0.056086	193.8	0.053833333	0.000694
60	12:48	2.94	0.05105	176.4	0.049	0.000694
60	12:49	2.95	0.051224	177	0.049166667	0.000694
60	12:50	2.95	0.051224	177	0.049166667	0.000694
60	12:51	2.95	0.051224	177	0.049166667	0.000694
60	12:52	2.95	0.051224	177	0.049166667	0.000694
60	12:53	2.95	0.051224	177	0.049166667	0.000694
60	12:54	2.96	0.051398	177.6	0.049333333	0.000694
60	12:55	2.95	0.051224	177	0.049166667	0.000694
60	12:56	2.95	0.051224	177	0.049166667	0.000694
60	12:57	2.95	0.051224	177	0.049166667	0.000694
60	12:58	2.95	0.051224	177	0.049166667	0.000694
60	12:59	2.95	0.051224	177	0.049166667	0.000694
60	13:0	2.96	0.051398	177.6	0.049333333	0.000694
60	13:1	2.96	0.051398	177.6	0.049333333	0.000694
60	13:2	2.96	0.051398	177.6	0.049333333	0.000694
60	13:3	2.96	0.051398	177.6	0.049333333	0.000694
60	13:4	2.96	0.051398	177.6	0.049333333	0.000694
60	13:5	2.95	0.051224	177	0.049166667	0.000694
60	13:6	2.95	0.051224	177	0.049166667	0.000694
60	13:7	2.95	0.051224	177	0.049166667	0.000694
60	13:8	2.95	0.051224	177	0.049166667	0.000694
60	13:9	2.95	0.051224	177	0.049166667	0.000694
60	13:10	2.95	0.051224	177	0.049166667	0.000694

60	13:11	2.95	0.051224	177	0.049166667	0.000694
60	13:12	2.95	0.051224	177	0.049166667	0.000694
60	13:13	2.95	0.051224	177	0.049166667	0.000694
60	13:14	2.95	0.051224	177	0.049166667	0.000694
60	13:15	2.95	0.051224	177	0.049166667	0.000694
60	13:16	2.95	0.051224	177	0.049166667	0.000694
60	13:17	2.95	0.051224	177	0.049166667	0.000694
60	13:18	2.95	0.051224	177	0.049166667	0.000694
60	13:19	2.95	0.051224	177	0.049166667	0.000694
60	13:20	2.95	0.051224	177	0.049166667	0.000694
60	13:21	2.95	0.051224	177	0.049166667	0.000694
60	13:22	2.96	0.051398	177.6	0.049333333	0.000694
60	13:23	2.95	0.051224	177	0.049166667	0.000694
60	13:24	2.96	0.051398	177.6	0.049333333	0.000694
60	13:25	2.96	0.051398	177.6	0.049333333	0.000694
60	13:26	2.96	0.051398	177.6	0.049333333	0.000694
60	13:27	2.96	0.051398	177.6	0.049333333	0.000694
60	13:28	2.95	0.051224	177	0.049166667	0.000694
60	13:29	2.95	0.051224	177	0.049166667	0.000694
60	13:30	2.96	0.051398	177.6	0.049333333	0.000694
60	13:31	2.96	0.051398	177.6	0.049333333	0.000694
60	13:32	2.96	0.051398	177.6	0.049333333	0.000694
60	13:33	2.96	0.051398	177.6	0.049333333	0.000694
60	13:34	2.96	0.051398	177.6	0.049333333	0.000694
60	13:35	2.96	0.051398	177.6	0.049333333	0.000694
60	13:36	2.95	0.051224	177	0.049166667	0.000694
60	13:37	2.95	0.051224	177	0.049166667	0.000694
60	13:38	2.95	0.051224	177	0.049166667	0.000694
60	13:39	2.95	0.051224	177	0.049166667	0.000694
60	13:40	2.95	0.051224	177	0.049166667	0.000694
60	13:41	2.95	0.051224	177	0.049166667	0.000694
60	13:42	2.95	0.051224	177	0.049166667	0.000694
60	13:43	2.95	0.051224	177	0.049166667	0.000694
60	13:45	2.95	0.051224	177	0.049166667	0.000694
60	13:46	2.95	0.051224	177	0.049166667	0.000694
60	13:47	2.96	0.051398	177.6	0.049333333	0.000694
60	13:48	2.96	0.051398	177.6	0.049333333	0.000694
60	13:49	2.96	0.051398	177.6	0.049333333	0.000694
60	13:50	2.96	0.051398	177.6	0.049333333	0.000694
60	13:51	2.96	0.051398	177.6	0.049333333	0.000694
60	13:52	2.96	0.051398	177.6	0.049333333	0.000694

60	13:53	2.96	0.051398	177.6	0.049333333	0.000694
60	13:54	2.95	0.051224	177	0.049166667	0.000694
60	13:55	2.95	0.051224	177	0.049166667	0.000694
60	13:56	2.95	0.051224	177	0.049166667	0.000694
60	13:57	2.95	0.051224	177	0.049166667	0.000694
60	13:58	2.95	0.051224	177	0.049166667	0.000694
60	13:59	2.96	0.051398	177.6	0.049333333	0.000694
60	14:0	2.96	0.051398	177.6	0.049333333	0.000694
60	14:1	2.96	0.051398	177.6	0.049333333	0.000694
60	14:2	2.96	0.051398	177.6	0.049333333	0.000694
60	14:3	2.96	0.051398	177.6	0.049333333	0.000694
60	14:4	2.96	0.051398	177.6	0.049333333	0.000694
60	14:5	2.96	0.051398	177.6	0.049333333	0.000694
60	14:6	2.95	0.051224	177	0.049166667	0.000694
60	14:7	2.95	0.051224	177	0.049166667	0.000694
60	14:8	2.95	0.051224	177	0.049166667	0.000694
60	14:9	2.95	0.051224	177	0.049166667	0.000694
60	14:10	2.95	0.051224	177	0.049166667	0.000694
60	14:11	2.96	0.051398	177.6	0.049333333	0.000694
60	14:12	2.96	0.051398	177.6	0.049333333	0.000694
60	14:13	2.96	0.051398	177.6	0.049333333	0.000694
60	14:14	2.96	0.051398	177.6	0.049333333	0.000694
60	14:15	2.96	0.051398	177.6	0.049333333	0.000694
60	14:16	2.96	0.051398	177.6	0.049333333	0.000694
60	14:17	2.96	0.051398	177.6	0.049333333	0.000694
60	14:18	2.96	0.051398	177.6	0.049333333	0.000694
60	14:19	2.96	0.051398	177.6	0.049333333	0.000694
60	14:20	2.96	0.051398	177.6	0.049333333	0.000694
60	14:21	2.96	0.051398	177.6	0.049333333	0.000694
60	14:22	2.96	0.051398	177.6	0.049333333	0.000694
60	14:23	2.96	0.051398	177.6	0.049333333	0.000694
60	14:24	2.96	0.051398	177.6	0.049333333	0.000694
60	14:25	2.96	0.051398	177.6	0.049333333	0.000694
60	14:26	2.96	0.051398	177.6	0.049333333	0.000694
60	14:27	2.96	0.051398	177.6	0.049333333	0.000694
60	14:28	2.96	0.051398	177.6	0.049333333	0.000694
60	14:29	2.96	0.051398	177.6	0.049333333	0.000694
60	14:30	2.96	0.051398	177.6	0.049333333	0.000694
60	14:31	2.96	0.051398	177.6	0.049333333	0.000694
60	14:32	2.96	0.051398	177.6	0.049333333	0.000694
60	14:33	2.96	0.051398	177.6	0.049333333	0.000694

60	14:34	2.96	0.051398	177.6	0.049333333	0.000694
60	14:35	2.96	0.051398	177.6	0.049333333	0.000694
60	14:36	2.96	0.051398	177.6	0.049333333	0.000694
60	14:37	2.96	0.051398	177.6	0.049333333	0.000694
60	14:38	2.96	0.051398	177.6	0.049333333	0.000694
60	14:39	2.96	0.051398	177.6	0.049333333	0.000694
60	14:40	2.97	0.051571	178.2	0.0495	0.000694
60	14:41	2.97	0.051571	178.2	0.0495	0.000694
60	14:42	2.97	0.051571	178.2	0.0495	0.000694
60	14:43	2.97	0.051571	178.2	0.0495	0.000694
60	14:44	2.96	0.051398	177.6	0.049333333	0.000694
60	14:45	2.96	0.051398	177.6	0.049333333	0.000694
60	14:46	2.96	0.051398	177.6	0.049333333	0.000694
60	14:47	2.96	0.051398	177.6	0.049333333	0.000694
60	14:48	2.96	0.051398	177.6	0.049333333	0.000694
60	14:49	2.96	0.051398	177.6	0.049333333	0.000694
60	14:50	2.96	0.051398	177.6	0.049333333	0.000694
60	14:51	2.96	0.051398	177.6	0.049333333	0.000694
60	14:52	2.96	0.051398	177.6	0.049333333	0.000694
60	14:53	2.96	0.051398	177.6	0.049333333	0.000694
60	14:54	2.96	0.051398	177.6	0.049333333	0.000694
60	14:55	2.96	0.051398	177.6	0.049333333	0.000694
60	14:56	2.96	0.051398	177.6	0.049333333	0.000694
60	14:57	2.96	0.051398	177.6	0.049333333	0.000694
60	14:58	2.96	0.051398	177.6	0.049333333	0.000694
60	14:59	2.96	0.051398	177.6	0.049333333	0.000694
60	15:0	2.96	0.051398	177.6	0.049333333	0.000694
60	15:1	2.96	0.051398	177.6	0.049333333	0.000694
60	15:2	2.96	0.051398	177.6	0.049333333	0.000694
60	15:3	2.96	0.051398	177.6	0.049333333	0.000694
60	15:4	2.96	0.051398	177.6	0.049333333	0.000694
60	15:5	2.96	0.051398	177.6	0.049333333	0.000694
60	15:6	2.96	0.051398	177.6	0.049333333	0.000694
60	15:7	2.96	0.051398	177.6	0.049333333	0.000694
60	15:8	2.96	0.051398	177.6	0.049333333	0.000694
60	15:9	2.96	0.051398	177.6	0.049333333	0.000694
60	15:10	2.96	0.051398	177.6	0.049333333	0.000694
60	15:11	2.96	0.051398	177.6	0.049333333	0.000694
60	15:12	2.96	0.051398	177.6	0.049333333	0.000694
60	15:13	2.96	0.051398	177.6	0.049333333	0.000694
60	15:14	2.96	0.051398	177.6	0.049333333	0.000694

60	0:8	2.97	0.051571	178.2	0.0495	0.000694
60	0:9	2.97	0.051571	178.2	0.0495	0.000694
60	0:10	2.97	0.051571	178.2	0.0495	0.000694
60	0:11	2.97	0.051571	178.2	0.0495	0.000694
60	0:12	2.96	0.051398	177.6	0.049333333	0.000694
60	0:13	2.96	0.051398	177.6	0.049333333	0.000694
60	0:14	2.96	0.051398	177.6	0.049333333	0.000694
60	0:15	2.96	0.051398	177.6	0.049333333	0.000694
60	0:16	2.96	0.051398	177.6	0.049333333	0.000694
60	0:17	2.96	0.051398	177.6	0.049333333	0.000694
60	0:18	2.96	0.051398	177.6	0.049333333	0.000694
60	0:19	2.96	0.051398	177.6	0.049333333	0.000694
60	0:20	2.96	0.051398	177.6	0.049333333	0.000694
60	0:21	2.96	0.051398	177.6	0.049333333	0.000694
60	0:22	2.96	0.051398	177.6	0.049333333	0.000694
60	0:23	2.97	0.051571	178.2	0.0495	0.000694
60	0:24	2.97	0.051571	178.2	0.0495	0.000694
60	0:25	2.97	0.051571	178.2	0.0495	0.000694
60	0:26	2.97	0.051571	178.2	0.0495	0.000694
60	0:27	2.96	0.051398	177.6	0.049333333	0.000694
60	0:28	2.96	0.051398	177.6	0.049333333	0.000694
60	0:29	2.96	0.051398	177.6	0.049333333	0.000694
60	0:30	2.96	0.051398	177.6	0.049333333	0.000694
60	0:31	2.96	0.051398	177.6	0.049333333	0.000694
60	0:32	2.96	0.051398	177.6	0.049333333	0.000694
60	0:33	2.96	0.051398	177.6	0.049333333	0.000694
60	0:34	2.96	0.051398	177.6	0.049333333	0.000694
60	0:35	2.96	0.051398	177.6	0.049333333	0.000694
60	0:36	2.96	0.051398	177.6	0.049333333	0.000694
60	0:37	2.96	0.051398	177.6	0.049333333	0.000694
60	0:38	2.96	0.051398	177.6	0.049333333	0.000694
60	0:39	2.96	0.051398	177.6	0.049333333	0.000694
60	0:40	2.96	0.051398	177.6	0.049333333	0.000694
60	0:41	2.96	0.051398	177.6	0.049333333	0.000694
60	0:42	2.96	0.051398	177.6	0.049333333	0.000694
60	0:43	2.96	0.051398	177.6	0.049333333	0.000694
60	0:44	2.96	0.051398	177.6	0.049333333	0.000694
60	0:45	2.96	0.051398	177.6	0.049333333	0.000694
60	0:46	2.96	0.051398	177.6	0.049333333	0.000694
60	0:47	2.96	0.051398	177.6	0.049333333	0.000694
60	0:48	2.97	0.051571	178.2	0.0495	0.000694

60	0:49	2.97	0.051571	178.2	0.0495	0.000694
60	0:50	2.97	0.051571	178.2	0.0495	0.000694
60	0:51	2.97	0.051571	178.2	0.0495	0.000694
60	0:52	2.97	0.051571	178.2	0.0495	0.000694
60	0:53	2.96	0.051398	177.6	0.049333333	0.000694
60	0:54	2.96	0.051398	177.6	0.049333333	0.000694
60	0:55	2.96	0.051398	177.6	0.049333333	0.000694
60	0:56	2.96	0.051398	177.6	0.049333333	0.000694
60	0:57	2.96	0.051398	177.6	0.049333333	0.000694
60	0:58	2.96	0.051398	177.6	0.049333333	0.000694
60	0:59	2.96	0.051398	177.6	0.049333333	0.000694
60	1:0	2.96	0.051398	177.6	0.049333333	0.000694
60	1:1	2.96	0.051398	177.6	0.049333333	0.000694
60	1:2	2.96	0.051398	177.6	0.049333333	0.000694
60	1:3	2.96	0.051398	177.6	0.049333333	0.000694
60	1:4	2.96	0.051398	177.6	0.049333333	0.000694
60	1:5	2.96	0.051398	177.6	0.049333333	0.000694
60	1:6	2.96	0.051398	177.6	0.049333333	0.000694
60	1:7	2.96	0.051398	177.6	0.049333333	0.000694
60	1:8	2.96	0.051398	177.6	0.049333333	0.000694
60	1:9	2.96	0.051398	177.6	0.049333333	0.000694
60	1:10	2.96	0.051398	177.6	0.049333333	0.000694
60	1:11	2.96	0.051398	177.6	0.049333333	0.000694
60	1:12	2.96	0.051398	177.6	0.049333333	0.000694
60	1:13	2.96	0.051398	177.6	0.049333333	0.000694
60	1:14	2.96	0.051398	177.6	0.049333333	0.000694
60	1:15	2.96	0.051398	177.6	0.049333333	0.000694
60	1:16	2.96	0.051398	177.6	0.049333333	0.000694
60	1:17	2.96	0.051398	177.6	0.049333333	0.000694
60	1:18	2.96	0.051398	177.6	0.049333333	0.000694
60	1:19	2.96	0.051398	177.6	0.049333333	0.000694
60	1:20	2.96	0.051398	177.6	0.049333333	0.000694
60	1:21	2.96	0.051398	177.6	0.049333333	0.000694
60	1:22	2.96	0.051398	177.6	0.049333333	0.000694
60	1:23	2.96	0.051398	177.6	0.049333333	0.000694
60	1:24	2.96	0.051398	177.6	0.049333333	0.000694
60	1:25	2.96	0.051398	177.6	0.049333333	0.000694
60	1:26	2.96	0.051398	177.6	0.049333333	0.000694
60	1:27	2.96	0.051398	177.6	0.049333333	0.000694
60	1:28	2.96	0.051398	177.6	0.049333333	0.000694
60	1:29	2.96	0.051398	177.6	0.049333333	0.000694

60	1:30	2.96	0.051398	177.6	0.049333333	0.000694
60	1:31	2.96	0.051398	177.6	0.049333333	0.000694
60	1:32	2.96	0.051398	177.6	0.049333333	0.000694
60	1:33	2.96	0.051398	177.6	0.049333333	0.000694
60	1:34	2.96	0.051398	177.6	0.049333333	0.000694
60	1:35	2.96	0.051398	177.6	0.049333333	0.000694
60	1:36	2.96	0.051398	177.6	0.049333333	0.000694
60	1:37	2.96	0.051398	177.6	0.049333333	0.000694
60	1:38	2.97	0.051571	178.2	0.0495	0.000694
60	1:39	2.96	0.051398	177.6	0.049333333	0.000694
60	1:40	2.96	0.051398	177.6	0.049333333	0.000694
60	1:41	2.96	0.051398	177.6	0.049333333	0.000694
60	1:42	2.96	0.051398	177.6	0.049333333	0.000694
60	1:43	2.96	0.051398	177.6	0.049333333	0.000694
60	1:44	2.96	0.051398	177.6	0.049333333	0.000694
60	1:45	2.96	0.051398	177.6	0.049333333	0.000694
60	1:46	2.96	0.051398	177.6	0.049333333	0.000694
60	1:47	2.96	0.051398	177.6	0.049333333	0.000694
60	1:48	2.96	0.051398	177.6	0.049333333	0.000694
60	1:49	2.96	0.051398	177.6	0.049333333	0.000694
60	1:50	2.96	0.051398	177.6	0.049333333	0.000694
60	1:51	2.96	0.051398	177.6	0.049333333	0.000694
60	1:52	2.96	0.051398	177.6	0.049333333	0.000694
60	1:53	2.96	0.051398	177.6	0.049333333	0.000694
60	1:54	2.96	0.051398	177.6	0.049333333	0.000694
60	1:55	2.96	0.051398	177.6	0.049333333	0.000694
60	1:56	2.96	0.051398	177.6	0.049333333	0.000694
60	1:57	2.96	0.051398	177.6	0.049333333	0.000694
60	1:58	2.96	0.051398	177.6	0.049333333	0.000694
60	1:59	2.96	0.051398	177.6	0.049333333	0.000694
60	2:0	2.96	0.051398	177.6	0.049333333	0.000694
60	2:1	2.96	0.051398	177.6	0.049333333	0.000694
60	2:2	2.96	0.051398	177.6	0.049333333	0.000694
60	2:3	2.96	0.051398	177.6	0.049333333	0.000694
60	2:4	2.96	0.051398	177.6	0.049333333	0.000694
60	2:5	2.96	0.051398	177.6	0.049333333	0.000694
60	2:6	2.96	0.051398	177.6	0.049333333	0.000694
60	2:7	2.96	0.051398	177.6	0.049333333	0.000694
60	2:8	2.96	0.051398	177.6	0.049333333	0.000694
60	2:9	2.96	0.051398	177.6	0.049333333	0.000694
60	2:10	2.96	0.051398	177.6	0.049333333	0.000694

60	2:52	2.96	0.051398	177.6	0.049333333	0.000694
60	2:53	2.96	0.051398	177.6	0.049333333	0.000694
60	2:54	2.96	0.051398	177.6	0.049333333	0.000694
60	2:55	2.96	0.051398	177.6	0.049333333	0.000694
60	2:56	2.96	0.051398	177.6	0.049333333	0.000694
60	2:57	2.96	0.051398	177.6	0.049333333	0.000694
60	2:58	2.96	0.051398	177.6	0.049333333	0.000694
60	2:59	2.96	0.051398	177.6	0.049333333	0.000694
60	3:0	2.96	0.051398	177.6	0.049333333	0.000694
60	3:1	2.96	0.051398	177.6	0.049333333	0.000694
60	3:2	2.96	0.051398	177.6	0.049333333	0.000694
60	3:3	2.96	0.051398	177.6	0.049333333	0.000694
60	3:4	2.96	0.051398	177.6	0.049333333	0.000694
60	3:5	2.96	0.051398	177.6	0.049333333	0.000694
60	3:6	2.97	0.051571	178.2	0.0495	0.000694
60	3:7	2.96	0.051398	177.6	0.049333333	0.000694
60	3:8	2.96	0.051398	177.6	0.049333333	0.000694
60	3:9	2.96	0.051398	177.6	0.049333333	0.000694
60	3:10	2.96	0.051398	177.6	0.049333333	0.000694
60	3:11	2.96	0.051398	177.6	0.049333333	0.000694
60	3:12	2.96	0.051398	177.6	0.049333333	0.000694
60	3:13	2.96	0.051398	177.6	0.049333333	0.000694
60	3:14	2.96	0.051398	177.6	0.049333333	0.000694
60	3:15	2.96	0.051398	177.6	0.049333333	0.000694
60	3:16	2.96	0.051398	177.6	0.049333333	0.000694
60	3:17	2.96	0.051398	177.6	0.049333333	0.000694
60	3:18	2.96	0.051398	177.6	0.049333333	0.000694
60	3:19	2.96	0.051398	177.6	0.049333333	0.000694
60	3:20	2.96	0.051398	177.6	0.049333333	0.000694
60	3:21	2.96	0.051398	177.6	0.049333333	0.000694
60	3:22	2.96	0.051398	177.6	0.049333333	0.000694
60	3:23	2.96	0.051398	177.6	0.049333333	0.000694
60	3:24	2.96	0.051398	177.6	0.049333333	0.000694
60	3:25	2.96	0.051398	177.6	0.049333333	0.000694
60	3:26	2.97	0.051571	178.2	0.0495	0.000694
60	3:27	2.96	0.051398	177.6	0.049333333	0.000694
60	3:28	2.96	0.051398	177.6	0.049333333	0.000694
60	3:29	2.96	0.051398	177.6	0.049333333	0.000694
60	3:30	2.96	0.051398	177.6	0.049333333	0.000694
60	3:31	2.96	0.051398	177.6	0.049333333	0.000694
60	3:32	2.96	0.051398	177.6	0.049333333	0.000694

60	3:33	2.96	0.051398	177.6	0.049333333	0.000694
60	3:34	2.96	0.051398	177.6	0.049333333	0.000694
60	3:35	2.96	0.051398	177.6	0.049333333	0.000694
60	3:36	2.96	0.051398	177.6	0.049333333	0.000694
60	3:37	2.96	0.051398	177.6	0.049333333	0.000694
60	3:38	2.96	0.051398	177.6	0.049333333	0.000694
60	3:39	2.96	0.051398	177.6	0.049333333	0.000694
60	3:40	2.96	0.051398	177.6	0.049333333	0.000694
60	3:41	2.96	0.051398	177.6	0.049333333	0.000694
60	3:42	2.96	0.051398	177.6	0.049333333	0.000694
60	3:43	2.97	0.051571	178.2	0.0495	0.000694
60	3:44	2.97	0.051571	178.2	0.0495	0.000694
60	3:45	2.97	0.051571	178.2	0.0495	0.000694
60	3:46	2.97	0.051571	178.2	0.0495	0.000694
60	3:47	2.96	0.051398	177.6	0.049333333	0.000694
60	3:48	2.96	0.051398	177.6	0.049333333	0.000694
60	3:49	2.96	0.051398	177.6	0.049333333	0.000694
60	3:50	2.96	0.051398	177.6	0.049333333	0.000694
60	3:51	2.96	0.051398	177.6	0.049333333	0.000694
60	3:52	2.96	0.051398	177.6	0.049333333	0.000694
60	3:53	2.96	0.051398	177.6	0.049333333	0.000694
60	3:54	2.96	0.051398	177.6	0.049333333	0.000694
60	3:55	2.96	0.051398	177.6	0.049333333	0.000694
60	3:56	2.96	0.051398	177.6	0.049333333	0.000694
60	3:57	2.96	0.051398	177.6	0.049333333	0.000694
60	3:58	2.96	0.051398	177.6	0.049333333	0.000694
60	3:59	2.96	0.051398	177.6	0.049333333	0.000694
60	4:0	2.96	0.051398	177.6	0.049333333	0.000694
60	4:1	2.96	0.051398	177.6	0.049333333	0.000694
60	4:2	2.96	0.051398	177.6	0.049333333	0.000694
60	4:3	2.96	0.051398	177.6	0.049333333	0.000694
60	4:4	2.96	0.051398	177.6	0.049333333	0.000694
60	4:5	2.96	0.051398	177.6	0.049333333	0.000694
60	4:6	2.96	0.051398	177.6	0.049333333	0.000694
60	4:7	2.96	0.051398	177.6	0.049333333	0.000694
60	4:8	2.96	0.051398	177.6	0.049333333	0.000694
60	4:9	2.96	0.051398	177.6	0.049333333	0.000694
60	4:10	2.96	0.051398	177.6	0.049333333	0.000694
60	4:11	2.96	0.051398	177.6	0.049333333	0.000694
60	4:12	2.96	0.051398	177.6	0.049333333	0.000694
60	4:13	2.96	0.051398	177.6	0.049333333	0.000694

60	4:14	2.96	0.051398	177.6	0.049333333	0.000694
60	4:15	2.96	0.051398	177.6	0.049333333	0.000694
60	4:16	2.96	0.051398	177.6	0.049333333	0.000694
60	4:17	2.96	0.051398	177.6	0.049333333	0.000694
60	4:18	2.96	0.051398	177.6	0.049333333	0.000694
60	4:19	2.96	0.051398	177.6	0.049333333	0.000694
60	4:20	2.96	0.051398	177.6	0.049333333	0.000694
60	4:21	2.96	0.051398	177.6	0.049333333	0.000694
60	4:22	2.96	0.051398	177.6	0.049333333	0.000694
60	4:23	2.96	0.051398	177.6	0.049333333	0.000694
60	4:24	2.96	0.051398	177.6	0.049333333	0.000694
60	4:25	2.96	0.051398	177.6	0.049333333	0.000694
60	4:26	2.96	0.051398	177.6	0.049333333	0.000694
60	4:27	2.96	0.051398	177.6	0.049333333	0.000694
60	4:28	2.96	0.051398	177.6	0.049333333	0.000694
60	4:29	2.96	0.051398	177.6	0.049333333	0.000694
60	4:30	2.96	0.051398	177.6	0.049333333	0.000694
60	4:31	2.96	0.051398	177.6	0.049333333	0.000694
60	4:32	2.96	0.051398	177.6	0.049333333	0.000694
60	4:33	2.97	0.051571	178.2	0.0495	0.000694
60	4:34	2.97	0.051571	178.2	0.0495	0.000694
60	4:35	2.97	0.051571	178.2	0.0495	0.000694
60	4:36	2.97	0.051571	178.2	0.0495	0.000694
60	4:37	2.96	0.051398	177.6	0.049333333	0.000694
60	4:38	2.96	0.051398	177.6	0.049333333	0.000694
60	4:39	2.96	0.051398	177.6	0.049333333	0.000694
60	4:40	2.96	0.051398	177.6	0.049333333	0.000694
60	4:41	2.96	0.051398	177.6	0.049333333	0.000694
60	4:42	2.96	0.051398	177.6	0.049333333	0.000694
60	4:43	2.96	0.051398	177.6	0.049333333	0.000694
60	4:44	2.96	0.051398	177.6	0.049333333	0.000694
60	4:45	2.96	0.051398	177.6	0.049333333	0.000694
60	4:46	2.96	0.051398	177.6	0.049333333	0.000694
60	4:47	2.96	0.051398	177.6	0.049333333	0.000694
60	4:48	2.96	0.051398	177.6	0.049333333	0.000694
60	4:49	2.96	0.051398	177.6	0.049333333	0.000694
60	4:50	2.96	0.051398	177.6	0.049333333	0.000694
60	4:51	2.96	0.051398	177.6	0.049333333	0.000694
60	4:52	2.97	0.051571	178.2	0.0495	0.000694
60	4:53	2.96	0.051398	177.6	0.049333333	0.000694
60	4:54	2.96	0.051398	177.6	0.049333333	0.000694

60	4:55	2.96	0.051398	177.6	0.049333333	0.000694
60	4:56	2.96	0.051398	177.6	0.049333333	0.000694
60	4:57	2.96	0.051398	177.6	0.049333333	0.000694
60	4:58	2.96	0.051398	177.6	0.049333333	0.000694
60	4:59	2.96	0.051398	177.6	0.049333333	0.000694
60	5:0	2.96	0.051398	177.6	0.049333333	0.000694
60	5:1	2.96	0.051398	177.6	0.049333333	0.000694
60	5:2	2.96	0.051398	177.6	0.049333333	0.000694
60	5:3	2.96	0.051398	177.6	0.049333333	0.000694
60	5:4	2.96	0.051398	177.6	0.049333333	0.000694
60	5:5	2.96	0.051398	177.6	0.049333333	0.000694
60	5:6	2.96	0.051398	177.6	0.049333333	0.000694
60	5:7	2.96	0.051398	177.6	0.049333333	0.000694
60	5:8	2.96	0.051398	177.6	0.049333333	0.000694
60	5:9	2.96	0.051398	177.6	0.049333333	0.000694
60	5:10	2.96	0.051398	177.6	0.049333333	0.000694
60	5:11	2.96	0.051398	177.6	0.049333333	0.000694
60	5:12	2.96	0.051398	177.6	0.049333333	0.000694
60	5:13	2.96	0.051398	177.6	0.049333333	0.000694
60	5:14	2.96	0.051398	177.6	0.049333333	0.000694
60	5:15	2.96	0.051398	177.6	0.049333333	0.000694
60	5:16	2.96	0.051398	177.6	0.049333333	0.000694
60	5:17	2.96	0.051398	177.6	0.049333333	0.000694
60	5:18	2.96	0.051398	177.6	0.049333333	0.000694
60	5:19	2.96	0.051398	177.6	0.049333333	0.000694
60	5:20	2.96	0.051398	177.6	0.049333333	0.000694
60	5:21	2.96	0.051398	177.6	0.049333333	0.000694
60	5:22	2.96	0.051398	177.6	0.049333333	0.000694
60	5:23	2.96	0.051398	177.6	0.049333333	0.000694
60	5:24	2.96	0.051398	177.6	0.049333333	0.000694
60	5:25	2.96	0.051398	177.6	0.049333333	0.000694
60	5:26	2.96	0.051398	177.6	0.049333333	0.000694
60	5:27	2.96	0.051398	177.6	0.049333333	0.000694
60	5:28	2.97	0.051571	178.2	0.0495	0.000694
60	5:29	2.97	0.051571	178.2	0.0495	0.000694
60	5:30	2.97	0.051571	178.2	0.0495	0.000694
60	5:31	2.97	0.051571	178.2	0.0495	0.000694
60	5:32	2.97	0.051571	178.2	0.0495	0.000694
60	5:33	2.96	0.051398	177.6	0.049333333	0.000694
60	5:34	2.96	0.051398	177.6	0.049333333	0.000694
60	5:35	2.96	0.051398	177.6	0.049333333	0.000694

60	5:36	2.96	0.051398	177.6	0.049333333	0.000694
60	5:37	2.96	0.051398	177.6	0.049333333	0.000694
60	5:38	2.96	0.051398	177.6	0.049333333	0.000694
60	5:39	2.96	0.051398	177.6	0.049333333	0.000694
60	5:40	2.96	0.051398	177.6	0.049333333	0.000694
60	5:41	2.96	0.051398	177.6	0.049333333	0.000694
60	5:42	2.96	0.051398	177.6	0.049333333	0.000694
60	5:43	2.96	0.051398	177.6	0.049333333	0.000694
60	5:44	2.96	0.051398	177.6	0.049333333	0.000694
60	5:45	2.96	0.051398	177.6	0.049333333	0.000694
60	5:46	2.96	0.051398	177.6	0.049333333	0.000694
60	5:47	2.96	0.051398	177.6	0.049333333	0.000694
60	5:48	2.96	0.051398	177.6	0.049333333	0.000694
60	5:49	2.96	0.051398	177.6	0.049333333	0.000694
60	5:50	2.96	0.051398	177.6	0.049333333	0.000694
60	5:51	2.96	0.051398	177.6	0.049333333	0.000694
60	5:52	2.96	0.051398	177.6	0.049333333	0.000694
60	5:53	2.96	0.051398	177.6	0.049333333	0.000694
60	5:54	2.96	0.051398	177.6	0.049333333	0.000694
60	5:55	2.96	0.051398	177.6	0.049333333	0.000694
60	5:56	2.96	0.051398	177.6	0.049333333	0.000694
60	5:57	2.96	0.051398	177.6	0.049333333	0.000694
60	5:58	2.96	0.051398	177.6	0.049333333	0.000694
60	5:59	2.96	0.051398	177.6	0.049333333	0.000694
60	6:0	2.96	0.051398	177.6	0.049333333	0.000694
60	6:1	2.96	0.051398	177.6	0.049333333	0.000694
60	6:2	2.96	0.051398	177.6	0.049333333	0.000694
60	6:3	2.96	0.051398	177.6	0.049333333	0.000694
60	6:4	2.96	0.051398	177.6	0.049333333	0.000694
60	6:5	2.96	0.051398	177.6	0.049333333	0.000694
60	6:6	2.96	0.051398	177.6	0.049333333	0.000694
60	6:7	2.96	0.051398	177.6	0.049333333	0.000694
60	6:8	2.96	0.051398	177.6	0.049333333	0.000694
60	6:9	2.96	0.051398	177.6	0.049333333	0.000694
60	6:10	2.96	0.051398	177.6	0.049333333	0.000694
60	6:11	2.96	0.051398	177.6	0.049333333	0.000694
60	6:12	2.96	0.051398	177.6	0.049333333	0.000694
60	6:13	2.97	0.051571	178.2	0.0495	0.000694
60	6:14	2.96	0.051398	177.6	0.049333333	0.000694
60	6:15	2.96	0.051398	177.6	0.049333333	0.000694
60	6:16	2.96	0.051398	177.6	0.049333333	0.000694

60	6:17	2.96	0.051398	177.6	0.049333333	0.000694
60	6:18	2.96	0.051398	177.6	0.049333333	0.000694
60	6:19	2.96	0.051398	177.6	0.049333333	0.000694
60	6:20	2.96	0.051398	177.6	0.049333333	0.000694
60	6:21	2.96	0.051398	177.6	0.049333333	0.000694
60	6:22	2.96	0.051398	177.6	0.049333333	0.000694
60	6:23	2.97	0.051571	178.2	0.0495	0.000694
60	6:24	2.97	0.051571	178.2	0.0495	0.000694
60	6:25	2.97	0.051571	178.2	0.0495	0.000694
60	6:26	2.97	0.051571	178.2	0.0495	0.000694
60	6:27	2.97	0.051571	178.2	0.0495	0.000694
60	6:28	2.96	0.051398	177.6	0.049333333	0.000694
60	6:29	2.96	0.051398	177.6	0.049333333	0.000694
60	6:30	2.96	0.051398	177.6	0.049333333	0.000694
60	6:31	2.96	0.051398	177.6	0.049333333	0.000694
60	6:32	2.96	0.051398	177.6	0.049333333	0.000694
60	6:33	2.96	0.051398	177.6	0.049333333	0.000694
60	6:34	2.96	0.051398	177.6	0.049333333	0.000694
60	6:35	2.96	0.051398	177.6	0.049333333	0.000694
60	6:36	2.96	0.051398	177.6	0.049333333	0.000694
60	6:37	2.96	0.051398	177.6	0.049333333	0.000694
60	6:38	2.96	0.051398	177.6	0.049333333	0.000694
60	6:39	2.96	0.051398	177.6	0.049333333	0.000694
60	6:40	2.96	0.051398	177.6	0.049333333	0.000694
60	6:41	2.96	0.051398	177.6	0.049333333	0.000694
60	6:42	2.96	0.051398	177.6	0.049333333	0.000694
60	6:43	2.96	0.051398	177.6	0.049333333	0.000694
60	6:44	2.96	0.051398	177.6	0.049333333	0.000694
60	6:45	2.96	0.051398	177.6	0.049333333	0.000694
60	6:46	2.96	0.051398	177.6	0.049333333	0.000694
60	6:47	2.96	0.051398	177.6	0.049333333	0.000694
60	6:48	2.96	0.051398	177.6	0.049333333	0.000694
60	6:49	2.96	0.051398	177.6	0.049333333	0.000694
60	6:50	2.96	0.051398	177.6	0.049333333	0.000694
60	6:51	2.96	0.051398	177.6	0.049333333	0.000694
60	6:52	2.96	0.051398	177.6	0.049333333	0.000694
60	6:53	2.96	0.051398	177.6	0.049333333	0.000694
60	6:54	2.96	0.051398	177.6	0.049333333	0.000694
60	6:55	2.96	0.051398	177.6	0.049333333	0.000694
60	6:56	2.96	0.051398	177.6	0.049333333	0.000694
60	6:57	2.96	0.051398	177.6	0.049333333	0.000694

60	6:58	2.96	0.051398	177.6	0.049333333	0.000694
60	6:59	2.96	0.051398	177.6	0.049333333	0.000694
60	7:0	2.96	0.051398	177.6	0.049333333	0.000694
60	7:1	2.96	0.051398	177.6	0.049333333	0.000694
60	7:2	2.96	0.051398	177.6	0.049333333	0.000694
60	7:3	2.96	0.051398	177.6	0.049333333	0.000694
60	7:4	2.96	0.051398	177.6	0.049333333	0.000694
60	7:5	2.96	0.051398	177.6	0.049333333	0.000694
60	7:6	2.96	0.051398	177.6	0.049333333	0.000694
60	7:7	2.96	0.051398	177.6	0.049333333	0.000694
60	7:8	2.96	0.051398	177.6	0.049333333	0.000694
60	7:9	2.96	0.051398	177.6	0.049333333	0.000694
60	7:10	2.96	0.051398	177.6	0.049333333	0.000694
60	7:11	2.96	0.051398	177.6	0.049333333	0.000694
60	7:12	2.96	0.051398	177.6	0.049333333	0.000694
60	7:13	2.97	0.051571	178.2	0.0495	0.000694
60	7:14	2.97	0.051571	178.2	0.0495	0.000694
60	7:15	2.97	0.051571	178.2	0.0495	0.000694
60	7:16	2.97	0.051571	178.2	0.0495	0.000694
60	7:17	2.97	0.051571	178.2	0.0495	0.000694
60	7:18	2.97	0.051571	178.2	0.0495	0.000694
60	7:19	2.97	0.051571	178.2	0.0495	0.000694
60	7:20	2.97	0.051571	178.2	0.0495	0.000694
60	7:21	2.97	0.051571	178.2	0.0495	0.000694
60	7:22	2.97	0.051571	178.2	0.0495	0.000694
60	7:23	2.97	0.051571	178.2	0.0495	0.000694
60	7:24	2.96	0.051398	177.6	0.049333333	0.000694
60	7:25	2.96	0.051398	177.6	0.049333333	0.000694
60	7:26	2.96	0.051398	177.6	0.049333333	0.000694
60	7:27	2.96	0.051398	177.6	0.049333333	0.000694
60	7:28	2.96	0.051398	177.6	0.049333333	0.000694
60	7:29	2.96	0.051398	177.6	0.049333333	0.000694
60	7:30	2.96	0.051398	177.6	0.049333333	0.000694
60	7:31	2.96	0.051398	177.6	0.049333333	0.000694
60	7:32	2.96	0.051398	177.6	0.049333333	0.000694
60	7:33	2.96	0.051398	177.6	0.049333333	0.000694
60	7:34	2.96	0.051398	177.6	0.049333333	0.000694
60	7:35	2.96	0.051398	177.6	0.049333333	0.000694
60	7:36	2.96	0.051398	177.6	0.049333333	0.000694
60	7:37	2.96	0.051398	177.6	0.049333333	0.000694
60	7:38	2.96	0.051398	177.6	0.049333333	0.000694

60	7:39	2.96	0.051398	177.6	0.049333333	0.000694
60	7:40	2.96	0.051398	177.6	0.049333333	0.000694
60	7:41	2.96	0.051398	177.6	0.049333333	0.000694
60	7:42	2.96	0.051398	177.6	0.049333333	0.000694
60	7:43	2.96	0.051398	177.6	0.049333333	0.000694
60	7:44	2.96	0.051398	177.6	0.049333333	0.000694
60	7:45	2.96	0.051398	177.6	0.049333333	0.000694
60	7:46	2.96	0.051398	177.6	0.049333333	0.000694
60	7:47	2.96	0.051398	177.6	0.049333333	0.000694
60	7:48	2.96	0.051398	177.6	0.049333333	0.000694
60	7:49	2.96	0.051398	177.6	0.049333333	0.000694
60	7:50	2.96	0.051398	177.6	0.049333333	0.000694
60	7:51	2.96	0.051398	177.6	0.049333333	0.000694
60	7:52	2.96	0.051398	177.6	0.049333333	0.000694
60	7:53	2.96	0.051398	177.6	0.049333333	0.000694
60	7:54	2.96	0.051398	177.6	0.049333333	0.000694
60	7:55	2.96	0.051398	177.6	0.049333333	0.000694
60	7:56	2.96	0.051398	177.6	0.049333333	0.000694
60	7:57	2.96	0.051398	177.6	0.049333333	0.000694
60	7:58	2.97	0.051571	178.2	0.0495	0.000694
60	7:59	2.96	0.051398	177.6	0.049333333	0.000694
60	8:0	2.96	0.051398	177.6	0.049333333	0.000694
60	8:1	2.96	0.051398	177.6	0.049333333	0.000694
60	8:2	2.96	0.051398	177.6	0.049333333	0.000694
60	8:3	2.96	0.051398	177.6	0.049333333	0.000694
60	8:4	2.96	0.051398	177.6	0.049333333	0.000694
60	8:5	2.96	0.051398	177.6	0.049333333	0.000694
60	8:6	2.96	0.051398	177.6	0.049333333	0.000694
60	8:7	2.96	0.051398	177.6	0.049333333	0.000694
60	8:8	2.97	0.051571	178.2	0.0495	0.000694
60	8:9	2.97	0.051571	178.2	0.0495	0.000694
60	8:10	2.97	0.051571	178.2	0.0495	0.000694
60	8:11	2.97	0.051571	178.2	0.0495	0.000694
60	8:12	2.97	0.051571	178.2	0.0495	0.000694
60	8:13	2.96	0.051398	177.6	0.049333333	0.000694
60	8:14	2.96	0.051398	177.6	0.049333333	0.000694
60	8:15	2.96	0.051398	177.6	0.049333333	0.000694
60	8:16	2.96	0.051398	177.6	0.049333333	0.000694
60	8:17	2.96	0.051398	177.6	0.049333333	0.000694
60	8:18	2.96	0.051398	177.6	0.049333333	0.000694
60	8:19	2.96	0.051398	177.6	0.049333333	0.000694

60	9:1	2.96	0.051398	177.6	0.049333333	0.000694
60	9:2	2.96	0.051398	177.6	0.049333333	0.000694
60	9:3	2.96	0.051398	177.6	0.049333333	0.000694
60	9:4	2.96	0.051398	177.6	0.049333333	0.000694
60	9:5	2.96	0.051398	177.6	0.049333333	0.000694
60	9:6	2.96	0.051398	177.6	0.049333333	0.000694
60	9:7	2.96	0.051398	177.6	0.049333333	0.000694
60	9:8	2.96	0.051398	177.6	0.049333333	0.000694
60	9:9	2.96	0.051398	177.6	0.049333333	0.000694
60	9:10	2.96	0.051398	177.6	0.049333333	0.000694
60	9:11	2.96	0.051398	177.6	0.049333333	0.000694
60	9:12	2.96	0.051398	177.6	0.049333333	0.000694
60	9:13	2.96	0.051398	177.6	0.049333333	0.000694
60	9:14	2.96	0.051398	177.6	0.049333333	0.000694
60	9:15	2.96	0.051398	177.6	0.049333333	0.000694
60	9:16	2.96	0.051398	177.6	0.049333333	0.000694
60	9:17	2.96	0.051398	177.6	0.049333333	0.000694
60	9:18	2.96	0.051398	177.6	0.049333333	0.000694
60	9:19	2.96	0.051398	177.6	0.049333333	0.000694
60	9:20	2.96	0.051398	177.6	0.049333333	0.000694
60	9:21	2.96	0.051398	177.6	0.049333333	0.000694
60	9:22	2.96	0.051398	177.6	0.049333333	0.000694
60	9:23	2.96	0.051398	177.6	0.049333333	0.000694
60	9:24	2.96	0.051398	177.6	0.049333333	0.000694
60	9:25	2.96	0.051398	177.6	0.049333333	0.000694
60	9:26	2.96	0.051398	177.6	0.049333333	0.000694
60	9:27	2.96	0.051398	177.6	0.049333333	0.000694
60	9:28	2.96	0.051398	177.6	0.049333333	0.000694
60	9:29	2.97	0.051571	178.2	0.0495	0.000694
60	9:30	2.96	0.051398	177.6	0.049333333	0.000694
60	9:31	2.96	0.051398	177.6	0.049333333	0.000694
60	9:32	2.96	0.051398	177.6	0.049333333	0.000694
60	9:33	2.96	0.051398	177.6	0.049333333	0.000694
60	9:34	2.96	0.051398	177.6	0.049333333	0.000694
60	9:35	2.97	0.051571	178.2	0.0495	0.000694
60	9:36	2.96	0.051398	177.6	0.049333333	0.000694
60	9:37	2.96	0.051398	177.6	0.049333333	0.000694
60	9:38	2.96	0.051398	177.6	0.049333333	0.000694
60	9:39	2.96	0.051398	177.6	0.049333333	0.000694
60	9:40	2.97	0.051571	178.2	0.0495	0.000694
60	9:41	2.97	0.051571	178.2	0.0495	0.000694

60	9:42	2.97	0.051571	178.2	0.0495	0.000694
60	9:43	2.97	0.051571	178.2	0.0495	0.000694
60	9:44	2.97	0.051571	178.2	0.0495	0.000694
60	9:45	2.96	0.051398	177.6	0.0493333333	0.000694
60	9:46	2.96	0.051398	177.6	0.0493333333	0.000694
60	9:47	2.96	0.051398	177.6	0.0493333333	0.000694
60	9:48	2.96	0.051398	177.6	0.0493333333	0.000694
60	9:49	2.96	0.051398	177.6	0.0493333333	0.000694
60	9:50	2.96	0.051398	177.6	0.0493333333	0.000694
60	9:51	2.96	0.051398	177.6	0.0493333333	0.000694
60	9:52	2.96	0.051398	177.6	0.0493333333	0.000694
60	9:53	2.96	0.051398	177.6	0.0493333333	0.000694
60	9:54	2.96	0.051398	177.6	0.0493333333	0.000694
60	9:55	2.96	0.051398	177.6	0.0493333333	0.000694
60	9:56	2.96	0.051398	177.6	0.0493333333	0.000694
60	9:57	2.97	0.051571	178.2	0.0495	0.000694
60	9:58	2.97	0.051571	178.2	0.0495	0.000694
60	9:59	2.97	0.051571	178.2	0.0495	0.000694
60	10:0	2.97	0.051571	178.2	0.0495	0.000694
60	10:1	2.96	0.051398	177.6	0.0493333333	0.000694
60	10:2	2.97	0.051571	178.2	0.0495	0.000694
60	10:3	2.97	0.051571	178.2	0.0495	0.000694
60	10:4	2.97	0.051571	178.2	0.0495	0.000694
60	10:5	2.97	0.051571	178.2	0.0495	0.000694
60	10:6	2.96	0.051398	177.6	0.0493333333	0.000694
60	10:7	2.96	0.051398	177.6	0.0493333333	0.000694
60	10:8	2.96	0.051398	177.6	0.0493333333	0.000694
60	10:9	2.96	0.051398	177.6	0.0493333333	0.000694
60	10:10	2.96	0.051398	177.6	0.0493333333	0.000694
60	10:11	2.96	0.051398	177.6	0.0493333333	0.000694
60	10:12	2.96	0.051398	177.6	0.0493333333	0.000694
60	10:13	2.97	0.051571	178.2	0.0495	0.000694
60	10:14	2.96	0.051398	177.6	0.0493333333	0.000694
60	10:15	2.96	0.051398	177.6	0.0493333333	0.000694
60	10:16	2.96	0.051398	177.6	0.0493333333	0.000694
Continue for 37 days : Cumulative result are given below						
-	-	-	3256.22890	-	3125.441514	37.1382060
			1			2

Appendix B: Crack patterns of RC beams

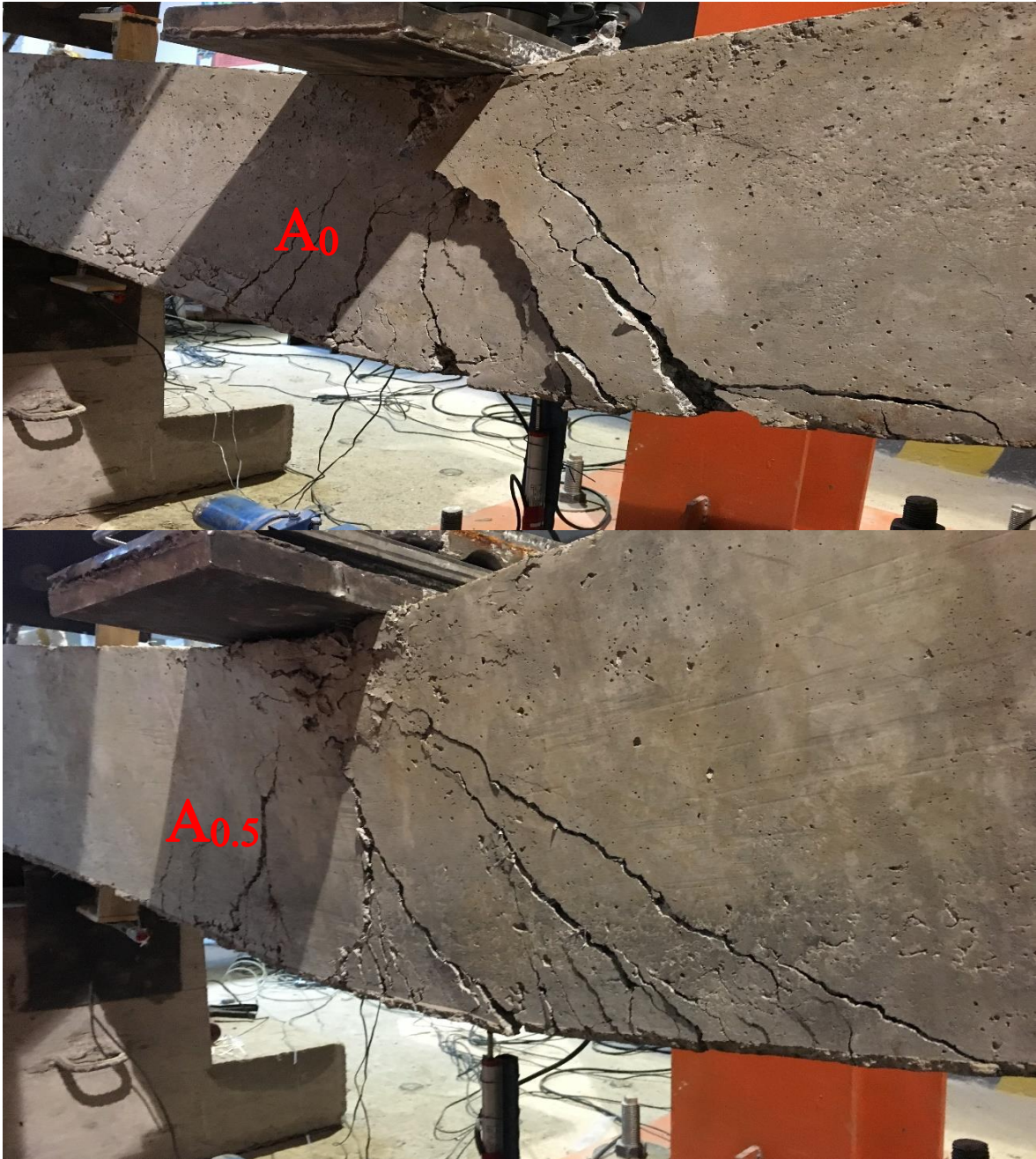


Figure 1. Load-displacement relationships of corroded RC beams for A₀ and A_{0.5}

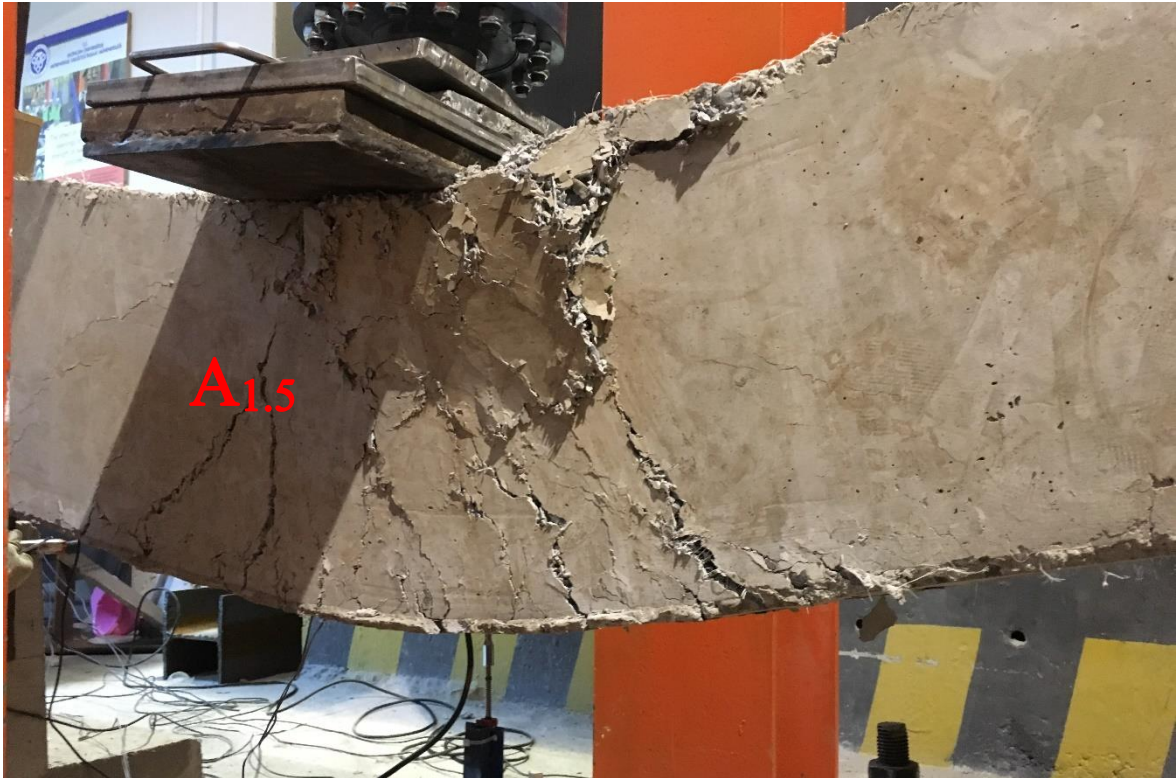


Figure 2. Load-displacement relationships of corroded RC beams for A1.5



Figure 3. Buckling of compression bars

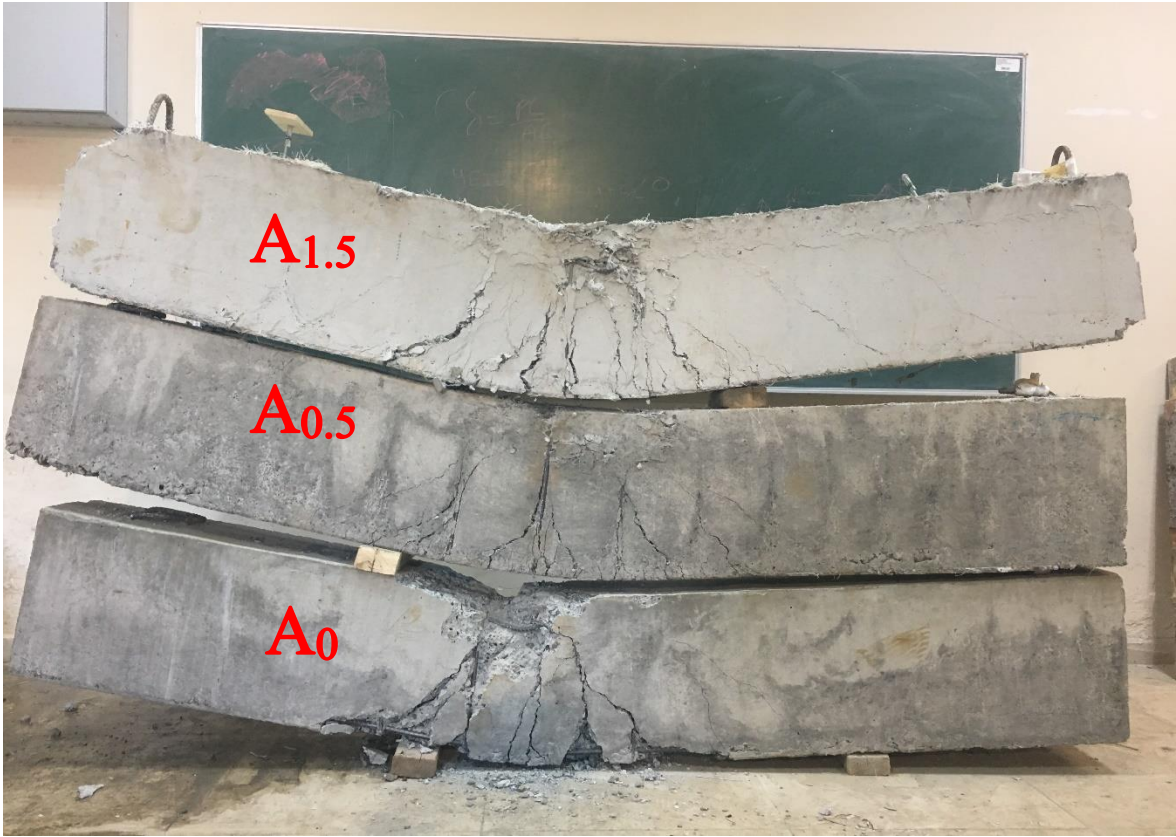


Figure 4. Load-displacement relationships of corroded RC beams for group A



Figure 5. Load-displacement relationships of corroded RC beams for B₀



Figure 6. Load-displacement relationships of corroded RC beams for B_{0.5}

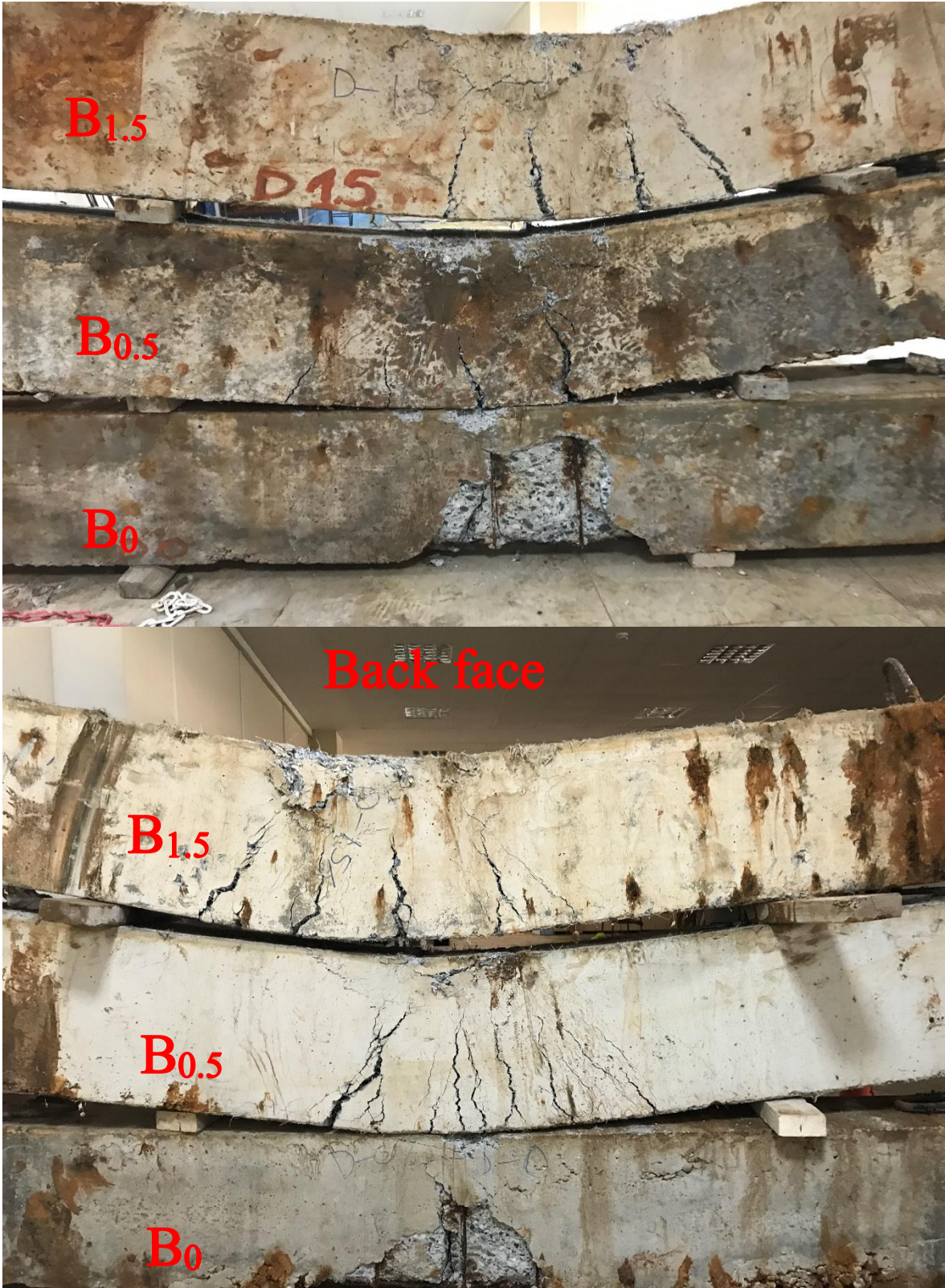


Figure 7. Load-displacement relationships of corroded RC beams for group B



Figure 8. Load-displacement relationships of corroded RC beams for C₀



Figure 9. Load-displacement relationships of corroded RC beams for C1.5

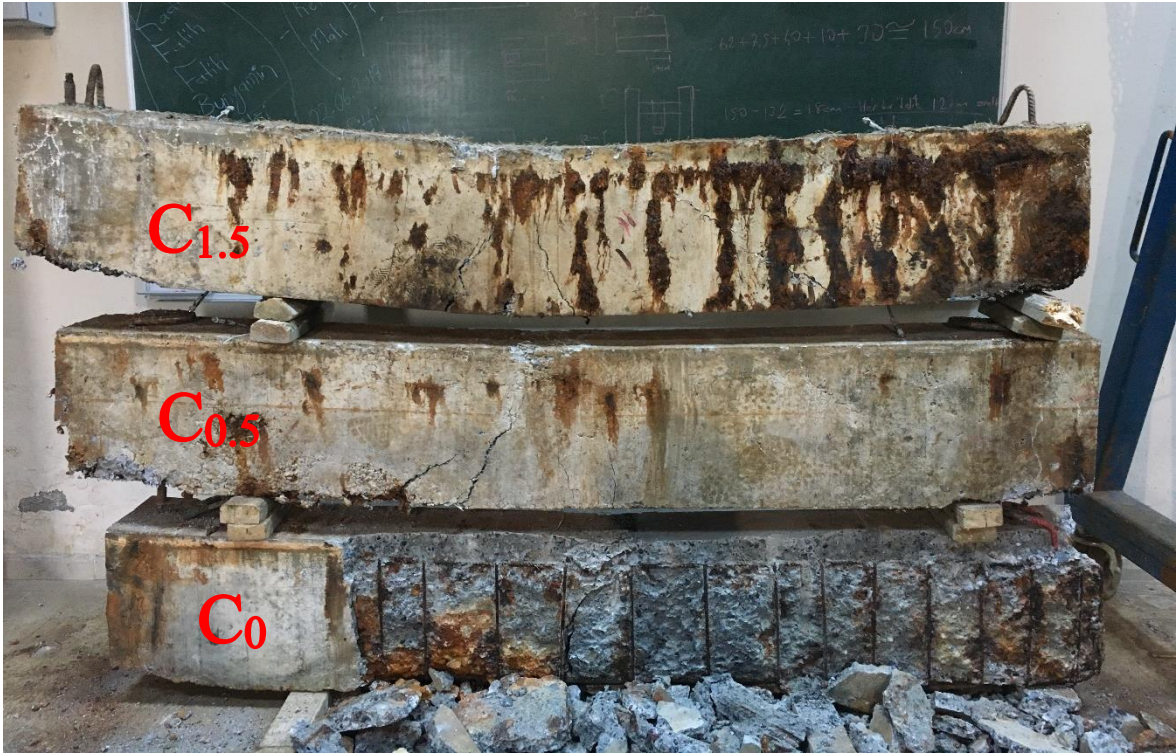


Figure 10. Load-displacement relationships of corroded RC beams for group C



Figure 11. Load-displacement relationships of corroded RC beams for D0



Figure 12. Load-displacement relationships of corroded RC beams for D0.5 and D1.5



Figure 13. Load-displacement relationships of corroded RC beams for group D

ÖZ GEÇMİŞ

Adı Soyadı: Kamil BİÇER

Doğum Tarihi: 18.06.1990

Unvanı: İnşaat Yüksek Mühendisi

İletişim Bilgileri Telefon: 05488324582

Email adresi: bicerkamil@gmail.com –bicerkamil@yahoo.com

5. Öğrenim Durumu: Yüksek Lisans- Doktora (tez aşaması)

Derece	Alan	Üniversite	Yıl
Lisans	İnşaat Mühendisliği	Doğu Akdeniz Üniv.	2007-2012
Y. Lisans	İnşaat Mühendisliği	Uluslararası Kıbrıs Üniv.	2012-2014
Doktora	İnşaat Mühendisliği	Uluslararası Kıbrıs Üniv.	2014 – Şubat 19
Doktora	İş Sağlığı ve Güvenliği	İ.M.B.L	2015 - güncel

Yayınlar

Uluslararası hakemli dergilerde yayınlanan makaleler (SCI & SSCI & Arts and Humanities)

- Bicer,K., Yalciner,H., Balkız,A., Kumbasaroglu,A., (2018).Flexural strength and structural behavior of corroded reinforced concrete beams with confinement effect of polypropylene fibers from fully extracted reinforcement bars from concrete. Construction and Building Materials
- Bicer,K., Yalciner,H., Balkız,A., Kumbasaroglu,A., (2018). FLEXURAL STRENGTH OF CORRODED REINFORCED CONCRETE BEAMS. ACI Structural and Materials Journals (Yayın Aşamassında)
- Biçer, K., Dikmen, D.C. (2018). Implementation of BIM in North Cyprus Construction Sector and its Effect on Economic Growth. The Russian Academic Journal. (Yayın Aşamasında)

Ulusal bilimsel toplantılarda sunulan ve bildiri kitabında basılan bildiriler

- Biçer, K., Sağlık Hizmetlerinde İş kazalarının değerlendirilmesinin İş sağlığı ve Güvenliği Açısından Önemi, 6. Uluslararası Sağlık ve Hastane Yönetimi Kongresi, Antalya, 2015
- Biçer, K., Kordal, N., Sağlık Hastanelerde görev yapan sağlık öğrencilerinin iş sağlığı ve Güvenliği konularında bilgilendirilmesi, 8. Uluslararası Sağlık ve Hastane Yönetimi Kongresi, Antalya, 2017

Projeler

- KKTC Akıncılar Köyünün İyileştirme, Koruma Ve Yenileme Projesi (TÜBİTAK Projesi) (2012-2015) Kendiliğinden Yerleşen Beton Projesi (Levent İnşaat Şirketi) (2013-2014)
- Korozyona maruz kalan betonarme yapıların fiber kullanılarak korozyona karşı davranışlarının Araştırılması. (Erzincan Üniv. –Bap Projesi,2018)

İdari Görevler

İş Sağlığı ve Güvenliği Program Sorumlusu (2015-2016)

İnşaat Mühendisliği Laboratuvar Sorumlusu (2012-2018)

Levent İnşaat Proje, Şantiye ve Beton Santrali Kalite Kontrol Sorumlusu (2012-2018)

Bilimsel ve Mesleki Kuruluşlara Üyelikler

İnşaat Mühendisleri Odası (KKTC)

Ödüller ve Sertifika

MUDEK Akreditasyon Başarı Hizmet Belgesi (2015)

İMO Yapı Denetim ve İş Sağlığı Güvenliği Sertifikası (2014)

Laboratuvar Deneyimleri

Kullanılan Aletler

- Windsor Probe for Concrete Compressive Strength Test
- MIRA A1040 Imaging device for Ultrasonic Tomography
- Profometer 5+ for Concrete Cover Measurement

- Hammer Rebound for Schmidt Concrete Compressive Strength Test
- Beton Karot Makinesi

Kullanılan Bilgisayar Programlari

Kullandığım programlar AutoCAD, IdeCAD, Sap2000, ArchiCAD, SteelPro, Microsoft Project, Word, Excel, Power point, MKA Steel, Probina ve MS Project (İş Programı)

İş Deneyimleri

Lisans eğitimi bitirdiğim yıldan itibaren aktif olarak bugüne kadar sayısız çelik ve betonarme projenin yapmış bulunmaktayım. (İMO'dan yapmış olduğum projeler hakkında bilgi alabilirsiniz.)

Bu güne kadar işlemiş olduğum firmalar aşağıdaki listedeki gibidir.

- Uzun inşaat ait apartman projeleri ve atölye tipi yapılar
- Erbatu inşaat ait otel, atölye, konut ve apartman projeler,
- Gerçek inşaat ait konut ve apartman tipi projeler,
- Aras Construction ait apartman projeleri,
- Hebo inşaat ait çelik konutlar,
- Tuğçe Construction ait konut ve atölye projeleri,
- Argeta Construction ait otel , toplu konut, apartman ve atölye projeleri yaptım.
- Levent veya DRN inşaat ait yurt projeleri, derslikler, apartmanlar ve çelik yapılar.(Şantiye aşamasında kontrolü)

Projelerini yapmış olduğumun binaların %70'nin uygulamalarını şantiyede denetlemekteyim.

Çelik Projelerinin %90'nın uygulama aşamasında kontrolör olarak denetlemekteyim.

Argeta Construction – Proje Mühendisi (Haziran 2018- Ocak 2019)

Öğretim Görevlisi- Uluslararası Kıbrıs Üniversitesi (2014 –Haziran 2018)

Yapı Mühendisliği – Levent İnşaat – (2014-2018)

Beton Kalite Kontrol Sorumlusu – Gerçek İnşaat – (2014- 2015)

İnşaat Laboratuvarı Sorumlusu — Uluslararası Kıbrıs Üniversitesi (2012-...)